KU LEUVEN

FACULTEIT BIO-INGENIEURSWETENSCHAPPEN

Studying the role of persistence in the emergence of antibiotic resistance through experimental evolution

Studie van de rol van persistentie in het ontstaan van antibioticumresistentie via experimentele evolutie

Promotoren:
Prof. Jan Michiels
Departement Microbiële en Moleculaire Systemen
Centrum voor Microbiële en Plantengenetica

Prof. Tom Wenseleers
Departement Biologie
Afdeling Ecologie, Evolutie en Biodiversiteitsbehoud

Masterproef voorgedragen
tot het behalen van het diploma van
Master of science in de bio-ingenieurswetenschappen:
cel- en gentechnologie

Etthel Windels

juni 2016

KU LEUVEN

FACULTEIT BIO-INGENIEURSWETENSCHAPPEN

Studying the role of persistence in the emergence of antibiotic resistance through experimental evolution

Studie van de rol van persistentie in het ontstaan van antibioticumresistentie via experimentele evolutie

Promotoren:
Prof. Jan Michiels
Departement Microbiële en Moleculaire Systemen
Centrum voor Microbiële en Plantengenetica

Prof. Tom Wenseleers
Departement Biologie
Afdeling Ecologie, Evolutie en Biodiversiteitsbehoud

Masterproef voorgedragen
tot het behalen van het diploma van
Master of science in de bio-ingenieurswetenschappen:
cel- en gentechnologie

Etthel Windels

juni 2016

Voorwoord

Deze thesis vormt een waardige afsluiter van een uiterst boeiend en vruchtbaar, maar ook intensief en uitdagend jaar. Verschillende mensen hebben elk op hun manier een bijdrage geleverd aan dit werk. Een woord van dank is dan ook zeker op zijn plaats voor iedereen die mij gedurende het voorbije jaar ondersteund heeft.

Eerst en vooral bedank ik graag mijn promotor, prof. Jan Michiels, voor het vertrouwen en de kansen die ik gekregen heb. Daarnaast ben ik ook mijn co-promotor, prof. Tom Wenseleers, dankbaar voor de mogelijkheid om van dit werk een boeiende mix van labowerk en modelleerwerk te maken.

Joran, uiteraard is dit ook jouw werk. Bedankt voor de vele uren die je in mij geïnvesteerd hebt, waarin je me de kneepjes van het vak leerde, ontelbare vragen beantwoordde, mijn teksten met grote zorgvuldigheid verbeterde,... en dat alles met eindeloos veel geduld. Zowel mijn enthousiasme over het onderwerp als alles wat ik dit jaar heb bijgeleerd, heb ik in de eerste plaats aan jou te danken.

Daarnaast ben ik ook mijn mede-thesisstudenten Evelien, Michiel, Isolde en Annelies, en alle leden van SPI en S&P dankbaar voor de gezellige sfeer in het labo en voor alle raad en hulp. Een bijzondere dankjewel aan Bram, voor je aanstekelijk enthousiasme en de inspirerende discussies.

Ook achter de schermen kon ik steeds op ondersteuning rekenen. Dankjewel mama en papa, voor alle kansen die ik krijg, voor jullie onvoorwaardelijke steun en voor het begrip tijdens het voorbije jaar, als ik het weer eens te druk had of niet naar huis kon komen tijdens het weekend. Ook bedankt aan mijn grootouders, voor de eeuwige bezorgdheid en interesse. Een heel bijzondere dankjewel is ten slotte weggelegd voor mijn vriend, die alles van op de eerste rij gevolgd heeft. Bedankt om me steeds weer perfect aan te vullen, samen zijn we er geraakt.

Etthel

Abstract

Our ability to treat bacterial infections is compromised worldwide by the emergence of antibiotic-resistant pathogens, which pose an ever-increasing global health threat. Apart from this major challenge, antibiotic treatment failure can also be caused by a small fraction of specialized survivor cells called persisters. Unlike genetically resistant mutants, persisters are rare phenotypic variants that are transiently capable of surviving exposure to lethal antibiotic doses. As persisters can re-initiate infection once the antibiotic pressure declines, they are held responsible for the recalcitrance of chronic infections. Despite fundamental differences between resistance and persistence, both survival strategies may be more related than currently anticipated. In particular, it has been proposed that persistence accelerates the emergence of resistance. The viability of persisters in the face of antibiotic treatment could indeed be an important factor in the evolution towards resistance. In addition, many of the processes involved in persistence, e.g. stress responses, have also been found to promote adaptive evolution.

In this work, we investigated the persistence-resistance link in *Escherichia coli* using experimental evolution, mechanistic experiments, and mathematical modelling. Long-term incubation of cultures on solid growth medium revealed a stronger and faster emergence of ciprofloxacin- and ampicillin-resistant colonies in mutants with elevated persister levels. The same trend was observed in experiments with environmental *E. coli* isolates. Nevertheless, evolution experiments that simulated an *in vivo*-like pharmacokinetic profile did not support these findings, indicating that the contribution of persistence to resistance largely depends on the treatment conditions.

The persister level of a population was not only shown to correlate with resistance development on solid medium, but also with the population-wide SOS response activity and stress-induced mutation rate. Due to its stimulating effects on adaptive mutagenesis, the elevated SOS response activity in high persistence strains can provide an important link between persistence and resistance.

Novel insights into the contribution of persistence to resistance development should stimulate the search for anti-persister therapies or strategies that target stress responses, in order to combat the emergence and spread of antibiotic resistance.

Samenvatting

De behandeling van bacteriële infecties wordt steeds moeilijker door de toenemende opkomst en verspreiding van antibioticumresistente pathogenen. Therapiefalen kan echter ook het gevolg zijn van een kleine fractie zogenaamde persistorcellen, die een bijkomende uitdaging vormen in de strijd tegen infectieziektes. In tegenstelling tot genetisch resistente mutanten zijn persistors zeldzame fenotypische varianten die tijdelijk in staat zijn om letale antibioticumdosissen te overleven. Eens de antibioticumstress wegvalt, kunnen persistors de groei hervatten en opnieuw infectie veroorzaken. Om die reden wordt persistentie vaak aangeduid als de onderliggende oorzaak van chronische infecties. Ondanks de fundamentele verschillen tussen resistentie en persistentie zijn beide overlevingsstrategieën misschien meer verwant dan aanvankelijk verondersteld. Er werd immers reeds gespeculeerd dat persistentie kan bijdragen aan het ontstaan van resistentie. De evolutie van resistentie zou inderdaad versneld kunnen worden door een kleine fractie persistors die de antibioticumbehandeling overleeft. Bovendien zijn verschillende processen die een rol spelen in persistentie, zoals bijvoorbeeld stressresponsen, ook in staat om adaptieve evolutie versnellen.

In dit werk werd de persistentie-resistentie link onderzocht in *Escherichia coli* via experimentele evolutie, mechanistische experimenten en wiskundige modellen. Langdurige incubatie van culturen op een vaste voedingsbodem toonde aan dat ciprofloxacine- en ampicillineresistente kolonies sneller en veelvuldiger ontstaan in mutanten met hogere persistorlevels. Dezelfde trend werd geobserveerd in experimenten met natuurlijke *E. coli* isolaten. We konden deze bevindingen evenwel niet ondersteunen aan de hand van evolutie-experimenten waarin een *in vivo* farmacokinetisch profiel werd nagebootst. De variërende uitkomst voor diverse experimenten toont aan dat de bijdrage van persistentie aan resistentie-ontwikkeling sterk afhangt van de behandelingscondities.

Persistorlevels bleken echter niet alleen te correleren met resistentie-ontwikkeling op vaste voedingsbodem, maar ook met de algemene SOS respons activiteit en stress-geïnduceerde mutatiesnelheid. Als gevolg van het stimulerend effect op adaptieve mutagenese kan de toegenomen SOS respons activiteit een belangrijke link vormen tussen persistentie en resistentie.

Nieuwe inzichten in de bijdrage van persistentie aan resistentie-ontwikkeling moeten een stimulans vormen in de zoektocht naar anti-persistortherapieën of strategieën die stressresponsen als doelwit hebben, om zodoende het ontstaan en de verspreiding van antibioticumresistentie tegen te gaan.

List of abbreviations

AMK	amikacin
AMP	ampicillin
ANOVA	analysis of variance
AUC	area under curve
CAR	carbenicillin
CEF	ceftazidime
CFU	colony-forming unit
CIP	ciprofloxacin
CRE	carbapenem-resistant *Enterobacteriaceae*
DSB	double-stranded break
GFP	green fluorescent protein
hip	high persistence
KAN	kanamycin
LB	lysogeny broth
LPS	lipopolysaccharide
MBC	minimum bactericidal concentration
MDR	multidrug resistance
MHB	Mueller-Hinton broth
MMC	mitomycin C
MPC	mutant prevention concentration
MSC	minimal selective concentration
MSW	mutant selection window
OD	optical density
OMP	outer membrane protein
PD	pharmacodynamic
PK	pharmacokinetic
(p)ppGpp	guanosine tetra(penta-)phosphate
PQ	paraquat

QRDR	quinolone resistance-determining region
RIF	rifampicin
RNAP	RNA polymerase
ROS	reactive oxygen species
rRNA	ribosomal RNA
SHX	serine hydroxamate
sRNA	small RNA
ssDNA	single-stranded DNA
TA	toxin-antitoxin
TDR	totally drug-resistant
TET	tetracycline
tRNA	transfer RNA
UTR	untranslated region
VRE	vancomycin-resistant enterococci
VRSA	vancomycin-resistant *Staphylococcus aureus*

List of Figures

List of Tables

Contents

Context and aims

The bacterial arsenal of antibiotic resistance mechanisms is expanding rapidly, causing an escalating burden on public healthcare. In addition to this widely acknowledged threat, treatment of infectious diseases is further complicated by persistence. The transient multidrug tolerance of a small number of persister cells is a major cause of the recalcitrance of chronic infections. Especially in immunocompromised hosts, or when shielded from the immune system in biofilms, persisters are held responsible for the chronic nature of infectious diseases.

Theoretical hypotheses point out a potential contribution of persistence to the evolution of resistance [39, 126]. So far, these theoretical arguments largely remained unexplored experimentally. In this master's thesis, we aimed to establish a link between persistence and the potential to develop resistance in *Escherichia coli*, using experimental evolution and focusing on widely used antibiotics such as fluoroquinolones and β-lactams. The alarmingly fast spread of fluoroquinolone resistance among *Enterobacteriaceae* [204] underscores the need for research focusing on underlying causes and catalysts, of which persistence may be one, of this dangerous phenomenon. To gain more insight into the dynamics of bacterial populations under antibiotic treatment, we intended to construct a model that incorporates both persisters and resistant mutants. By measuring the activity of various stress responses, we wished to identify possible mechanisms that could connect persistence to an accelerated resistance development. The identification of such mechanisms can offer opportunities to combat persistence as well as to counteract the spread of resistance.

Recent cancer research demonstrated that the impact of the current study reaches beyond infectious diseases. Persistence- and resistance-related phenomena have indeed been associated with cancer cell populations [200]. Importantly, Ramirez *et al.* [185] reported the emergence of diverse drug resistance mechanisms from persisters, indicating that persisters may provide a reservoir of resistant cancer cells.

The first part of this thesis provides an overview of the currently available literature on antibiotic survival strategies, experimental evolution, the persistence-resistance link, and mathematical modelling of persistence. The materials and methods used in this work are described in the second part. The third part focuses on experimental work and mathematical modelling and is followed by a discussion of the obtained results.

Part I

Literature review

Chapter 1

Evading antibiotics: from phenotypic tolerance to genetic resistance

The discovery of antibiotics radically changed human healthcare and saved millions of lives worldwide. However, the introduction of these drugs was inevitably accompanied by the emergence of pathogens resistant to their action [43]. The selection pressure exerted by antibiotics resulted in an alarmingly fast spread of resistance genes, which are making previously treatable infections lethal again [233].

The clinical burden posed by antibiotic resistance is widely acknowledged, but resistance is not the only reason for treatment failure. Even in the absence of genetic resistance, bacteria exhibit a spectrum of survival strategies allowing them to escape the action of antibiotics. Either working population-wide or only at a subpopulation level, these defense mechanisms provide phenotypic tolerance and avoid extinction of the bacterial population. This chapter gives an overview of the most important bacterial survival strategies, starting with a concise introduction on the different antibiotic classes and genetically encoded resistance mechanisms. The second part deals with phenotypic tolerance, of which persistence is the most prominent example.

1.1 Antibiotics: a classification based on mode of action

The unprecedented success of antibiotics in the treatment of infections led to their widespread use in clinical settings. Fleming's famous discovery of the first natural antibiotic penicillin boosted the exploration of other major antibiotic classes. These natural products defined the scaffold of several generations of synthetically modified analogues [48]. Table 1.1 gives an overview of the major antibiotic classes and their characteristics. Antibiotics can be classified according to their mode of action, in which a distinction is made between bacteriostatic antibiotics, only inhibiting

cell growth, and bactericidal antibiotics, also leading to cell death by corrupting the function of their targets. The use of bactericidal drugs leads to the inhibition of essential cellular processes as well as the induction of lethal damage [110].

This first categorization can be fine-tuned by classifying antibiotics according to their primary cellular targets [110]. Fluoroquinolones comprise a synthetic class of broad-spectrum antibiotics that are derived from the quinolones, and include clinically relevant agents such as ciprofloxacin and levofloxacin [36]. These drugs corrupt the function of DNA gyrase (DNA topoisomerase II) and DNA topoisomerase IV, which modulate DNA supercoiling by introducing and ligating DNA breaks. Binding of the drug to these enzyme-DNA complexes prevents strand rejoining after DNA cleavage. The resulting DNA breaks lead to inhibition of DNA synthesis, induction of the SOS response, cell filamentation, and ultimately cell death [50, 110].

Rifamycins are a class of originally natural antibiotics that were modified by mutagenesis of the producing organism [48]. By binding to the β-subunit of RNA polymerase (RNAP), these drugs are efficient inhibitors of transcription initiation. The semi-synthetically derived compound rifampicin serves as an important first-line agent against *Mycobacterium tuberculosis* [30, 149].

β-lactams (including penicillins, cephalosporins, and carbapenems) are a widely used class of antibiotics that target cell wall synthesis. They inhibit the action of transpeptidases, also called penicillin-binding proteins, thereby blocking cross-linking of peptidoglycan units [110]. The use of β-lactams eventually results in lysis-dependent cell death, a complex process involving autolysins [110].

Several antibiotics target the ribosomes, leading to the inhibition of cellular protein synthesis. Examples are macrolides, lincosamides, streptogramins, amphenicols, and oxazolidinones, which are all 50S ribosome inhibitors [110]. 30S ribosome inhibitors include the tetracyclines and aminoglycosides, the latter being important bactericidal drugs. Whereas most protein synthesis inhibitors cause bacteriostasis by restricting ribosome functioning, aminoglycosides promote the synthesis of mistranslated proteins, the membrane incorporation of which contributes to cell death [110].

Despite substantial variability in primary targets, Kohanski *et al.* [111] proposed that all bactericidal antibiotics eventually kill bacteria through a common mechanism involving highly deleterious reactive oxygen species (ROS). However, since recent studies criticized this point of view [55, 101, 137, 189], the ROS hypothesis remains a matter of debate.

Table 1.1: Overview of the most important antibiotic classes and their characteristics

Antibiotic class	Intracellular target	Resistance mechanisms	Bacteriostatic/ bactericidal	Examples
Quinolones	Topoisomerase II (DNA gyrase), topoisomerase IV	Target modification, efflux pumps[148]	Bactericidal	Ciprofloxacin, levofloxacin
Rifamycins	RNA polymerase	Target modification[219], decreased cell permeability[219], antibiotic modifiying enzymes (e.g. Arr enzymes)[20]	Bactericidal	Rifamycin SV, rifampicin
β-lactams	Transpeptidase	Target modification[148], decreased cell permeability[219], antibiotic modifying enzymes (e.g. β-lactamases)[148]	Bactericidal	Ampicillin, ceftazidime, meropenem
Tetracyclines	30S ribosome	Ribosomal protection[203], efflux pumps[203]	Bacteriostatic	Minocycline, doxycycline
Aminoglycosides	30S ribosome	16S RNA methylation[148], efflux pumps[148], antibiotic modifying enzymes[148]	Bactericidal	Amikacin, kanamycin, tobramycin

1.2 Genetic resistance mechanisms

The efficacy of antibiotics in the battle against infectious diseases is restricted by several bacterial defense strategies. Through growth inhibition of susceptible cells, antibiotics strongly select for genetic mutants that are able to escape antibiotic action. Although many different resistance determinants exist, all aim at the prevention of antibiotic-target binding. The antibiotic can be degraded or modified, thereby rendering it inactive. Examples of these mechanisms include enzymes such as β-lactamases and aminoglycoside-modifying enzymes [148]. Furthermore, the entry of antibiotics into the cell can be prevented or their intracellular concentration can be decreased by means of non-specific or specific efflux pumps. Resistance can also be provided through target alteration by mutation, enzymatic changes, or target substitution [129]. For most antibiotics, multiple resistance mechanisms exist [127].

Resistance can be either intrinsic or acquired. As intrinsic resistance is attributed to inherent structural and functional characteristics of a species, it can be considered as a general property of all isolates [5]. Examples include *ampC*-encoded β-lactamases in Gram-negative bacteria and the intrinsic resistance of *Pseudomonas aeruginosa* to a wide range of antibiotics, which is largely due to the low permeability of its outer membrane and the constitutive expression of various efflux pumps [208]. Acquired resistance arises when a micro-organism gains resistance to an antimicrobial agent to which it was previously susceptible [27]. In some organisms, such as *M. tuberculosis*, vertical transmission of *de novo* point mutations serves as the predominant source of acquired antibiotic resistance. Nevertheless, many resistance genes are associated with mobile genetic elements such as plasmids, transposons, and integrons [174]. The horizontal dissemination of

these elements provides a means for the rapid spread of resistance determinants, whereas point mutations cause a much slower, gradual development from low to high resistance [127].

Treatment of infectious diseases is further complicated by the emergence of multidrug-resistant pathogens. The extensive and often unwarranted use of numerous antibiotics in healthcare, livestock production, and aquaculture selected for the presence of different resistance mechanisms in a single bacterium (e.g. multiple resistance-conferring plasmids) or non-selective mechanisms working against several drugs (e.g. drug efflux pumps). Moreover, some drug-specific resistance determinants reduce the susceptibility towards other drugs [5]. The serious threat posed by multidrug resistance is reflected in the emergence of virtually untreatable pathogens such as totally drug-resistant (TDR) *M. tuberculosis*, vancomycin-resistant enterococci (VRE), vancomycin-resistant *Staphylococcus aureus* (VRSA), multidrug-resistant (MDR) *P. aeruginosa*, and carbapenem-resistant *Enterobacteriaceae* (CRE) [41, 65, 168, 212, 217].

1.3 Persistence

1.3.1 General description

Under conditions of continuous antibiotic exposure, a genetically resistant mutant has a clear fitness advantage over a wild type strain. This advantage is however not definite in environments where antibiotics are only periodically present, since the maintenance of resistance mechanisms is often associated with a fitness cost under antibiotic-free conditions [8]. Fluctuating environments in which sudden, lethal catastrophes occur occasionally can favour bet-hedging strategies such as persistence [114]. Bet-hedging refers to a risk spreading strategy that aims to optimize the population fitness in unpredictable environments by generating phenotypic diversity. Unlike resistance, persistence is characterized by a genetically identical, but phenotypically distinct subpopulation containing a small number of non- or slowly growing cells called 'persisters' [105]. Persisters are rare phenotypic variants which are refractory to antibiotic concentrations that are lethal for normal cells, thereby preventing the complete eradication of the population under antibiotic stress [24, 129]. Exposure of the population to such lethal concentrations thus reveals the existence of the drug-tolerant subpopulation, resulting in a biphasic killing curve (Figure 1.1). Fast killing of normal cells is followed by a plateau where persisters are killed at a much slower rate [146]. After removal of the drug, the small surviving persister fraction resumes growth and gives rise to a new population, again containing a small fraction of persisters. The switch from the persister state to the normal, dividing state after the relief of antibiotic stress indicates the transient nature of the persister phenotype.

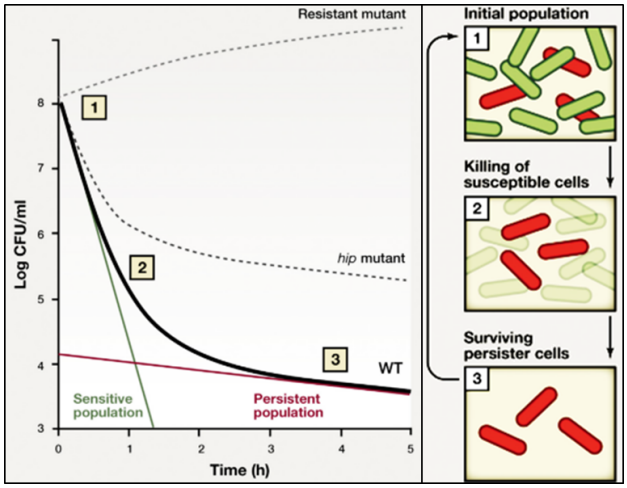

Figure 1.1: Biphasic killing pattern during antibiotic treatment of a population containing persisters. The susceptible subpopulation is killed at a constant rate (green slope) until only persisters remain viable. Killing of persisters occurs at a much slower rate, as revealed by the red slope, resulting in a persister plateau. For high persistence (*hip*) mutants, high persister levels translate into an increased survival at the plateau. As opposed to genetically resistant mutants, surviving persisters give rise to a drug-susceptible population, again containing a small persister fraction (adapted from [146]).

1.3.2 Switching to the persister state

The coexistence of different subpopulations in one isogenic population implies the action of an epigenetic mechanism, deciding which cells give up active growth in order to become tolerant persisters. Single-cell observations using microfluidic devices allowed Balaban *et al.* [17] to prove that stochastic processes generate non-growing, tolerant phenotypic variants prior to antibiotic treatment. Phenotypic heterogeneity can be triggered by noise in transcription and translation of a certain persister protein, generating a distribution of the expression level around an average value [53]. However, noise alone is insufficient to generate considerable phenotypic heterogeneity unless it is amplified by regulatory processes. When the expression level reaches a certain threshold, noise amplification through positive or double negative feedback loops can convert a continuous expression distribution into a discrete (e.g. bimodal) one [194]. This process enables two or more phenotypic states to stably coexist in a genetically identical population.

However, persister levels are not entirely independent on the environment. Deterministic components, such as the growth phase, significantly affect persister levels, with the highest number of persisters emerging during late-exponential and stationary phase [100]. Furthermore, other environmental cues such as nutrient limitation [64], diauxic carbon source transitions [7], heat stress [162], osmotic stress [162], oxidative stress [84, 240], acid stress [84], antibiotic stress [46, 91, 116], quorum sensing [23, 96, 124, 158], host macrophages [79], etc. can potentially shift the average expression level of persister proteins to a higher value, resulting in more cells crossing the threshold

and switching to the persister state (Figure 1.2). Importantly, many of these triggers are present in an *in vivo* infection environment, and persister levels can even increase during antibiotic exposure [15, 46, 91, 116].

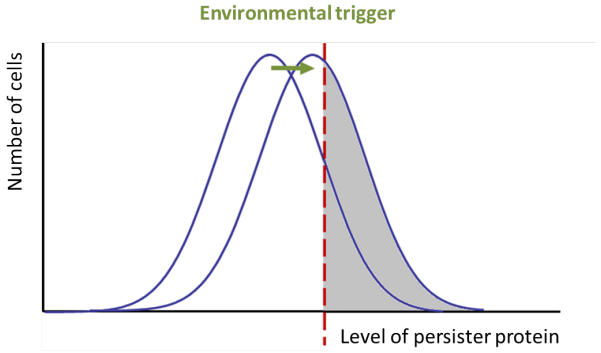

Figure 1.2: Both stochastic and deterministic components are involved in persister formation. Stochasticity in transcription and translation of a certain persister protein results in a distribution of the expression around an average value. Cells with an expression level above a particular threshold value switch to the persister state. Certain environmental triggers, such as the growth phase and several stress conditions, can shift the average expression level and result in a higher persister fraction.

1.3.3 Physiological state of persisters

Given the absence of genetic resistance mechanisms that prevent antibiotic-target binding, the (multi)drug tolerance of persisters must be ascribed to physiological processes avoiding the action of the drug. Since persister are supposed to be non- or slowly growing cells [17], a global downregulation of processes targeted by antibiotics is thought to prevent the lethal effects of target-bound drugs on persisters [130]. It is known since long that the efficacy of antibiotics indeed correlates with the bacterial growth rate [54, 218]. Although this dormancy itself can passively contribute to the drug tolerance of persisters, it is not sufficient to define their complete phenotype, as demonstrated by their tolerance towards antibiotics targeting non-growing cells and their expression pattern that is distinct from stationary phase cells [198]. Furthermore, it was reported that rapidly dividing cells can give rise to persisters, and that the majority of dormant cells are not persisters [171].

In addition, many studies provide evidence for the involvement of active processes in persister differentiation. Examples include a starvation-induced stringent response [167], oxidative stress defense mechanisms [103], stochastic expression of an intracellular antibiotic-activating enzyme [229], and activation of efflux pumps [240], all of which prevent the damage induced by antibiotics. As will be discussed in paragraph 1.3.4, stress responses seem to play an important role in the establishment and maintenance of the persister state [182]. However, the involvement of active

processes in persister formation should not be considered inconsistent with persister-associated dormancy. Instead, these processes could represent the active mechanisms by which cells reach this dormant state [237].

1.3.4 Persistence mechanisms

Although some authors suggest that there may be no specific mechanism underlying persistence [125, 223], others consider the environmental induction of persistence as evidence for an active persister formation mechanism [130]. In any case, the processes responsible for the differentiation to a persister cell still hold many unclarities [16]. No single gene knock-out results in a mutant lacking persisters, indicating the high redundancy of persistence mechanisms [85]. Studies reporting decreased persister levels in mutants lacking global regulators confirm this redundancy [78, 132, 162, 225]. The involvement of many parallel mechanisms makes persistence hard to study and to target therapeutically.

Toxin-antitoxin modules

Different transcriptome studies indicated a central role for toxin-antitoxin (TA) modules in the generation of persisters [98, 100, 198]. A TA module encodes a stable toxin, inhibiting some essential cellular function, and an unstable antitoxin, preventing the action of the toxin. Through the negative effect exerted on processes such as protein translation or the proton motive force, high toxin/antitoxin ratios in persisters are supposed to be an important cause of both the stochastic and the deterministic establishment of growth arrest and multidrug tolerance [116, 130]. Indeed, overexpression of toxins causes growth arrest and persistence, which can be rescued by overexpression of the cognate antitoxin [113, 177]. Although the deletion of a single TA module does not affect persister levels in most cases, Maisonneuve *et al.* [147] reported a progressive reduction in persister levels upon successive deletion of all 10 type II mRNase TA modules.

Selection for high persistence mutants by mutagenesis and repeated ampicillin exposure led to the discovery of HipA, the first toxin shown to be involved in persistence [160]. Mutants bearing the gain-of-function allele *hipA7* exhibit a high persistence phenotype [112]. While the translation elongation factor EF-Tu was first suggested as the intracellular target of HipA [196], it has been shown recently that HipA phosphorylates glutamyl-tRNA synthetase (GltX) instead of EF-Tu [70, 94]. Phosphorylation of GltX inhibits its aminoacylation activity and provokes the accumulation of uncharged transfer RNAs (tRNAs), thereby stimulating the stringent response and associated (p)ppGpp (guanosine tetra(penta-)phosphate) synthesis.

Stress responses

Correlated to their high toxin expression levels, persisters are characterized by the general activation of stress response pathways. The upregulation of various stress responses was already observed in transcriptome analyses of persisters [99, 198]. The role of these stress responses was further examined by different research groups, often focusing on well-known pathways such as the stringent response and the SOS response. Consistent with the observed dependence of the *hipA7* phenotype on the stringent response alarmone (p)ppGpp [112], Maisonneuve *et al.* [145] proposed a central role for (p)ppGpp in TA-mediated stochastic switching to the persister state [145]. Through (p)ppGpp-dependent accumulation of polyphosphate (PolyP), the stringent response stimulates the activation of Lon protease, which degrades type II antitoxins [147]. (Figure 1.3). However, (p)ppGpp-induced persistence can also occur independently of Lon. An example is persistence mediated by the membrane depolarizing toxin HokB, the expression of which is dependent on the conserved GTPase ObgE as well as (p)ppGpp [224]. Additionally, Amato *et al.* [7] provided evidence for another (p)ppGpp persister formation pathway relying on inhibition of the fluoroquinolone target DNA gyrase. The induction of the stringent response in several stress conditions, most notably amino acid or other nutrient limitation, also links this regulator to environmentally induced persistence [145].

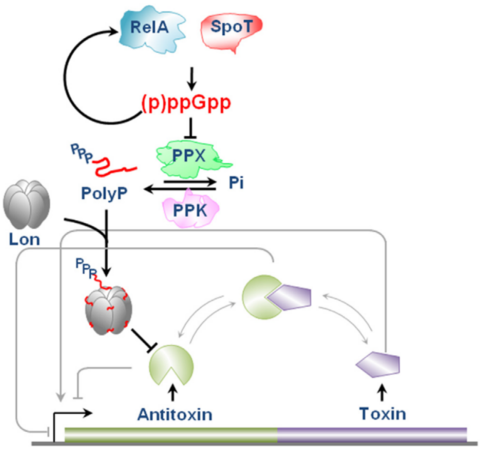

Figure 1.3: Mechanisms underlying (p)ppGpp controlled persistence. (p)ppGpp is synthesized through the action of both RelA and SpoT and inhibits the degradation of polyphosphate (PolyP) by exopolyphosphatase (PPX). The constitutive synthesis of PolyP by polyphosphate kinase (PPK) promotes the accumulation of PolyP, which stimulates the activity of Lon protease. The degradation of antitoxins causes increasing concentration of free toxins, resulting in persistence (adapted from [145]).

Dörr *et al.* [46] reported a major role of the SOS response in the induction of TA-mediated persistence to ciprofloxacin. They observed strongly decreased persister levels in a Δ*recA* and *lexA3* mutant, both lacking a proper SOS induction. Remarkably, pre-exposure to ciprofloxacin

itself promotes DNA damage and activates the SOS response. This process eventually leads to the insertion of the toxin TisB into the membrane, reducing the proton motive force and initiating a dormant state in a similar way as HokB [47].

1.3.5 Clinical relevance of persistence

As persistence is supposed to be a universal survival strategy, it should not be overlooked when it comes to human pathogens. Indeed, the presence of persisters has been described in notable pathogens such as uropathogenic *Escherichia coli* [25], *P. aeruginosa* [161], *M. tuberculosis* [231], *S. aureus* [99], and *Candida albicans* [118]. Further extending the clinical impact of persistence, small fractions of transiently drug-tolerant cells have even been observed in cancer cell populations [200].

Despite their low frequencies, multidrug tolerant persister cells in a population of pathogenic bacteria can have life-threatening implications. In most cases, small number of persisters do not cause major problems as they are easily eliminated by the host's immune system. However, in immunocompromised hosts such as HIV or cancer patients, the presence of these survivor cells can be detrimental [130]. Furthermore, persisters are often protected from the immune system by the extracellular matrix of biofilms, where they constitute a predominant cause of chronic infections [205]. However, the association with biofilms is not always required in order for persisters to cause health problems. Pathogens can be protected by several niches in the human body, including the central nervous system, the gastrointestinal tract, and host cells in the case of intracellular pathogens [90, 130].

Examples of well-known diseases in which persistence has harmful implications include tuberculosis, cystic fibrosis, chronic urinary tract infections, and gastritis [57, 74]. The clinical relevance of persistence is further sustained by experiments demonstrating the presence and antibiotic tolerance of persisters in *in vivo* infection models [37, 79, 93] and experimental support for the *in vivo* selection of high persistence mutants of *P. aeruginosa* and *C. albicans* in patients with cystic fibrosis and oral candidiasis respectively [118, 161].

1.4 Other antibiotic survival strategies

1.4.1 Drug indifference

Although dormancy is not sufficient to explain a persister's tolerant state, it is generally accepted that the dormancy-associated shutdown of processes targeted by antibiotics can cause reduced

drug sensitivity, a phenomenon called 'drug indifference' [150]. Metabolic dormancy, whether or not induced by resource limitation, renders bacteria phenotypically refractory to drugs that require active growth. Antibiotics such as ampicillin effectively kill exponentially growing cells, but only slightly affect densities of stationary phase cultures [126, 218]. This population-wide survival of nutrient-limited cells is essentially different from persistence, which only affects a small proportion of the population and is also manifest in favorable, nutrient-rich growth conditions. The clinical impact of drug indifference is especially prominent in *M. tuberculosis* infections. The presence of a latent population of non-dividing bacteria is a major cause of the remarkably extended treatment duration [231]. However, recent studies on the physiological state of these latent bacteria suggest that their dormancy is in fact a regulated process instead of a passive side effect of resource limitation [2, 13]. Moreover, it seems plausible that at least some metabolic activity is required for the maintenance of the non-replicating mycobacterial state [186].

1.4.2 Collective antibiotic tolerance

Another strategy conferring antibiotic tolerance is the so-called 'inoculum effect'. This term refers to the reduced efficacy of antibiotics with increasing population densities and can be achieved in different ways [210]. Release of resistance-conferring enzymes, e.g. β-lactamases, in the environment can protect the whole population [238]. When the production of such enzymes is costly, their synthesis can be delayed until a sufficiently high density is attained [45]. Such density-dependent effects on collective gene expression are often regulated by quorum sensing molecules [154]. Collective antibiotic tolerance can also result from antibiotic-mediated altruistic cell death, leading to an increased concentration of protective extracellular agents for surviving cells [154]. In still other cases, only a few highly resistant individuals produce the signaling molecule indole, which induces phenotypic tolerance in more susceptible cells and enhances population survival at the cost of a small number of altruistic individuals [121]. Finally, bistability in ribosome inhibition, caused by certain antibiotics, can result in the complete eradication of low density populations but ensure survival when the population is at a sufficiently high density. At low densities, the intracellular concentration is high enough to inhibit ribosome functioning, whereas positive feedback in ribosome synthesis overcomes inhibition at lower concentrations [210].

Chapter 2

Evolution under antibiotic stress

In recent years, experimental evolution has emerged as an important tool in addressing fundamental evolutionary questions and unraveling the genetic basis of complex traits. This chapter discusses recent progress in the field of experimental evolution, with the focus on bacterial adaptation to antibiotic stress.

2.1 Experimental evolution

2.1.1 Introduction

Evolutionary questions are traditionally addressed with comparative studies of living organisms, fossil records, and molecular phylogeny. However, complete evolutionary trajectories and forces yielding current phenotypes are difficult to unravel based on these data alone. Experimental evolution provides an alternative way of studying evolution in the lab. Under strictly controlled laboratory conditions, populations evolve as they would when subject to natural selective forces, allowing the observation of evolutionary dynamics in real time [95].

The short generation times and large population sizes of microbial organisms enable the study of evolutionary processes at a reasonable timescale [123]. In 1988, Richard Lenski embarked on a famous, long-term evolution experiment starting from 12 identical ancestral populations of *E. coli* [122]. More than 28 years and 64,000 generations later, the experiment is still running and has answered many questions about genome dynamics during evolution, the relationship with phenotypic adaptation, and other evolutionary issues [143]. Parallel evolution of identical starting populations under the same conditions can reveal the contribution of chance to evolutionary outcomes. Furthermore, cryogenic preservation allows direct comparisons of ancestor, intermediate, and evolved strains, and aids in the reconstruction of evolutionary trajectories [235]. The reproducibility combined with the strict control over the growth conditions contributes to the versatility of experimental evolution in the study of evolutionary dynamics.

Although very useful to study evolutionary forces, genetic changes underlying adaptations, mutation rates, fitness trajectories, and numerous other evolutionary processes, experimental evolution still holds some limitations. Long-term processes such as speciation can be too slow to study at a human timescale. Furthermore, the maintenance of populations is often a labor-intensive and time-consuming process, and contamination of the populations can impose an important practical issue [95].

2.1.2 Dynamics during experimental evolution

Even in the absence of selective pressure, mutations spontaneously arise during the cell cycle due to DNA replication errors, insertion of mobile elements, or DNA damage caused by environmental factors such as UV radiation or chemical mutagens. Despite their low rate, spontaneous mutations can account for a great deal of the genetic variation in a population.

In adaptive evolution experiments, changes in the population's gene pool are however often driven in a certain direction through the selection pressure exerted by constant or fluctuating environmental conditions imposed by the researcher. The result is a fitness increase relative to the ancestral population, due to the accumulation of adaptive genetic changes [18]. The rate of fitness increase usually slows down during adaptation as a result of genetic interactions between new and already existing mutations, a process termed 'diminishing-return epistasis' [34]. Early beneficial mutations with large fitness impacts generally precede small-impact mutations, and adaptation in this stage is said to be in the optimization regime [18]. Occasionally, small-impact mutations can prepare the genetic background for a highly beneficial mutation, which is called innovation [18].

When a beneficial mutation initially arises, it is present at low frequency and risks being lost by the random process of genetic drift. If the mutation overcomes this accidental loss, it can gradually reach fixation in a so-called selective sweep and pave the way for new beneficial mutations. This sequential follow-up of mutations is termed periodic selection [18] (Figure 2.1). When alternative beneficial mutations are present in a population, due to a high mutation rate or large population size, competition between the different mutants slows down the spread of each individual mutation. Eventually, the mutation rendering the highest fitness advantage outcompetes the alternative mutations and reaches genetic fixation [71] (Figure 2.1). This 'clonal interference' only occurs in asexual populations, since competing beneficial mutations have the potential to be recombined in sexual populations.

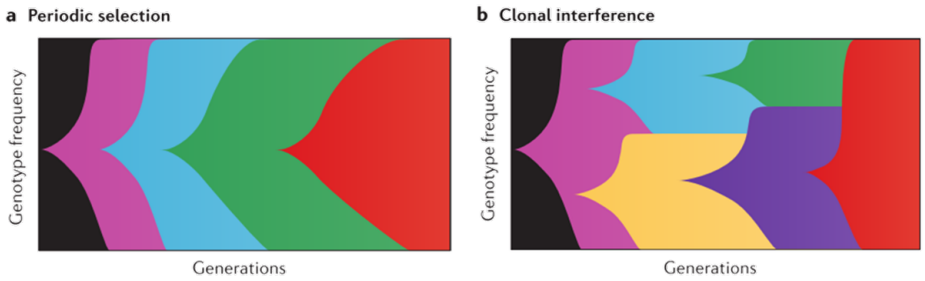

Figure 2.1: Dynamics during experimental evolution. Evolutionary trajectories are commonly represented in Muller plots, which show the frequency of different genotypes over time. a) In the case of periodic selection, one mutation sweeps at a time, resulting in a step-like trajectory. As the rate of fitness increase generally slows down due to diminishing-return epistasis, successive sweeps gradually take longer. b) Clonal interference occurs when beneficial mutations emerge at a high rate, resulting in competition between alternative mutations which slows down genetic fixation (adapted from [18]).

2.1.3 Experimental setup

Batch culture

Bacterial populations are often grown and evolved in a closed batch system. After a lag period of adaptation to the new environment, cells start to grow exponentially. As nutrients become exhausted and waste products accumulate, growth slows down and eventually ceases upon reaching stationary phase. A fraction of the maximal density population is then inoculated into fresh medium during serial transfer. Selection pressure can drive evolution towards some interesting phenotype. However, transfer of a small fraction of the genetic variation generates a population bottleneck, resulting in the loss of some beneficial mutations. Indeed, bottlenecks imposed in serial transfer experiments significantly reduce the probability that a beneficial mutation reaches fixation and can slow down adaptive evolutionary dynamics [228].

Continuous culture

In some experiments, it is desirable to keep the cell physiology and environmental conditions fixed. In these cases, bacteria can be grown in a continuous culture system, most commonly a chemostat. The continuous addition of fresh medium and outflow of waste products and cells result in steady-state growth under stable environmental conditions, subject to experimental control (see also paragraph 6.11.2). In a nutrient-limited chemostat, the concentration of a particular limiting resource determines the maximal cell density. At steady-state, cells grow at a rate that is equal to the dilution rate, thereby enabling precise experimental control [87].

A potential problem associated with growth in a chemostat is the selection of 'sticky mutations',

generating cells attaching to the wall of the vessel. This wall growth can create a subpopulation of cells that experience other environmental conditions and that can again migrate into the liquid. In most cases however, wall growth does not cause major problems [52].

2.2 Experimental evolution under antibiotic stress

As summarized in paragraph 2.1, experimental evolution provides important insights in fundamental evolutionary processes. On the other hand, experimental evolution is also emerging as an important tool to unravel the genetic basis of complex phenotypes such as antibiotic resistance, phenotypic tolerance, multicellular behavior, etc. [88, 187, 221]. As these complex phenotypes often result from interactions between multiple genes and regulation by redundant genetic mechanisms, they are challenging to study with classical experimental methods. This paragraph focuses on the use of experimental evolution to investigate the emergence of bacterial survival strategies in the face of antibiotics.

2.2.1 Evolution of antibiotic resistance

Given its clinical importance, a thorough understanding of resistance evolution is required for the optimization of antibiotic dosage and treatment period. Decisions on therapeutical strategies often rely on *in vitro* studies considering only short periods of bacterial growth. However, these studies might not adequately predict therapy outcome as they do not capture resistance evolution. After all, the acquisition of resistance is often a multistep process and antibiotic therapies usually last several days to months. In this light, experimental evolution serves as an appropriate tool to track down the genetic adaptation of bacterial populations facing antibiotics [88].

Homogeneous environments

Dependent on the subject under study, evolution under antibiotic stress can be monitored using different experimental set-ups. Serial transfer of cultures in a batch system containing a fixed antibiotic concentration provides constant environmental conditions. In this way, Lázár *et al.* [120] propagated *E. coli* cultures in a batch system with fixed concentrations of different antibiotics and tracked the susceptibility patterns of the evolved strains. They noticed a significant increase in resistance levels towards all antibiotics.

Heterogeneous environments

Given the heterogeneity in space and time of biological environments, the relevance of studying resistance evolution in homogeneous environments can be limited. Moreover, once a resistance-conferring mutation becomes fixed in the population, the selection pressure exerted by the antibiotic drops and further adaptation is slowed down. In a microfluidics approach, Zhang *et al.* [246] mimicked spatial heterogeneity of biological environments. Connections between populations growing under different degrees of stress allowed migration between the populations and accelerated the emergence of resistance.

In order to overcome the decreasing selection pressure associated with fixed antibiotic concentrations, Lázár *et al.* [120] performed serial transfer experiments with gradually increasing antibiotic concentrations. Comparable experiments were executed by Oz *et al.* [172], who reported a similar increase of resistance levels over time. Increasing the antibiotic concentration in order to keep the selection pressure constant is however not restricted to batch systems. Lee *et al.* [121] evolved *E. coli* in a chemostat, imposing gradually increasing antibiotic concentrations based on the minimum inhibitory concentration (MIC; see also paragraph 2.2.3) of the population. They noticed the emergence of highly resistant mutants producing indole in order to stimulate more susceptible cells to protect themselves. Using a more sophisticated approach, Toprak *et al.* [215] developed the morbidostat, a continuous culture device that allows to monitor gradual evolution of antibiotic resistance. As the population becomes more drug-resistant, the antibiotic concentration is gradually increased in order to keep the growth rate fixed. Tuning the drug concentration to growth using feedback regulation gives an indication of the rate of evolutionary adaptation. The same researchers used the morbidostat to evolve *E. coli* under a constant selection pressure of either chloramphenicol, doxycycline, or trimethoprim, which resulted in a dramatic increase of resistance levels [214].

Cross-resistance and hypersensitivity

In addition to resistance emerging in the presence of a single antibiotic, interactions between different resistance mechanisms are another matter of concern. Some mutations can confer resistance to more than one drug, a phenomenon called cross-resistance. Oz *et al.* [172] observed high levels of cross-resistance under strong selection regimens with a single drug. On the other hand, resistance against a certain drug can enhance sensitivity to other drugs. This so-called collateral sensitivity gives rise to a trade-off which is especially prominent in the case of aminoglycoside resistance [120, 172, 173].

2.2.2 Evolution of antibiotic tolerance and persistence

Clearly, the permanent presence of antibiotic stress strongly selects for resistant mutants which are able to grow under these conditions. However, in fluctuating environments with alternating periods of antibiotic stress, other evolutionary dynamics can occur. Under such conditions, resistance does not always come out as the most successful strategy, as a consequence of the fitness cost associated with the maintenance of resistance mechanisms [8]. The lower the frequency of antibiotic exposures, the higher this fitness cost. Furthermore, when resistance requires an adaptive response (i.e. induction of a resistance mechanism), the response can be too slow to cope with sudden, high antibiotic concentrations [115]. When evolving a wild type strain under such conditions, resistant mutants should instantaneously exhibit high resistance levels. High-level resistance usually emerges in a stepwise fashion by accumulation of multiple mutations. As such, these conditions only allow growth of pre-existing, highly resistant mutants and exclude *de novo* mutants. The experimental results discussed below indicate how more appropriate survival strategies, involving phenotypic tolerance, have recently been shown to flourish under such environmental conditions.

Experimental evolution of *E. coli* intermittently treated with ampicillin resulted in a lengthening of the lag time, matching the duration of antibiotic exposure [61]. Evolved strains displayed increased survival upon antibiotic challenge while their MIC was unaffected. As ampicillin targets actively dividing cells, dilution of stationary phase cultures into ampicillin-containing, fresh medium specifically favored cells in which the first cell division was delayed. This temporal dormancy was introduced as 'tolerance by lag'. Although the evolved population as a whole became tolerant due to an extended mean lag time, an increased variance of the single-cell lag time distribution was also observed.

Experimental evolution of phenotypic tolerance was also performed by Van den Bergh *et al.* [221], who observed the early emergence of strains with strongly elevated persister levels when *E. coli* cultures were treated daily with aminoglycosides. Importantly, the obtained persister levels were found to correlate with the treatment frequency, according to models of bet-hedging and persistence [66, 114, 175] (see also paragraph 4.2.2). Despite similarities with the experimental approach of Fridman *et al.* [61], important differences are the timing of antibiotic treatment (stationary phase) and the use of antibiotics that also target normal, non-growing cells. These results provide experimental evidence for persistence as a highly evolvable trait, confirm that persistence can be considered as a bet-hedging strategy, and support theoretical models considering long-term fitness of persistence.

In a similar approach, Mechler *et al.* [152] repeatedly treated *S. aureus* stationary phase cultures with daptomycin, alternated with periods of growth under antibiotic-free conditions. They de-

tected a dramatic increase of drug tolerance after 6 treatment cycles, which confirms the results of Van den Bergh *et al.* [221] and justifies their extrapolation to other species and antibiotics.

2.2.3 Evolution in PK/PD models and *in vivo*

Pharmacokinetics and pharmacodynamics

The *in vivo* response of bacteria to antibiotic therapy largely depends on pharmacokinetic (PK) as well as pharmacodynamic (PD) parameters. Pharmacokinetics describe how the antibiotic concentration varies as a function of time, defined in the context of a living organism. After administration, drugs are characterized by a certain absorption, distribution, and elimination profile [211]. Chemical or enzymatic degradation as well as excretion processes are factors that limit the *in vivo* half-life of antibiotics.

In addition, bacterial behavior in the presence of a certain antibiotic concentration can differ considerably between strains. The functional relationship between the antibiotic concentration and the growth characteristics of a particular strain is contained in pharmacodynamic parameters [188]. The best known and most frequently used parameter is the minimum inhibitory concentration (MIC), which is defined as the lowest antibiotic concentration entirely inhibiting growth [10]. Another measure for the effectiveness of a bactericidal antibiotic is the minimum bactericidal concentration (MBC), indicating the minimal concentration able to kill the bacterial strain. As concentrations above the MIC inhibit growth of normal cells, the MIC defines the lower limit of the so-called mutant selection window (MSW). In this concentration range, with an upper limit defined by the mutant prevention concentration (MPC), selection for drug-resistant mutants is likely to take place [49] (Figure 2.2).

The pharmacodynamic function

In addition to the MIC, which is typically used as the only guide in the optimization of antibiotic treatment regimens, Regoes *et al.* [188] advocate the use of three other pharmacodynamic parameters to measure the antibiotic susceptibility of bacteria. These parameters are contained in the pharmacodynamic function, a Hill function describing the relationship between the bacterial growth rate ψ and the antibiotic concentration a. This model can be formulated as:

$$\psi(a) = \psi_{max} - \frac{(\psi_{max} - \psi_{min})(\frac{a}{MIC})^{\kappa}}{(\frac{a}{MIC})^{\kappa} - \frac{\psi_{min}}{\psi_{max}}} \tag{2.1}$$

In Eq. 2.1, ψ_{max} represents the bacterial growth rate in the absence of antibiotics, whereas ψ_{min} is the minimum growth rate in the presence of high antibiotic concentrations. Given the fact that ψ_{min} mostly has a negative value, it actually represents a killing rate. κ is called the Hill coefficient, serving as a measure of the steepness of the curve (Figure 2.2). Knowledge of the pharmacodynamic function, combined with the pharmacokinetics, plays a crucial role in the design of antimicrobial therapies [188].

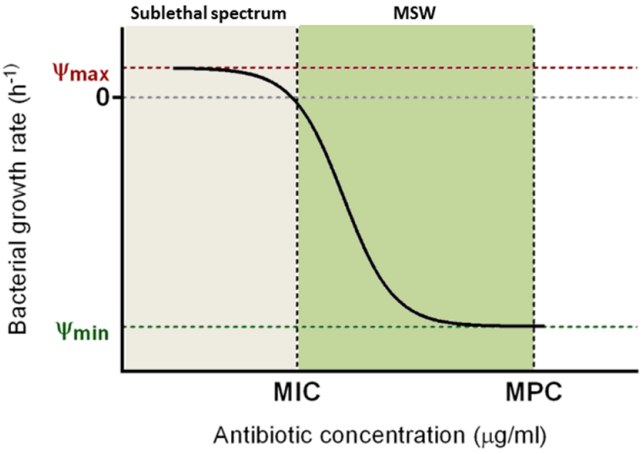

Figure 2.2: Graphical representation of the pharmacodynamic function, defined by Regoes *et al.* [188] and describing the relationship between the antibiotic concentration and the bacterial growth rate. The model contains four pharmacodynamic parameters: the maximum growth rate in the absence of antibiotics (ψ_{max}), the minimum growth rate at high antibiotic concentrations (ψ_{min}), the minimum inhibitory concentration (MIC), and the Hill coefficient (κ), which is a measure of the steepness of the sigmoid curve. The mutant selection window (MSW), defined by the MIC and the mutant prevention concentration (MPC), represents a range of concentrations that favour resistant mutants.

Experimental evolution in PK/PD models

As mentioned earlier, environments characterized by intermittent, high antibiotic doses apparently do not select for *de novo* resistance mutations. In the context of infections though, the antibiotic concentrations to which bacteria are exposed depend on the pharmacokinetic properties of the drug. The approximately exponential decay of antibiotics observed *in vivo* can be simulated *in vitro* in a continuous culture, with the periodic addition of a bolus of the drug. Such *in vitro* models have been used extensively to predict the pharmacodynamic effects of antibiotics, providing useful information for therapeutic design.

Using a simple PK/PD model, Louie *et al.* [141] demonstrated that the conditions described above can select for antibiotic resistance. By simulating realistic pharmacokinetic parameters for levofloxacin and ciprofloxacin treatment of *Streptococcus pneumoniae* infections, they observed

the emergence of resistance after a few days of treatment. Additionally, Tam *et al.* [209] used the ratio of the area under the concentration-time curve over the MIC (AUC/MIC) as a PK/PD index, and demonstrated that the emergence of resistant mutants is characterized by an initial increase, followed by a decline when AUC/MIC is raised.

In vivo experimental evolution

In vitro evolution experiments have proven very useful to study evolutionary adaptation under strictly controlled laboratory conditions. Still, they neglect some essential properties of a human host environment. Probably one of the most important factors interplaying with antibiotics in the clearance of infections is the host's immune system. Despite the fact that some theoretical models advocate the incorporation of the immune response in treatment optimizations [11, 68], few studies actually take it into account. In addition to the immune system, the complex structure of a host environment can strongly influence evolutionary dynamics [244].

Given these disadvantages of *in vitro* model systems, attention should be drawn to the study of evolutionary dynamics in more natural environments. Although still *in vitro*, Wong *et al.* [236] already made one step in this direction by evolving *P. aeruginosa* under growth conditions that mimic the environment of a cystic fibrosis lung. They investigated the genetic basis of fluoroquinolone resistance under these conditions and observed the co-occurrence of resistance mutations with compensatory mutations reducing the cost of resistance.

The *in vivo* counterpart of this experiment was conducted by Yang *et al.* [244], who followed the evolutionary dynamics of *P. aeruginosa* adapting to the host environment of cystic fibrosis patients and observed that diversification was more limited than predicted from *in vitro* experiments. Furthermore, sampling of longitudinal clinical isolates of cystic fibrosis patients led to the discovery of increasing persister levels during the course of infection [161]. The prolonged infection term in cystic fibrosis patients was also exploited by Lieberman *et al.* [133], who tracked the *in vivo* evolutionary adaptation of *Burkholderia dolosa* to its human host and identified genes important for its pathogenicity. Recently, Klemm *et al.* [107] reported remarkable within-host evolution of *Salmonella* Enteriditis in an immunocompromised patient. Except for these efforts in human, extensive animal infection models that are appropriate for experimental evolution studies are currently still lacking.

2.3 Effects of antibiotics at sublethal concentrations

2.3.1 Selection of antibiotic resistance

The MSW hypothesis proposed by Drlica [49] suggests that antibiotic concentrations should be higher than he MIC in order to select for resistant mutants, since the growth of susceptible cells is not inhibited at sub-MIC levels. However, according to the pharmacodynamic function (Figure 2.2), bacterial growth behavior in the sub-MIC range is still concentration-dependent. Although often neglected, low antibiotic concentrations can have important effects on the selection of resistant mutants [9]. Experimental studies including competition experiments demonstrate that the minimal selective concentration (MSC) can be significantly lower than the MIC [75, 135].

In addition to the enrichment of pre-existing mutants, sub-MIC antibiotic concentrations can also result in an increased number of *de novo* mutations [75, 92]. The presence of antibiotics can activate bacterial stress responses, of which the SOS response is most frequently reported. The SOS response has known effects on the induction of mutagenesis, recombination, and horizontal gene transfer, all of which are important contributors to the emergence of resistance [21, 76, 80, 109, 139]. Since susceptible cells are still able to grow at sub-MIC concentrations, the fitness cost of resistance-conferring mutations should be small enough in order to outcompete the wild type strain. These low-cost mutations usually have small effects, but they can prepare the genetic background for higher impact mutations. Furthermore, the obligatory low cost of these mutations can contribute to the limited reversibility of antibiotic resistance [8].

2.3.2 Induction of persistence

The importance of stress responses in persister formation was already discussed in paragraph 1.3.4. As antibiotics at sublethal concentrations trigger these stress responses, their presence can significantly affect persister levels. Indeed, *E. coli* cultures pretreated with sub-MIC concentrations of fluoroquinolones showed dramatically increased persister levels, underlining the importance of sublethal concentrations in the survival of bacterial populations [46]. Johnson and Levin [91] observed the same effects when pretreating *S. aureus* with gentamicin, vancomycin, and oxacillin, and provided a mathematical framework for these experimental observations.

Chapter 3

Persistence and the evolution of resistance

3.1 Persisters: a potential reservoir of resistant mutants

As discussed in more detail in paragraph 1.3, persisters can be considered as a slowly dividing subpopulation of cells that are protected from lethal stresses. In the face of antibiotic treatment, normal cells are killed rapidly, barely leaving time for *de novo* resistance mutations to occur. However, as persisters constitute a protected compartment in the population, they remain viable in the presence of antibiotics and can accumulate mutations. Although the slow division rate of persisters could point at a low mutation frequency, it has been shown that even non-dividing cells accumulate mutations at a substantial rate through mechanisms that do not rely on DNA replication [106, 138] (see also paragraph 3.2.2). Hence, the refractory subpopulation of persisters can act as a reservoir of resistant mutants. This hypothesis was considered by Levin and Rozen [126] by means of a theoretical model of a continuous culture. Their model suggests an acceleration of resistance evolution when persisters are present.

3.2 Stress responses in persisters can accelerate adaptive evolution

In theory, the presence of a refractory subpopulation is sufficient to promote the emergence of resistance. However, as the maintenance of the persister state seems to depend on stress responses, Cohen *et al.* [39] postulated that these may strongly accelerate evolution towards resistance. This paragraph further elaborates this potential connection between persistence and resistance, starting with a brief overview of the most important bacterial stress responses, largely based on findings in *E. coli*.

3.2.1 Bacterial stress responses

General stress response

In contrast to most stress responses which are rather specific, the general stress response leads to a global transcriptional reprogramming of the cell, resulting in tolerance towards several stresses. The general stress response is controlled by the sigma factor RpoS or σ^S. The vast set of genes under direct or indirect control of RpoS (approximately 10 % of all genes in *E. coli*) explains the global and drastic effects on cell physiology [232]. Several unfavorable growth conditions can trigger the general stress response, including starvation, stationary phase, DNA damage, heat or cold stress, pH stress, energy limitation, high osmolarity, oxidative stress, etc. [19]. Independent of the stress that activates it, the outcome of the general stress response is a global adaptation of the cell to several stressful environments, as well as to stationary phase conditions. This general cross-protection and metabolic downregulation is the result of several morphological, transcriptional, and metabolic adaptations [19]. Examples include a smaller and spherical cell shape, the repression of aerobic metabolism, and the production of ribosome modulating factor (RMF) [164].

Similar to other sigma factors, *rpoS* expression is regulated at multiple levels to avoid an increase of the cellular RpoS concentration under favorable growth conditions [119]. Transcription of *rpoS* can occur from the promoter of *nlpD*, a gene located upstream of *rpoS*, or from the *rpoS* promoter itself [19]. Increased *rpoS* transcription is observed during entry into stationary phase, which is positively regulated by (p)ppGpp, among others [51]. The response regulator ArcA of the two-component ArcB/ArcA system, which is sensitive to the cellular energy status, is an example of a negative regulator of *rpoS* transcription [157]. Although (p)ppGpp also seems to play a role [81], translational control of RpoS is largely dependent on small RNAs (sRNAs) induced by several types of stress conditions. Binding of sRNAs to the 5' untranslated region (5' UTR) of *rpoS* mRNA exposes its ribosome binding site, thereby inducing translation [28]. RpoS is a highly unstable protein in exponential phase, due to rapid degradation by ClpXP protease in cooperation with the adaptor protein RssB [22, 197]. A more exhaustive overview of the regulation mechanisms of RpoS is provided by Battesti *et al.* [19].

Stringent response

The stringent response is activated by amino acid starvation and other kinds of nutrient limitation. The result is an adaptation of the cell to nutrient-limited growth conditions, mainly through the reduction of RNA and protein synthesis. The main effector molecule of the stringent response, (p)ppGpp, induces dissociation of the unstable RNA polymerase-promoter open complex

of ribosomal RNA (rRNA) genes and ribosomal proteins [183]. (p)ppGpp-synthesis is RelA- and SpoT-dependent. RelA is a (p)ppGpp synthethase associated with the ribosomal A-site. It is activated in the presence of uncharged tRNAs at the ribosomes, as a consequence of amino acid starvation [38]. SpoT is both able to synthesize (p)ppGpp in response to other kinds of nutrient limitation and to hydrolyze (p)ppGpp in the absence of amino acid starvation [241]. Increased levels of (p)ppGpp cause a global shutdown of macromolecular synthesis processes such as the production rRNA and tRNA, DNA, lipids, and ribosomal proteins (Figure 3.1). Furthermore, amino acid supplies are replenished through amino acid biosynthesis and proteolysis [144]. As mentioned above, (p)ppGpp is an important transcriptional and translational activator of RpoS expression, establishing a link between starvation and the activation of the general stress response.

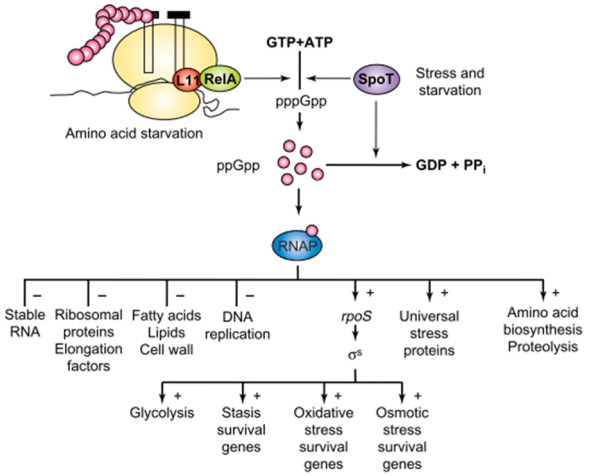

Figure 3.1: Schematic overview of the activation and effects of the stringent response. The synthesis of (p)ppGpp is controlled by RelA, in response to amino acid starvation, and SpoT, in response to other types of stress and nutrient limitation. (p)ppGpp binds to RNA polymerase (RNAP), inducing transcription of stress resistance and starvation survival genes (adapted from [144]).

SOS response

The presence of DNA damage, arisen spontaneously or induced by genotoxic stress, can be catastrophic for the normal functioning of a bacterial cell. Under these circumstances, the SOS response acts as a life-saver by organizing DNA repair. Since some of the mechanisms activated by the SOS response are intrinsically mutagenic, SOS genes are under tight control of the LexA repressor. LexA binds as a dimer to cognate LexA box sequences in SOS gene promoters and prevents their induction under normal growth conditions [29] (Figure 3.2). The presence of single-stranded DNA (ssDNA) warns the cell for DNA damage. The subsequent recruitment of RecA to this ssDNA results in the formation of nucleoprotein filaments which induce autocleavage of the LexA repressor and expression of SOS genes [29] (Figure 3.2). Generally, the induction of the SOS response leads

to the activation of repair systems such as homologous recombination, nucleotide excision repair, and translaesion synthesis [14]. Homologous recombination usually results in an error-free repair of ssDNA lesions or double-stranded breaks (DSB). Recombination proteins such as RecFOR and RecBCD generate ssDNA recognized by RecA and rely on the sequence of the sister chromosome to carry out error-free repair [14]. Damaged or mismatching nucleotides can be replaced through the nucleotide excision repair mechanism based on the UvrABC endonuclease and UvrD helicase.

Only after a sufficiently long induction of the SOS response, translaesion synthesis is activated as a last resort to repair the damage that still remains [155]. This mutagenic DNA repair is performed by error-prone polymerases such as PolV, PolII, and PolIV, encoded by *umuCD*, *polB*, and *dinB* respectively. RecA-ssDNA nucleoprotein filaments cleave UmuD to generate UmuD', which constitutes the active PolV complex UmuD'$_2$C. The incorporation of nucleotides by these polymerases is not guided by base paring, nor corrected with proofreading activity. In addition to the repair of DNA damage, the mutagenic effects of the SOS response can be considered as an additional adaptive response to stress conditions (Figure 3.2). A higher mutability increases the chances of beneficial mutations and can play a major role in survival and adaptation to changing environments [14, 151].

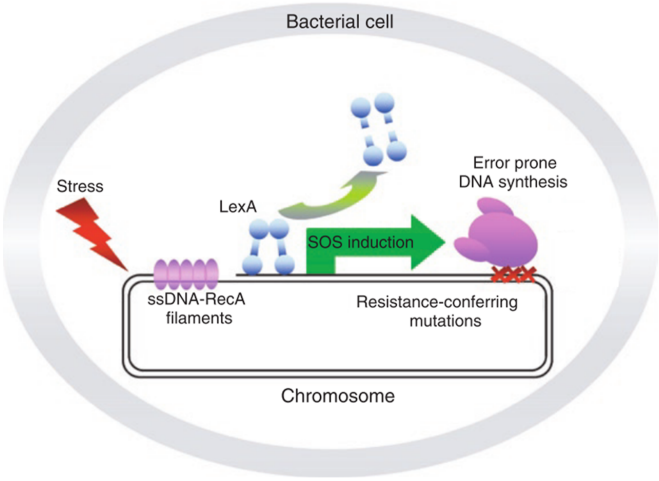

Figure 3.2: Schematic overview of the activation and effects of the SOS response. In the absence of DNA damage, the LexA repressor binds to the promoter of SOS genes, thereby preventing their transcription. Upon DNA damage, RecA nucleoprotein filaments are formed and activate autocleavage of LexA, enabling transcription of SOS genes. Derepression of error-prone polymerases through this mechanism can cause adaptive mutagenesis, which confers resistance towards the stress (adapted from [202]).

Oxidative stress response

While oxygen is by far the most efficient electron acceptor in terms of energy, the oxidative stress intrinsically associated with aerobic respiration provides a major challenge to cellular systems.

The harmful ROS generated as a byproduct from oxygen reduction as well as from exogenous sources need to be eliminated properly in order to prevent cellular damage. Two major oxidative stress regulons, the *soxRS* and *oxyR* regulons, have been unraveled in *E. coli* [180].

The *soxRS* regulon is mainly concerned with superoxide radicals ($O_2^{-\cdot}$) and is induced by SoxR, which acts as a redox sensor and activates transcription of the downstream regulator SoxS (Figure 3.3). The SoxR protein is produced continuously and functions as a homodimer containing two [2Fe-2S] clusters that sense oxidative stress. Oxidation of the iron-sulfur clusters in SoxR by superoxide radicals or other oxidizing agents renders it active, resulting in the induction of the *soxS* promoter. SoxS, in turn, regulates the expression of various genes important in the protection against oxidative stress. An example is the superoxide dismutase gene *sodA*, the product of which plays a role in the conversion of $O_2^{-\cdot}$ to hydrogen peroxide (H_2O_2) [33, 63].

Similar to SoxR, OxyR functions as a redox sensor (Figure 3.3). However, since the reversible formation of disulfide bonds now underlies the sensing mechanism, OxyR mainly initiates the response to H_2O_2. In its oxidized, active state, OxyR regulates the expression of various genes, including *katG* (catalase), *ahp* (alkylhydroxyperoxide reductase), and *dps* (iron sequestration protein) [6, 63].

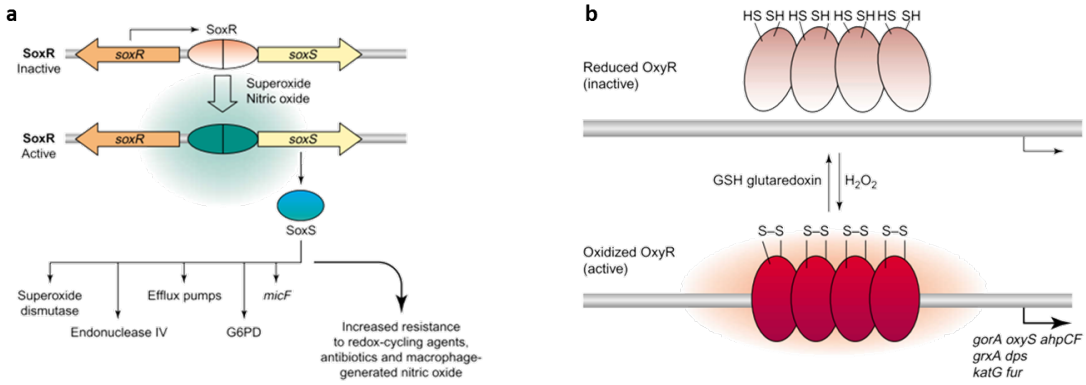

Figure 3.3: Schematic overview of the activation and effects of the oxidative stress response. a) The *soxRS* locus encodes the continuously produced SoxR protein, which is activated in the presence of superoxide-generating agents or nitric oxide and induces transcription of *soxS*. SoxS regulates transcription of various stress resistance genes. b) The *oxyR* regulon is activated upon oxidation of OxyR by hydrogen peroxide (H_2O_2). Oxidized OxyR regulates transcription of genes with antioxidant functions (adapted from [180]).

Extracytoplasmic stress response

Changes in the extracellular environment are initially sensed at the cellular envelope. Stressful conditions can cause envelope perturbations, warning the cell of the changing environment. Furthermore, since many crucial physiological processes occur at the envelope, an appropriate

response to extracytoplasmic stress is required in order to maintain its functionalities. Of the multiple envelope stress response pathways found in bacteria, the σ^E-dependent pathway is the best studied and most important one (Figure 3.4). The activity of this sigma factor, encoded by *rpoE*, is induced by misfolded outer membrane proteins (OMPs) in a proteolytic cascade involving RseB, RseA, and DegS [3, 102].

In the absence of stress, the activity of σ^E is inhibited by tight interaction with the inner membrane protein RseA, which serves as an anti-sigma factor [102]. Misfolding of OMPs exposes a C-terminal motif that is recognized by the protease DegS, which targets RseA [230]. However, DegS-mediated RseA degradation is prevented by binding of RseB with RseA. The accumulation of lipopolysaccharide (LPS) in the periplasm attracts RseB, thereby dissociating from RseA and resulting in the cleavage of RseA. RseA is further cleaved in its transmembrane region by the protease RseP and degraded completely by ClpXP [4, 102]. The resulting release of σ^E generally influences transcription of genes involved in the synthesis and assembly of OMPs and LPS and the degradation of misfolded OMPs [190]. In addition, σ^E seems to play a species-specific role in bacterial pathogenicity [195].

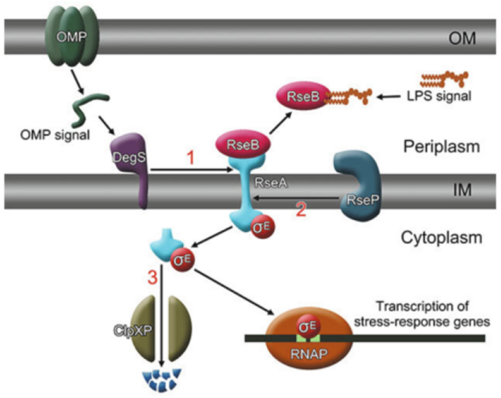

Figure 3.4: Schematic overview of the activation and effects of the extracytoplasmic stress response. The activity of the sigma factor σ^E is inhibited by tight interaction with the inner membrane protein RseA. Binding of OMPs activates DegS, while RseB is relieved from RseA by LPS. RseA is sequentially digested by DegS, RseP, and ClpXP, resulting in the release of σ^E in the cytoplasm (adapted from [102]).

3.2.2 The role of stress responses in adaptive evolution

The contribution of elevated stress responses to the maintenance of the persister state was already discussed in paragraph 1.3.4. Especially, the role of the stringent response and the SOS response has recently been verified experimentally [46, 145]. The same stress responses have been associated with a higher adaptive potential by promoting mutagenesis. The general outcome of these stress-induced mutations is an increased genetic diversity and accelerated evolution when the population

is maladapted to the current environment.

Ponder *et al.* [181] demonstrated that PolIV-mediated error-prone repair of DSBs is dependent on the general stress response mediator RpoS. Furthermore, RpoE was also shown to be involved in this type of DNA repair, suggesting a role for extracytoplasmic stressors in stress-induced mutagenesis [72]. Through the investigation of copy number variants emerging under starvation stress, Lin *et al.* [134] observed chromosomal structural changes associated with amplification events, which were dependent on RpoS as well as RpoE. As mentioned in paragraph 3.2.1, the mutagenic effects of the SOS response can also strongly contribute to the increased evolvability observed under stressful conditions [151]. Additionally, the SOS response promotes the spread of resistance genes on mobile genetic elements via horizontal gene transfer [21].

Based on these observations, Rosenberg *et al.* [193] proposed a general model for DSB-dependent stress-induced mutagenesis, as a result of three simultaneous events: the formation and repair of DSBs, induction of the SOS response, and a second stress that induces RpoS. DSBs can be generated by DNA damaging agents, but spontaneous DNA breaks have also been shown to occur frequently [178]. The repair of these DSBs by homologous recombination is a frequent cause of SOS response induction. Under the control of both the SOS response and RpoS, the repair of DSBs is switched from a high-fidelity to a mutagenic process through the activation of error-prone polymerases. The result is an accumulation of replication errors that are fixed as mutations (Figure 3.5).

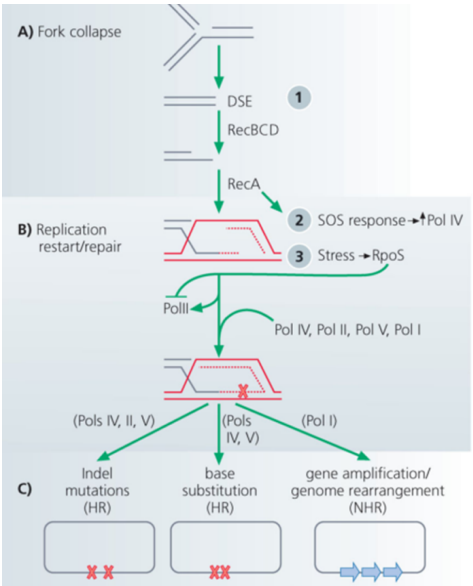

Figure 3.5: A general model of DSB-dependent stress-induced mutagenesis. A) a double-stranded end (DSE) or DSB can be generated spontaneously by replication fork collapse. B) Repair of the resulting break by homologous recombination involves RecBCD and RecA, and can potentially induce the SOS response. Together with the SOS response, the induction of RpoS by a second stress activates error-prone polymerases that generate mutations (C) (adapted from [193]).

3.3 Persistence and resistance: overlapping mechanisms?

Although the population heterogeneity associated with persistence is purely phenotypic, the persister fraction of a strain is a genetically determined trait. A number of genetic mutations affecting persister levels have already been reported. Examples of mutated genes that result in increased persister levels are *hipA* [160], *nuoN*, *gadC*, and *oppB* [221]. In addition to their effects on persister levels, mutations in genes of the *nuo* and *opp* operons have also been found in resistant mutants [1, 120, 191], suggesting that phenotypic persister variants and resistant mutants rely on similar tactics to avoid antibiotic action. Therefore, it could be speculated that the evolutionary pathway towards resistance is easier to take for a high persistence mutant.

Other experimental results also indicate that persistance and resistance are not totally independent. For example, cross-talk between fosfomycin resistance and ofloxacin persistence has already been observed. Overexpression of *fosA* or a mutation in *glpT*, both conferring resistance to fosfomycin, reduces the number of persisters after ofloxacin treatment [44]. Furthermore, bacterial efflux pumps, which are known as important mediators of antibiotic resistance [131], have been shown to play a role in persistence in mycobacteria [2]. More generally, some studies have found that strains showing high antibiotic resistance also tend to be highly tolerant [136] or exhibit high persister levels [226].

Chapter 4

Mathematical modelling of persistence

As the complexity of biological systems often reaches beyond intuition, mathematical modelling can have an important added value in their study. Providing a quantitative description of the interactions between different variables, mathematics can be a useful language to reveal elements that are not obvious in a purely qualitative approach. The most important benefits offered by mathematical models are their predictive power, generating new and testable hypotheses, and their ability to guide the experimental setup.

Mathematical modelling has become an important tool in the study of bacterial persistence, as demonstrated by the various modelling papers published in the field. Two types of models have already proven their value. Mechanistic models focus on genetic modules and their regulation, aiming to provide a mechanistic explanation of persister formation and resuscitation. On the other hand, population models are used to predict the dynamics of persistence at the population level.

4.1 Mechanistic models

Over the last decade, persistence mechanisms have become a popular subject of mathematical modelling papers. The central role for type II TA modules in the generation of persisters (see also paragraph 1.3.4.) has been translated into a myriad of mechanistic models, focusing on the regulatory dynamics of these genetic elements and their ability to induce persistence.

Lou *et al.* [140] outlined a simple deterministic model of the regulation of the *hipBA* module. Apart from negative autoregulation through DNA binding of both free antitoxin and toxin-antitoxin complexes, they considered dilution of the toxin through cell division, and growth rate modulation. Growth rate modulation refers to the inhibitory effect of the toxin on cellular growth and is required to explain persister formation. Their system only shows potential for bistability

when the cooperative binding of free antitoxins as well as of toxin-antitoxin complexes to operator sequences is taken into account, suggesting an essential role for this cooperativity in phenotypic heterogeneity. Furthermore, the model provides a theoretical explanation for the strongly elevated persister levels observed in stationary phase as compared to early exponential phase [100].

Further extending the model of cooperativity [140], Cataudella *et al.* [32] pinpointed the possible contribution of conditional cooperativity to the bistability associated with persistence. Conditional cooperativity refers to the dependence of transcriptional autoregulation on the toxin concentration (Figure 4.1). Free antitoxin only serves as a weak transcriptional repressor, whereas toxin-antitoxin complexes with intermediate toxin-antitoxin ratios strongly repress transcription of the TA module. Further increasing the toxin concentration above a certain threshold results in the formation of toxin-antitoxin complexes with a high stoichiometric ratio, which have a low repressor activity and thereby enable transcription. Consequently, the low translation rate in persisters favors a high toxin-antitoxin ratio because of the unstability of the antitoxin, resulting in a high transcription level of TA modules in persisters [69]. When the antitoxin degradation rate lowers, the toxin-antitoxin ratio decreases. According to the model of conditional cooperativity, this leads to transcriptional repression of TA modules and lower toxin activity, both resulting in the resuscitation of a persister cell [69].

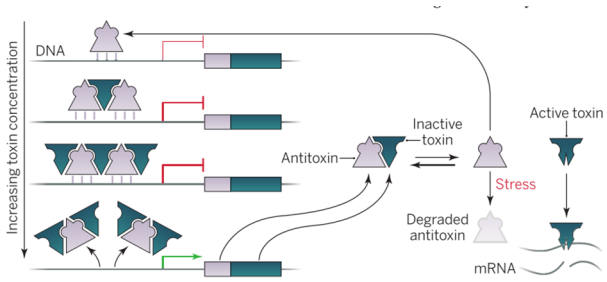

Figure 4.1: Conditional cooperativiy in toxin-antitoxin (TA) modules. The transcriptional autoregulation of TA modules depends on the toxin concentration. Free antitoxin serves as a weak transcriptional repressor, whereas complexes with intermediate toxin-antitoxin ratios strongly repress transcription. When the toxin concentration exceeds a certain threshold, transcription is enabled due to dissociation of the toxin-antitoxin complexes from the DNA. In the absence of stress, the antitoxin sequesters the toxin and counteracts its function. The antitoxin is prone to degradation by proteases, which are upregulated under stress conditions and can induce a dormant persister state (adapted from [83]).

The model of Lou *et al.* [140] also inspired Feng *et al.* [58] to build a more realistic model incorporating new insights into the organization of the *hipBA* module. In biological systems, transcription and translation are inherently associated with noise, which can play an important role in the expression dynamics of TA modules. A stochastic model, as built by Feng *et al.* [58] using the Gillespie algorithm [242], incorporates this noise and can lead to a drastic improvement of genetic models. By taking into account growth rate modulation but excluding conditional cooperativity, their model indicates the importance of the growth rate in persister bistability.

The stochastic model of Rotem *et al.* [194] predicts that cells become persisters when their toxin level exceeds a particular threshold, with the duration of growth arrest being dependent on the toxin level relative to the threshold. This hypothesis is further supported by the model of Koh and Dunlop [108]. The observation that multiple TA modules can cooperate to induce switching, was considered in a mathematical model of Fasani and Savageau [56]. Their model suggests that multiple TA modules can be coupled to create bistability and predicts a correlation between persister fractions and the number of TA modules.

The concepts described above (negative transcriptional autoregulation, conditional cooperativity, and growth rate modulation) are summarized mathematically in Eq. 4.1 [156].

$$\begin{cases} \dfrac{dA(t)}{dt} = \dfrac{\rho_A}{1+\frac{AT(t)^n}{K^n}}\gamma_T - \alpha_C A(t)T(t) + \theta_C AT(t) - d_A A(t) + \eta(t) \\ \dfrac{dT(t)}{dt} = \dfrac{\rho_T}{1+\frac{AT(t)^n}{K^n}}\gamma_T - \alpha_C A(t)T(t) + \theta_C AT(t) - \alpha_C AT(t)T(t) \\ \qquad\qquad + \theta_C TAT(t) - d_T\gamma_T T(t) + \eta(t) \\ \dfrac{dAT(t)}{dt} = \alpha_C A(t)T(t) - \theta_C AT(t) - d_{AT}\gamma_T AT(t) + \theta_C TAT(t) - \alpha_C AT(t)T(t) \\ \dfrac{dTAT(t)}{dt} = \alpha_C A(t)T(t) - \theta_C TAT(t) - d_{TAT}\gamma_T TAT(t) \end{cases} \tag{4.1}$$

In the differential equation system of Eq. 4.1, toxin and antitoxin are represented by T and A respectively, while AT and TAT denote toxin-antitoxin complexes with intermediate and high ratios respectively. ρ_A and ρ_T represent average rates of formation by transcription and translation, while dA, dT, dAT, and $dTAT$ are the average degradation rates. α_c, the rate of AT complex formation, and θ_c, the rate of complex dissociation, provide a means to take into account toxin sequestration by antitoxin. Negative transcriptional autoregulation is considered by multiplication of the formation rates with $\frac{1}{1+\frac{AT(t)^n}{K^n}}$ ($K = \theta_c/\alpha_c$). Conditional cooperativity is taken into account through the formation of a TAT complex, which is unable to repress transcription. Consequently, the concentration of the TAT complex does not influence the formation rates of both A and T, as does the concentration of the AT complex. Growth rate modulation can be formulated mathematically by introducing a modulation factor γ_T. This factor describes the negative, threshold-based effect of the toxin on the growth rate, and consequently on the rates of transcription and translation. $\eta(t)$, which is called a Langevin noise term, introduces stochastic effects as random, Gaussian noise. A more detailed description of the general model described in Eq. 4.1 is given by Vandervelde *et al.* [156].

4.2 Population models

The models described in the previous paragraph have shed light on the mechanisms that drive a single cell into the persister state. Nevertheless, this persister switch makes more sense when considered in the context of a whole bacterial population. Population models of persistence zoom out from the single-cell level to the population level, aiming to describe and understand the population dynamics associated with persistence. Their predictive power can be exploited to gain insight into the evolutionary and ecological implications of persistence and to predict the behavior of bacterial populations in the face of different therapeutic strategies.

4.2.1 Population models of phenotypic diversity

Under fixed environmental conditions, the fitness of a bacterial population is maximized when all individuals exhibit the best adapted phenotype. On the other hand, fluctuating environments seem to favor phenotypic diversity in an isogenic population. The evolutionary basis of phenotypic variability and corresponding 'bet-hedging' strategies has been examined through various theoretical models. Lachmann and Jablonka [117] demonstrated that the optimal transition rates between two phenotypes correspond to the environmental periodicity. Similarly, Thattai and Van Oudenaarden [213] built a general model of phenotypic heterogeneity. Their model demonstrates the benefits of a 'dynamically heterogeneous' population in a fluctuating environment and predicts that rates of switching between phenotypes can be evolutionary tuned to environmental changes in order to maximize long-term population fitness. In another model of phenotypic diversity, Kussell and Leibler [115] demonstrated that stochastic switching is favored over environmental sensing in environments that change infrequently.

4.2.2 Population models of persistence

A simple two-state population model of persistence was first introduced by Balaban *et al.* [17], describing the dynamics of both normal cells and persisters with a first-order, linear differential equation (Eq. 4.2).

$$\begin{cases} \frac{dn}{dt} = \mu_n \times n(t) - a \times n(t) + b \times p(t) \\ \frac{dp}{dt} = \mu_p \times p(t) - b \times p(t) + a \times n(t) \end{cases} \tag{4.2}$$

Switching from the normal state n to the persister state p occurs with a switching rate a, while persisters switch back to the normal state with a switching rate b. Growth or mortality rates

of normal cells and persisters are denoted by μ_n and μ_p respectively. When μ_n and μ_p have positive values, this model allows an infinite exponential growth. As this does not correspond to the population dynamics of batch growth, a factor N_{tot}/K for logistic growth can be added, with N_{tot} representing the total population size and K the carrying capacity. Apart from the ability to make theoretical predictions using relevant parameter estimations [114, 175], this model can be used to extract parameter values from experimental data [67, 221].

Kussell *et al.* [114] used the model described by Eq. 4.2 to investigate how switching rates determine long-term fitness of a population in fluctuating environments. They performed both deterministic and stochastic simulations of population dynamics in periodically changing environments, in which periods of growth with a fixed duration t_g are alternated with periods of antibiotic stress with a fixed duration t_s. By assuming that the presence of antibiotics influences the growth rates μ_n and μ_p, but has no short-term effects on the switching rates a and b, they calculated the switching rates that maximize long-term fitness in a specific changing environment. Importantly, they found that the optimal a is approximately inversely proportional to t_g ($a \approx 1/t_g$), while the optimal b is approximately inversely proportional to t_s ($b \approx 1/t_s$). This theoretical prediction indicates that switching rates, rather than growth or killing rates, are subject to evolution and that the frequency of environmental changes, rather than the specific characteristics of one environment, is the major determinant of the optimal switching rates. Furthermore, they suggest that persistence can be explained in the context of bet-hedging strategies, providing the strongest benefits when antibiotic stress is frequent and intense. Together, these results support theoretical predictions derived from previous, more general models concerning phenotypic diversity [117, 213] and were confirmed by recent experimental data and theoretical predictions [221].

A more detailed analysis of the population dynamics of persistence was performed by Patra and Klumpp [175]. Assuming that switching rates are low compared to growth and killing rates, they used the model described by Eq. 4.2 to derive analytical expressions of the persister fraction, switching rates, and other relevant parameters under different environmental conditions. In a periodically switching environment, they essentially derived the same estimation of the optimal switching rates as previous models [114, 117, 213]. However, the assumption that the environment changes infrequently was relaxed, which allowed the derivation of expressions of optimal switching rates for short environmental durations.

The prediction that high persister levels are favored when antibiotic stress occurs more frequently [114], was also inferred by Gardner *et al.* [66]. However, they consider the cost of persistence - a growth deficit - and the benefit of persistence - an increased survival in the face of antibiotic stress - as implications on direct, individual fitness instead of being part of a population level survival strategy. In their perspective, the benefits of persistence at the population level can be

explained more accurately when resource competition is taken into account. Their model predicts that nutritional stress, e.g. in stationary phase, which is associated with a decreased growth rate of normal cells, not only reduces the individual fitness cost of persistence but also increases population benefits of persistence by minimizing resource competition among genetically related individuals.

Despite the importance of mathematical models to gain insight in the mechanisms driving persistence and the evolutionary forces shaping persister levels, experimental validation of these theoretical findings is often lacking. However, experimental data are indispensable to discover limitations of existing models and to guide the development of more accurate models, as was pointed out by Stepanyan *et al.* [206]. Driven by the discrepancy between experimentally observed persister levels and theoretical predictions, they revealed additional costs of persistence that could explain the observed low persister levels. In addition to the direct growth cost of persistence, evolutionary stable persister levels also seem to result from a lengthened lag phase in the absence of antibiotic stress and an increased mortality in stationary phase. Consequently, these two pleiotropic costs of persistence which should be considered for incorporation in future models.

Part II

Materials and methods

Chapter 5

Materials

5.1 Strains

The bacterial strains used in this work are listed in Table 5.1. Additional strains originated from the ECOR collection [170] (ECOR 01, 08, 15, 16, 21, 26, 30, 36, 37, 41, 42, 43, 47, 49, 51, 57, 58, 59, 65, and 70).

Table 5.1: Overview of bacterial strains used in this work

Strain	Genotype	Reference
E. coli		
SX43	Δ(*araD-araB*)567 λ^- *rph-1* Δ*(rhaD-rhaB)*568 *hsdR*514 Δ*lacZ::tsr-venus*	[243]
*oppB**	SX43 *oppB*539 C>A	[221]
*nuoN**	SX43 *nuoN*1204 C>G	[221]
*gadC**	SX43 *gadC*1100 A>G	[221]
BW25113	Δ(*araD-araB*)567 λ^- *rph-1* Δ*(rhaD-rhaB)*568 *hsdR*514 Δ*lacZ4787(::rrnB-3)*	
JW0429	BW25113 Δ*lon*::Km^R	[12]
JW5437	BW25113 Δ*rpoS*::Km^R	[12]
Δ*(relAspoT)*	BW25113 Δ*relA* Δ*spoT*::Spc^R	[159]
MG1655	λ^- *rph-1*	[26]
Δ*10TA*	MG1655 Δ*mazF* Δ*chpB* Δ*relBE* Δ*(dinJ-yafQ)* Δ*(yefM-yoeB)* Δ*higBA* Δ*(prlF-yhaV)* Δ*yafNO* Δ*mqsRA* Δ*hicAB*	[147]
MG21	MG1655 *zde-264*::Tn*10*	[176]
MG1655A7	*zde-264*::Tn*10 hipA7*	[176]
TOP10	*recA1 araD*139 Δ*(ara-leu)*7697 *galU galK rpsL*(Str^R) *endA*1 *nupG*	Invitrogen™

5.2 Plasmids

The plasmids used in this work are listed in Table 5.2.

Table 5.2: Overview of plasmids used in this work

Plasmid	Relevant characteristics	Reference
pUA66	Km^R	[245]
P*relA-gfp*	promoter fusion with *gfpmut2*, Km^R	[245]
P*wrbA-gfp*	promoter fusion with *gfpmut2*, Km^R	[245]
P*osmE-gfp*	promoter fusion with *gfpmut2*, Km^R	[245]
P*recA-gfp*	promoter fusion with *gfpmut2*, Km^R	[245]
P*dinB-gfp*	promoter fusion with *gfpmut2*, Km^R	[245]
P*polB-gfp*	promoter fusion with *gfpmut2*, Km^R	[245]
P*umuCD-gfp*	promoter fusion with *gfpmut2*, Km^R	[245]
P*rpoE-gfp*	promoter fusion with *gfpmut2*, Km^R	[245]
P*rpoS-gfp*	promoter fusion with *gfpmut2*, Km^R	[245]
P*soxS-gfp*	promoter fusion with *gfpmut2*, Km^R	[245]
P*dps-gfp*	promoter fusion with *gfpmut2*, Km^R	[245]
pCP20	FLP recombinase, temperature-sensitive replication, Ap^R, Cm^R	[42]

5.3 Culture media

Liquid cultures were grown in lysogeny broth (LB), Mueller-Hinton broth (MHB), or 2x LB (low salt). Agar was added for solid media. All media were sterilized by autoclaving.

5.4 Medium additives

Medium additives were added after filter sterilization (0.2 μm) to autoclaved, cooled media. All relevant medium additives are listed in Table 5.3.

Table 5.3: Overview of medium additives used in this work

Additive	Abbreviation	Stock concentration	Working concentration[a]	Solvent
Antibiotics				
Amikacin	AMK	50 mg/ml		Distilled water
Ampicillin	AMP	100 mg/ml	100 μg/ml	Distilled water
Carbenicillin	CAR	100 mg/ml		Distilled water
Ceftazidime	CEF	50 mg/ml		Distilled water
Ciprofloxacin	CIP	5 mg/ml		Distilled water[b]
Kanamycin	KAN	50 mg/ml	50 μg/ml	Distilled water
Rifampicin	RIF	50 mg/ml	50 μg/ml	Dimethyl sulfoxide
Tetracycline	TET	10 mg/ml	10 μg/ml	70 % ethanol
Others				
Arabinose	Ara	200 mg/ml	2 mg/ml	Distilled water
Glucose	Glc	200 mg/ml	2 mg/ml	Distilled water
Calcium dichloride	$CaCl_2$	1 M	5 mM	Distilled water
Magnesium sulphate	$MgSO_4$	1 M	10 mM	Distilled water
Sodium citrate		1 M	5-200 mM	Distilled water[c]

[a] For antibiotics, working concentrations used for cloning purposes are given. Otherwise, applied concentrations are indicated elsewhere.

[b] addition of HCl enhances solubility

[c] pH was adjusted to 5.5 with NaOH

5.5 Buffers and mixtures

5.5.1 Polymerase chain reaction (PCR)

PCR was performed with either *Taq* DNA polymerase (New England Biolabs) or Q5 DNA polymerase (New England Biolabs), according to the manufacturer's instructions.

5.5.2 DNA gel electrophoresis

Tris-borate-ethylenediaminetetraacetic acid (EDTA) buffer (TBE) (10x) was prepared with 121 g Tris-base, 102 g boric acid, 6.4 g Na_2EDTA, and 1 l distilled water. Blue juice (5x) consisted of 500 ml glycerol, 37.25 g EDTA, 2 g bromophenol blue, and 30 g sodium dodecyl sulphate (SDS). The resulting mixture was diluted to 1 l with TBE buffer (1x).

5.5.3 Preparation of chemocompetent cells

Two buffers were used for the preparation of chemocompetent cells. Transformation buffer 1 (Tfb 1) consisted of 1.178 g potassium acetate, 4.83 g RbCl, 0.588 g $CaCl_2$, 3.958 g $MnCl_2.4H_2O$, 340 ml distilled water, and 60 ml glycerol. The mixture was adjusted to pH 5.8 with acetic acid (0.2 M) and stored at 4 °C. Transformation buffer 2 (Tfb 2) was prepared with 0.628 g 3-(N-morpholino)propanesulfonic acid (MOPS), 3.708 g $CaCl_2$, 0.362 g RbCl, and 85 ml distilled water.

5.5.4 Flow cytometry

Before sorting, cultures were diluted in phosphate-buffered saline (PBS) (8 g NaCl, 0.2 g KCl, 1.44 g Na_2HPO_4, 0.24 g KH_2PO_4, and 1 l distilled water).

5.6 Commercial kits

An overview of the commercial kits is given in Table 5.4.

Table 5.4: Overview of commercial kits used in this work

Kit	Company	Use
GenElute™ HP Plasmid Miniprep Kit	Sigma-Aldrich	Plasmid isolation
Wizard® SV Gel and PCR Clean-Up System	Promega	DNA extraction from agarose gel

5.7 Primers

All primers used for PCR amplification are listed in Table 5.5. Primers were designed with the Geneious software version 7.1.7 [97] and synthesized by Integrated DNA Technologies (IDT).

Table 5.5: Overview of primers used for PCR amplification

Primer	**Sequence**	**Target**
SPI10943 (forward)	AAATTACCGCCACCGCCATA	*ampC* promoter region
SPI10944 (reverse)	GTGGGTATTCTGCTGCCACT	
SPI11089 (forward)	TGCCAGATGTCCGAGAT	*gyrA* quinolone resistance-
SPI11090 (reverse)	GTATAACGCATTGCCGC	determining region
SPI11091 (forward)	GCCTTTCTTCACTTTGTACAGCG	*gyrB* quinolone resistance-
SPI11092 (reverse)	GTGACGGCGGTACTCACCTG	determining region
SPI11093 (forward)	TATGCGATGTCTGAAC	*parC* quinolone resistance-
SPI11094 (reverse)	GCTCAATAGCAGCTCGGAAT	determining region
SPI11095 (forward)	CTGACCGAAAGCTACGTCAACC	*parE* quinolone resistance-
SPI11096 (reverse)	CGTTCGGCTTGCCTTTCTTG	determining region

Chapter 6

Methods

6.1 Bacterial growth and storage

E. coli strains were grown at 37 °C in liquid LB or MHB medium or plated out on LB agar supplemented with appropriate antibiotics, except when stated otherwise. Liquid cultures were incubated shaking at 200 rpm (revolutions per minute) for sufficient oxygen supply. Oxygen permeable membranes were used for growth in microplates. Colonies on agar plates were stored up to one month at 4 °C. For longer term storage, equal volumes of a liquid overnight culture and 50 % (v/v) glycerol were mixed and frozen at -80 °C.

6.2 Determination of the number of CFU/ml

The number of colony-forming units per ml (CFU/ml) in a culture was determined by plating. Appropriate dilutions were prepared in an isotonic $MgSO_4$ (10 mM) solution and plated out using sterile glass beads or an Eddy Jet spiral plater (iUL Instruments). After overnight or twice overnight incubation, colonies were counted manually or with the Flash&Go automated colony counter (iUL instruments).

6.3 Determination of killing curves

Survival following antibiotic treatment was determined by measuring the number of CFU/ml as a function of treatment duration. A strain was inoculated in 5 ml MHB and grown for 24 hours. 1 ml of this culture was diluted in 100 ml of fresh medium and grown overnight (app. 16 hours). For determination of killing curves in stationary phase, 1 ml of the 100 ml culture was incubated for 8 hours in MHB medium supplemented with a lethal dose of the appropriate antibiotic. For exponential phase experiments, the culture was diluted 1:100 and incubated for 2.5 hours followed by 8 hours of antibiotic treatment. The number of CFU/ml was determined after 0, 0.5, 1, 2, 3, 5, and 8 hours of treatment by washing the samples with $MgSO_4$, plating out the appropriate dilution on LB agar, and incubating two times overnight. The persister fraction was calculated as the ratio of the number of CFU/ml after treatment and the number of CFU/ml before treatment.

6.4 Determination of minimum inhibitory concentration

The minimum inhibitory concentration (MIC) is a conventional measure for the susceptibility of bacterial strains towards a particular antibiotic. The MIC is defined as the lowest antibiotic concentration inhibiting visual growth of a bacterial population and was determined by the microdilution method. An overnight culture (app. 16 hours) was diluted in MHB to a cell density of approximately 10^5 CFU/ml and incubated in a 96-well microplate containing a twofold antibiotic dilution series that spanned the expected MIC of the population. Inoculum without antibiotics was used as a positive control, while MHB without inoculum was used as a negative control. After 16-20 hours of incubation at 37 °C, growth was examined visually and quantified by measuring the optical density at 595 nm ($OD_{595\ nm}$) with the Synergy™ Mx Microplate Reader (BioTek).

6.5 DNA manipulations

6.5.1 Plasmid isolation

Plasmid DNA was isolated using the GenElute™ HP Plasmid Miniprep Kit (Sigma-Aldrich). 1-3 ml of an overnight culture was centrifuged at 17,000 $\times g$. Resuspension in an alkaline solution caused cell lysis and precipitation of proteins and chromosomal DNA. After neutralization, plasmid DNA was adsorbed to a column, followed by a washing step and elution of the DNA. For a more detailed description of the protocol, we refer to the manual of the kit.

6.5.2 Polymerase chain reaction

The polymerase chain reaction (PCR) was performed to amplify DNA fragments *in vitro* in a highly specific manner. When an improved amplification fidelity was necessary, the commonly used *Taq* DNA polymerase (New England Biolabs) was replaced by Q5 DNA polymerase (New England Biolabs), which has proofreading activity. DNA was denatured by heating the mixture to 95 °C *Taq*) or 98 °C (Q5) for 30 seconds. For the annealing phase of 30 seconds, a temperature was chosen based on the melting temperature of the primer:template duplex, commonly between 50 and 65 °C. The duration of the elongation phase (68 °C for *Taq* polymerase and 72 °C for Q5 polymerase) depended on the elongation speed of the enzyme (1 min/kb for *Taq* polymerase and 30 s/kb for Q5 polymerase). Approximately 30 cycli were performed. The program was initiated by a denaturation step of 2 minutes (10 minutes for colony PCR) and completed with a final elongation step of 10 minutes.

6.5.3 Determination of DNA concentration

The concentration and purity of nucleic acids was determined spectrophotometrically (UV-Vis absorbance at 260 nm, with 260:230 and 260:280 nm ratios as measures for purity) using the NanoDrop® ND-1000 (Thermo Fischer Scientific).

6.5.4 Sanger sequencing

Sanger sequencing of PCR products was performed by GATC Biotech (Germany), for which DNA samples (10-100 ng/μl) and primers (10 pmol/μl) were prepared in 20 μl. Sequencing results were analyzed using the Geneious software version 7.1.7 [97].

6.6 Agarose gel electrophoresis

Gel electrophoresis was used for separation, purification, and size determination of PCR products. 0.7 % (w/v) agarose was dissolved in hot TBE buffer. Before the gel was formed by cooling the mixture, three drops of ethidium bromide (0.625 mg/ml) were added for visualization of the DNA under UV light. After the addition of blue juice loading buffer (1x), the samples were loaded into the wells of the gel. The size and concentration of the fragments were estimated by comparison to a size marker (SmartLadder, Eurogentec). A potential difference of 130 V ($\pm$ 8,6 V/cm) was applied during 1 hour. After electrophoresis, gel bands containing the desired DNA fragments were excised and DNA was extracted using the Wizard® SV Gel and PCR Clean-Up System kit (Promega). For this purpose, the agarose gel containing DNA was successively dissolved at 55-60 °C, loaded onto a column membrane, washed, and eluted using appropriate buffers. For a more detailed description of the protocol, we refer to the manual of the kit.

6.7 DNA transfer

6.7.1 Chemical transformation

Preparation of chemocompetent cells

An overnight culture of the recipient strain was diluted 1:100 in LB and incubated to exponential phase (3 hours at 37 °C). 1 ml of this culture was cooled on ice for 10 minutes and centrifuged for 5 minutes (1,200 $\times g$, 4 °C). After resuspension in ice-cold Tfb 1, the cells were kept on ice for 5 minutes, followed by centrifugation and resuspension in Tfb 2. Cells were kept on ice for another 10 minutes. The resulting chemocompetent cells were used immediately or stored at -80 °C.

Transformation

Chemocompetent cells were thawed on ice for 10 minutes, followed by the addition of 2 μl (high copy number plasmid) or 5-7 μl (low copy number plasmid) of DNA. After keeping this mixture on ice for 15 minutes, a 42 °C heat shock was applied for 2 minutes to permeabilize the membrane, after which cells were again kept on ice for 15 minutes. 500 μl LB was added and cells were allowed to recover at 37 °C for 45 minutes (or 20 minutes for selection on ampicillin). Selection of transformed colonies was performed by plating out on antibiotic-containing LB agar and overnight incubation at 37 °C (30 °C in the case of temperature-sensitive plasmid replication).

6.7.2 Electroporation

Preparation of electrocompetent cells

An overnight culture of the recipient strain was diluted 1:100 in LB and incubated to exponential phase (2-4 hours at 37 °C). When relevant, the expression of enzymes was induced by adding 0.2 % arabinose after 2 hours of incubation. 1.5 ml of this culture was centrifuged for 2 minutes (10,000 $\times g$, 0 °C). The pellet was resuspended in ice-cold MilliQ water and centrifuged again for 2 minutes. After repeating this washing step three times, the pellet was resuspended in 60 μl MilliQ. The resulting electrocompetent cells were used immediately.

Electroporation

1-5 μl (50-200 ng) of DNA was added to 60 μl of electrocompetent cells. After transfer of this mixture to a sterile, ice-cold electroporation cuvette (2 mm electrode gap), an electroshock was applied with the Gene/Pulse Controller (Bio-Rad) using a voltage of 2.5 kV, capacity of 25 μF, and resistance of 200 Ω. The mixture was added to 1 ml LB, followed by recovery at 37 °C during 45 minutes (or 20 minutes for selection on ampicillin). Selection of successful transformants was performed by plating out on antibiotic-containing LB agar and overnight incubation at 37 °C (30 °C in the case of temperature-sensitive plasmid replication).

6.8 Determination of pharmacodynamic functions

The pharmacodynamic function represents a mathematical relationship between the growth rate of a bacterial strain and the concentration of a particular antibiotic. A strain was inoculated in 5 ml MHB and grown for 24 hours. 1 ml of this culture was diluted in 100 ml of fresh medium and grown overnight (app. 16 hours). 1 ml of the 100 ml culture was then treated for 1 hour with different antibiotic concentrations (0, 1/64, 1/32, 1/16, 1/8, 1/4, 1/2, 1, 2, 4, 8, 16, 32,

and 64 times the MIC) either directly, or during exponential growth after 1:10,000 dilution and 2 hours of incubation. Cell densities were determined using the method described in paragraph 6.2. Growth rates were calculated by taking the logarithm of the ratio of the cell densities after and before treatment. By plotting the growth rates as a function of the antibiotic concentration and fitting the Hill function as defined by Regoes *et al.* [188], pharmacodynamic parameters such as the maximal and minimal growth rate, MIC, and Hill coefficient were extracted.

6.9 Fluctuation assay

A protocol based on the Luria-Delbrück fluctuation test [142] was used to measure the rate at which spontaneous mutations occur in a population. Starting from a small inoculum (5000 CFU/ml), 10 parallel cultures were grown separately in non-selective MHB medium. Assuming that the cultures contained approximately equal densities after 24 hours of growth, the number of spontaneous mutants resistant to rifampicin was then counted by plating out on rifampicin-containing (100 μg/ml) selective LB agar. Total cell densities before and after overnight growth were calculated by plating out on non-selective LB agar. The same protocol was used to measure mutation rates under conditions of subinhibitory antibiotic stress. To this end, the antibiotic concentration was optimized to obtain equally high cell densities after 24 hours of growth as compared to non-stressed cultures. The number of resistant mutants counted on selective plates (r) and the total cell density after 24 hours of growth (N_t) were used to calculate the number of mutational events (m) and the mutation rate with the Ma-Sandri-Sarkar Maximum Likelihood Estimator (MSS-MLE) method using the Fluctuation AnaLysis CalculatOR (FALCOR; [77]). When total cell densities could be assumed equal, mutation rates were compared statistically with a Student's t-test on the absolute numbers of mutational events m [192].

6.10 Measurement of stress response promoter activity

In order to measure the activity of stress responses under different conditions, reporter plasmids encoding transcriptional fusions of stress response promoters to *gfpmut2* were transformed to the desired strains. To this end, plasmids (pUA66 backbone) encoding the appropriate promoter fusions and a kanamycin resistance gene were first isolated from the Thermo Scientific *E. coli* Promoter Collection [245] by growing the clones overnight in 2x LB broth (low salt) with kanamycin (25 μg/ml), followed by plasmid isolation as described in paragraph 6.5.1. The resulting plasmids, including an empty pUA66 vector, were transformed to the desired strains as described in paragraph 6.7.1.

6.10.1 Population measurements

The promoter activity in the transformed strains was measured at the population level by growing cultures in 96-well microplates with MHB containing kanamycin (25 μg/ml) and varying doses of the appropriate antibiotics. After 24 hours of growth, the cultures were centrifuged and resuspended in $MgSO_4$. $OD_{595\ nm}$ and fluorescence (excitation at 488 nm, emission at 509 nm) were measured with the Synergy^{TM} Mx Microplate Reader (BioTek) in black, clear-bottom microplates to avoid fluorescent signal cross-talk. For each stress response, a positive control was established by subjecting exponential phase cultures of the reporter strains to 2 hour treatments known to activate the respective stress responses.

6.10.2 Single-cell measurements using flow cytometry

Single-cell fluorescence of the transformed strains was measured using a BD Influx cell sorter with 488 nm excitation and emission through a 530/40 nm band pass filter. Cultures were diluted in PBS before flow cytometry. For cell sorting, 100,000 cells were sorted in 500 μl of fresh MHB. When persister resuscitation was to be avoided, cells were sorted in spent MHB. Highly and weakly fluorescent subpopulations (100,000 cells) were analyzed further by plating or antibiotic treatment when relevant.

6.11 Evolution experiments

6.11.1 Resistant mutant plate assay

The emergence of resistant colonies on agar plates was monitored by plating out 200 μl of an overnight culture (app. 20 hours) on MHB agar containing an optimized antibiotic concentration, and incubating the plates at 37 °C. The initial cell density was determined by plating out on LB agar without antibiotics. The number of colonies on antibiotic-containing plates was counted daily during 10-12 days, after which resistance was confirmed by transferring colonies to new antibiotic-containing plates and incubating overnight.

6.11.2 Experimental evolution by serial transfer

Selection for antibiotic resistance was performed by propagating cultures under a constant selection pressure exerted by subinhibitory antibiotic concentrations. An overnight culture (app. 16 hours) was diluted to a cell density of approximately 10^5 CFU/ml and incubated in a 96-well microplate containing a twofold antibiotic dilution series that spanned the expected MIC of the population. After 22 hours of incubation at 37 °C, growth was quantified by measuring the $OD_{595\ nm}$ with the

Synergy^{TM} Mx Microplate Reader (BioTek). The culture grown in the drug concentration equal to half the MIC was diluted and incubated again in wells containing a range of drug concentrations spanning the expected MIC of the current population. This protocol was repeated on a daily basis for a period of 18 days. Evolution towards resistance was evaluated as the increase of the MIC over time.

6.11.3 Experimental evolution in a chemostat

Different strains were evolved in the chemostat, in a setup illustrated in Figure 6.1. The chemostat vessels (21x70 mm, total volume of 14 ml) were capped with open screw caps in which silicon septa were inserted, allowing repeated sterile sampling with a needle. MHB medium flowed from the reservoir through sterile Tygon tubing and a sterile needle into the vessels at a constant rate, driven by a peristaltic pump. At the same rate, spent medium and cells were washed out and collected. The volume of the cultures remained constant (6 ml) and was determined by the height of the needle used for effluent outflow. Atmospheric pressure was maintained in the medium reservoirs by allowing air inflow through a sterilizing filter. An air pump with sterilizing filter was used for culture aeration and mixing, and to generate overpressure to allow waste efflux. The risk of contamination in this setup was evaluated by verifying the sterility of non-inoculated culture medium.

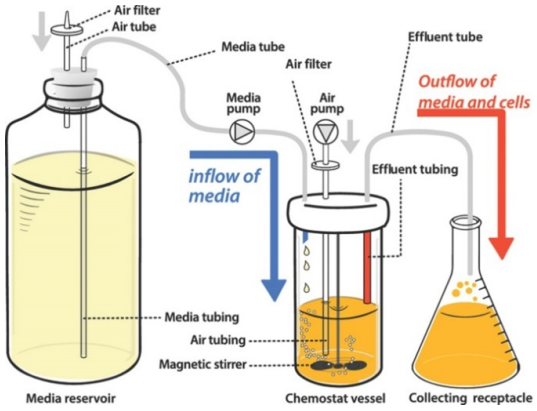

Figure 6.1: Experimental setup of a chemostat. Medium flows into the vessel containing the bacterial culture, while at the same rate, spent medium and cells are washed out and collected in a receptacle. Atmospheric pressure is maintained in the medium reservoirs by allowing air to flow in through a sterilizing filter. Oxygen is supplied by an air pump, which also ensures continuous mixing of the culture (adapted from [247]).

Experimental evolution was initiated by inoculating bacterial strains from overnight cultures into the chemostat vessels to a final density of 10^5 CFU/ml. After 24 hours of growth, bacterial cultures were treated on a daily basis with a bolus of antibiotics, followed by an exponential decay of the antibiotic concentration by dilution. The rate of antibiotic decay in the vessel equals the dilution

rate (0.231 ml/h) of the pump, as was verified by monitoring ciprofloxacin concentrations in a vessel filled with MilliQ water. For every strain, an additional, non-treated culture was evolved as a control. Three samples were taken daily from each culture. The first sample was taken after one half-life period of the antibiotic, the second sample was taken when the theoretically estimated antibiotic concentration in the vessel equaled the MIC, and the third sample was taken 24 hours after treatment, just before adding the new bolus. After washing the samples with $MgSO_4$, the cell density of each sample was determined by plating out on LB agar as described in paragraph 6.2. Cryogenic stocks of the evolving populations were stored daily. The number of resistant mutants was followed by plating out on MHB agar supplemented with antibiotic at a concentration corresponding to 2x or 4x the initial MIC of the strain. Additionally, the evolution of resistance was followed with disk diffusion susceptibility assays. To this end, an inoculum with an $OD_{595\ nm}$ of 0.15-0.5 was prepared and spread out on MHB agar, after which a disk containing the appropriate antibiotic was applied to the agar in the centre of the plate. As the antibiotic diffused rapidly from the disk into the agar, a zone of growth inhibition appeared after overnight incubation that was representative for the MIC of the culture.

Part III

Results and discussion

Chapter 7

Results

The alarmingly fast emergence and spread of bacterial resistance towards antibiotics strongly hampers the success of these drugs in healthcare. In addition to this widely acknowledged clinical burden, treatment of infections is further complicated by persistence. Although both survival strategies seem very different at first sight, it has been postulated that persistence can contribute to the emergence of resistance. By remaining viable in the presence of antibiotics, persister cells can accumulate mutations and constitute a reservoir of resistant mutants [126]. In addition, many of the stress responses involved in the generation and survival of persisters can promote evolutionary adaptation through stress-induced mutagenesis [39].

The first aim of the experimental work was to investigate the potential link between persistence and resistance using experimental evolution under antibiotic stress. For both high and low persistence mutants, the tendency to acquire resistance was compared in three different experimental setups. In a first evolution experiment, the emergence of resistant mutants was followed during incubation on solid growth medium. Next, strains were evolved in a serial transfer experiment with a constant antibiotic selection pressure, and changes in their MIC values were recorded over time. Finally, evolution of resistance was investigated in a chemostat, characterized by an *in vivo*-like pharmacokinetic profile. After each evolution experiment, we attempted to identify the resistance-conferring mutations in evolved clones.

Secondly, we sought general support for our hypothesis by looking for a correlation between persister fractions and resistance development in a collection of naturally occurring *E. coli* strains.

In a third part, we focused on potential mechanisms that could underlie the correlation between persistence and resistance. In particular, the contribution of stress-induced mutagenesis was investigated by comparing basal and stress-induced mutation rates, as well as stress response activation, among high and low persistence mutants.

Experimental results were complemented with a theoretical model that was built in order to simulate resistance development in a continuous culture. To be able to predict population dynamics, important model parameters including growth rates, killing rates, mutation rates, MIC values, and Hill coefficients, were either measured directly or extracted from experimental data.

7.1 Selection of strains and antibiotics

Recent studies pointed out various genes involved in *E. coli* persistence. Strains having either mutated or deleted alleles of the corresponding genes often show notable changes in their extent of phenotypic tolerance. Among them, a subset of *E. coli* strains was selected that was expected to cover a wide range of persister levels. For strains having mutations in *nuoN*, *gadC*, *oppB*, and *hipA*, high persister levels have been reported [160, 221]. RelA, SpoT, Lon, and TA modules play a central role in the model of (p)ppGpp-controlled persistence described by Maisonneuve and Gerdes [146], supported by the observation of low persister levels in Δ*relAspoT*, Δ*lon*, and Δ*10TA* mutants [145, 147]. RpoS has been described as an important regulator of gentamicin persistence in *E. coli* [239] and ofloxacin tolerance in *P. aeruginosa* [162], therefore persister levels were expected to be low in the Δ*rpoS* mutant. Moreover, the central role for RpoS in stress-induced mutagenesis was expected to affect resistance development [181]. As the Δ*lon* and Δ*rpoS* mutants originated from the Keio collection [12], they contained a kanamycin resistance cassette that could potentially interfere with experiments involving selection for aminoglycoside resistance. Therefore, kanamycin resistance cassettes were eliminated first by means of FLP recombinase expressed from pCP20. In all experiments, observations for mutant strains were compared to those for the corresponding isogenic wild type strain. Experimental data were collected for antibiotics representing the three major classes of bactericidal antibiotics: aminoglycosides (amikacin), quinolones (ciprofloxacin), and β-lactams (ampicillin, carbenicillin, and ceftazidime).

7.2 Experimental evolution of antibiotic resistance

The selected *E. coli* strains, consisting of both high and low persistence mutants, were tested for their potential to develop antibiotic resistance in evolution experiments with three different setups. Comparison of evolutionary dynamics among strains is only feasible when an equally strong selection pressure is applied. As the susceptibility of different strains towards a particular antibiotic may vary, antibiotic concentrations used for treatment were expressed relative to the MIC to take into account these potential variations. Therefore, the antibiotic susceptibility of all strains was first quantified by measuring MIC values of the different antibiotics.

7.2.1 Determination of antibiotic susceptibility

The MIC of three different antibiotics (amikacin, ciprofloxacin, and ampicillin) was determined for 12 strains. Additionally, the MIC of two other β-lactams (carbenicillin and ceftazidime) was measured for *hipA7* and its corresponding wild type strain. The MIC values of all strain-antibiotic combinations are listed in Table A.1 (Appendix A). For amikacin, the data revealed some vari-

ability. For all other antibiotics, very similar MIC values were observed for wild type and mutant strains with the same genetic background. Exceptions are Δ*lon* and *hipA7*, for which ciprofloxacin has a twofold higher MIC value than for the corresponding wild type strain.

7.2.2 Experimental evolution on solid medium

Monitoring the emergence of resistance on agar plates first required optimization of the antibiotic concentration and incubation time, in order to yield a suitable number of colonies for an accurate comparison of resistance evolution rates. Therefore, a preliminary assay was performed with the wild type strain MG1655. Resistant colonies appearing on MHB agar plates with different antibiotic concentrations (2x, 4x, 8x, 16x, 32x, and 64x MIC) were counted on a daily basis until a plateau was reached (Figure B.1, Appendix B). For each antibiotic, the optimal incubation time was approximately 10 days, with an optimal concentration being 4x MIC for amikacin, 2x MIC for ciprofloxacin, and 4x MIC for ampicillin.

The same plate assay was then performed for all strains with amikacin, ciprofloxacin, and ampicillin using the optimized treatment conditions (Figure B.2, Appendix B). Resistance levels of all strains were compared to those of the corresponding wild type strain. Resistance was confirmed by transferring a few, random colonies to fresh, selective plates. As colonies on amikacin plates often became transparent after a few days, possibly because of lysis, and mostly showed no growth after transfer to a new selective plate, these data should be considered as rough estimations.

For the strain-antibiotic combinations shown in Figure 7.1, a positive correlation was observed between resistance development and the persistence phenotype reported in literature. The frequency of resistant mutants, defined as the resistant proportion of the initial population size, is represented as a function of time. These data reveal a remarkably accelerated resistance development in *oppB** and *hipA7* as compared to their wild type. For both strains, high persister levels have been reported [160, 221]. In contrast, considerably less resistant mutants were encountered for Δ*10TA* and Δ*lon*, two strains for which persister levels were described to be low [145, 147]. Together, these results indicate a positive correlation between persister levels and the emergence of resistance in these strains.

On ampicillin plates, several colonies became surrounded by satellite colonies over time. This phenomenon has been reported before for β-lactams and is ascribed to the enzymatic degradation of the antibiotic by central, β-lactamase-producing resistant colonies [153]. Indeed, central colonies were able to grow after transfer to a fresh, selective plate, while satellite colonies were not. As an exception, all transferred colonies of *hipA7* were resistant. To avoid interference of enzymatic drug degradation, the assay was repeated for *hipA7* and its wild type with two other β-lactams,

carbenicillin and ceftazidime, known for their higher stability as compared to ampicillin (Figure 7.1).

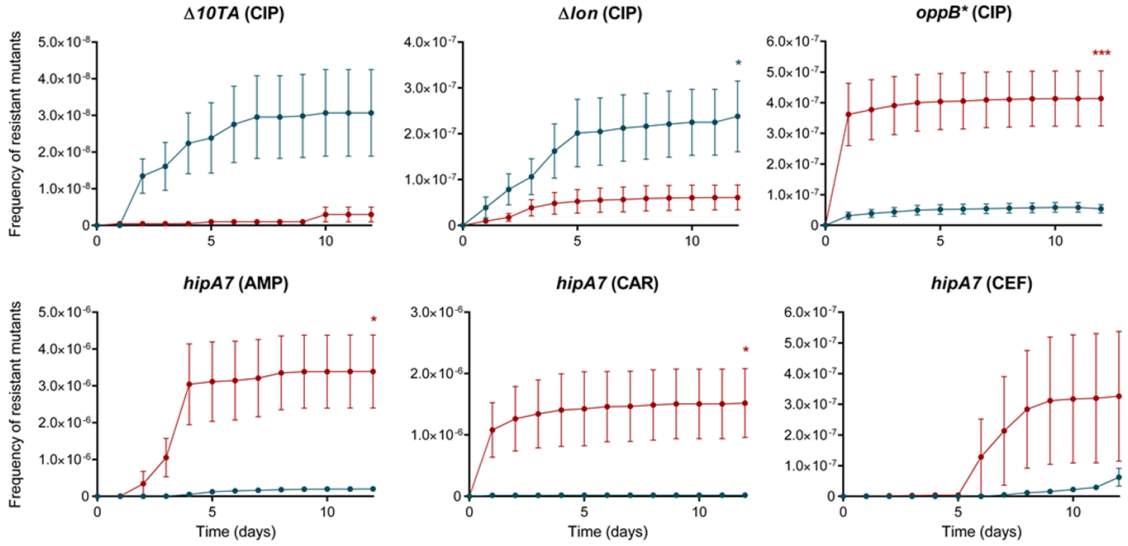

Figure 7.1: Frequencies of resistant mutants emerging on solid growth medium supplemented with ciprofloxacin (CIP; 2x MIC), ampicillin (AMP; 4x MIC), carbenicillin (CAR; 4x MIC), or ceftazidime (CEF; 4x MIC). Measurements for wild type strains are colored blue, while measurements for mutants are colored red. The number of resistant colonies appearing over time is represented as the mean proportion of the total population density, which was measured at the start of the experiment. Error bars indicate the standard error of the mean (n=9). End points were compared statistically with a two-sided Student's t-test ($* : P \leq 0.05; ** : P \leq 0.01; *** : P \leq 0.001$).

7.2.3 Validation of persistence phenotypes

For the strains that provided most evident results in the plate assays (Figure 7.1), killing dynamics were monitored to validate their persistence phenotype. Time-kill curves of both exponential and stationary phase cultures of Δ*10TA*, Δ*lon*, *oppB**, and their corresponding wild types were measured in the presence of ciprofloxacin. *hipA7* and its wild type were treated with three different β-lactams (ampicillin, carbenicillin, and ceftazidime). Only exponential phase cultures were investigated in this case, since β-lactams mainly affect actively dividing cells. In Figure 7.2, the number of surviving cells is plotted as a function of the antibiotic treatment time t. In all cases, a biphasic killing curve (Eq. 7.1) could be fitted.

$$\log_{10}(CFU/ml) = \log_{10}((N_0 - P_0) \times e^{-k_n t} + P_0 \times e^{-k_p t}) \tag{7.1}$$

From the best-fit killing curve, parameter values were extracted for the initial number of normal cells (N_0), the initial number of persisters (P_0), the killing rate of normal cells (k_n), and the

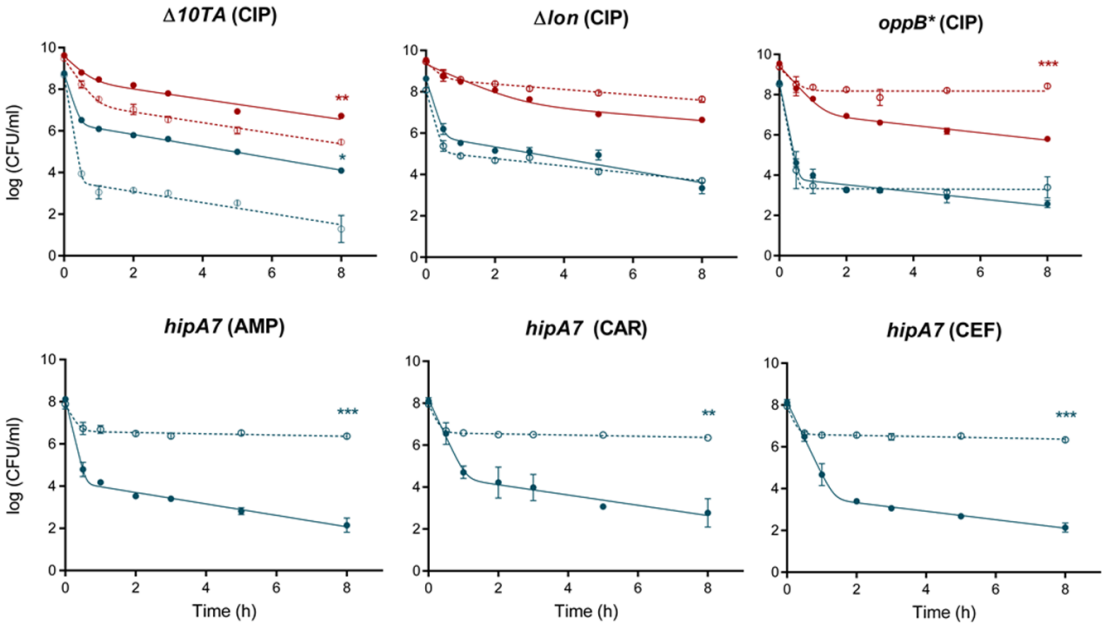

Figure 7.2: Time-kill curves of Δ*10TA*, Δ*lon*, *oppB**, *hipA7*, and their corresponding wild types in the presence of ciprofloxacin (CIP; 5 μg/ml), ampicillin (AMP; 100 μg/ml), carbenicillin (CAR; 100 μg/ml), or ceftazidime (CEF; 50 μg/ml). Red points represent measurements in stationary phase (solid circles for wild type strains, open circles for mutant strains), whereas blue points were measured in exponential phase (solid circles for wild type strains, open circles for mutant strains). Best-fit killing curves of wild type strains are represented by solid lines, the mutant counterparts are represented by dashed lines. Mean numbers of surviving cells are plotted, with error bars indicating the standard error of the mean (n=3). Persister fractions of the mutant strains were compared to those of the wild type strains with two-sided Student's *t*-tests ($* : P \leq 0.05; ** : P \leq 0.01; *** : P \leq 0.001$).

killing rate of persisters (k_p). Wild type and mutant strains were compared statistically using a two-sided Student's *t*-test on the logarithm of the persister fractions ($\log_{10}(P_0/(N_0 + P_0))$) after checking equality of variances with a two-sided F-test. When variances were found to be unequal, a two-sided Welch's test was executed.

Time-kill curves of Δ*10TA* reveal significantly lower persister fractions in both exponential and stationary phase as compared to the wild type (500-fold and 12-fold reduction respectively). These results correspond to observations of Maisonneuve *et al.* [147] and confirm that Δ*10TA* can be considered as a low persistence strain. Δ*lon* showed no significantly different survival in exponential and stationary phase as compared to its wild type, which is in contrast to the observations of Maisonneuve *et al.* [147]. As expected [221], persister levels in stationary phase cultures of *oppB** were significantly higher as compared to the wild type strain (600-fold increase), while no pronounced difference was observed in exponential phase. Also confirming previous observations [160], *hipA7* showed significantly increased persister levels in exponential phase when treated with three different β-lactam antibiotics (400-fold increase for ampicillin, 160-fold increase for carbenicillin, and 1200-fold increase for ceftazidime).

7.2.4 Experimental evolution by serial transfer

Based on the observed correlation between persister levels and the emergence of resistant colonies on plate, we decided to further investigate the low persistence mutant Δ*10TA* and the high persistence (*hip*) mutants *oppB** and *hipA7*. The evolution of antibiotic resistance in these mutants and their wild types was followed in a serial transfer experiment. Similar to the setup of Oz *et al.* [172], 4 parallel populations were evolved under a constant antibiotic selection pressure. After 22 hours of growth in a range of antibiotic concentrations, populations grown in the concentration equal to half the MIC were transferred to fresh medium with an equal or increased concentration range. This selection process was continued for 18 days. Δ*10TA*, *oppB**, and their wild types were evolved with ciprofloxacin, while *hipA7* and its wild type were evolved with ampicillin, carbenicillin, and ceftazidime. In Figure 7.3, resistance levels are represented by normalized MIC values as a function of time. Except for Δ*10TA* and its wild type, no correlation was observed between persister levels and resistance development.

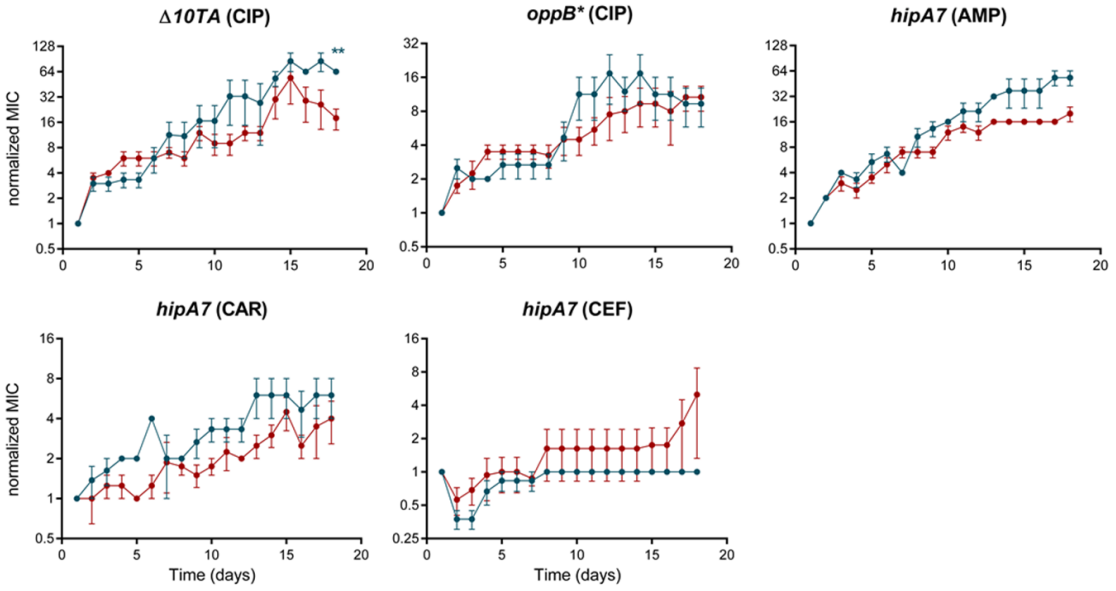

Figure 7.3: Evolution of resistance in serial transfer experiments with constant antibiotic selection pressure (half the MIC). Δ*10TA*, *oppB**, and their corresponding wild types were evolved with ciprofloxacin (CIP), while *hipA7* and its wild type was evolved with ampicillin (AMP), carbenicillin (CAR), and ceftazidime (CEF). Measurements for wild type strains are colored blue, while measurements for mutants are colored red. Daily recorded MIC values are normalized with the MIC at day 0 and represented on a $\log_2$ scale. Mean values are plotted, with error bars indicating the standard error of the mean (n=4).

7.2.5 Experimental evolution in continuous culture

As resistance evolution on plate and in batch cultures simplifies many complexities of an infection environment, strains were also evolved under biologically more relevant conditions. *oppB**, Δ*10TA*,

and their wild types were grown continuously in a chemostat for 6-10 days. A daily bolus of ciprofloxacin was added with a peak concentration of 0.37 μg/ml (app. 46x MIC), corresponding to the *in vivo* measured peak serum concentration after oral administration of a 100 mg dose [165]. Because of dilution, the antibiotic concentration in the chemostat vessels decayed exponentially, resulting in an *in vivo*-like pharmacokinetic profile. The constant dilution rate (0.231 ml/h) was tuned to obtain a ciprofloxacin half-life of 3 h, according to the serum half-life [165]. 16.5 hours after each treatment, the ciprofloxacin concentration was approximately equal to the initial MIC value of the population. The subsequent 7.5 hours of treatment with sub-MIC antibiotic concentrations were expected to have an important role in the evolution of resistance [9].

Total cell densities of samples taken just before each treatment, 3 hours after treatment (one half-life period), and 16.5 hours after treatment are plotted in Figure 7.4 for the *hip* mutant *oppB** and its wild type (three biological replicates) and for the low persistence mutant Δ*10TA* and its wild type. The number of resistant mutants was estimated by plating out a sample on MHB agar plates containing ciprofloxacin (4x MIC). For *oppB** and its wild type, resistance emerged in only one replicate, after 6 treatment cycles in the case of the wild type and after 8 treatment cycles in the case of *oppB**. Resistance evolution was more evident for Δ*10TA* and its wild type, as resistant mutants took over both populations after only two treatment cycles.

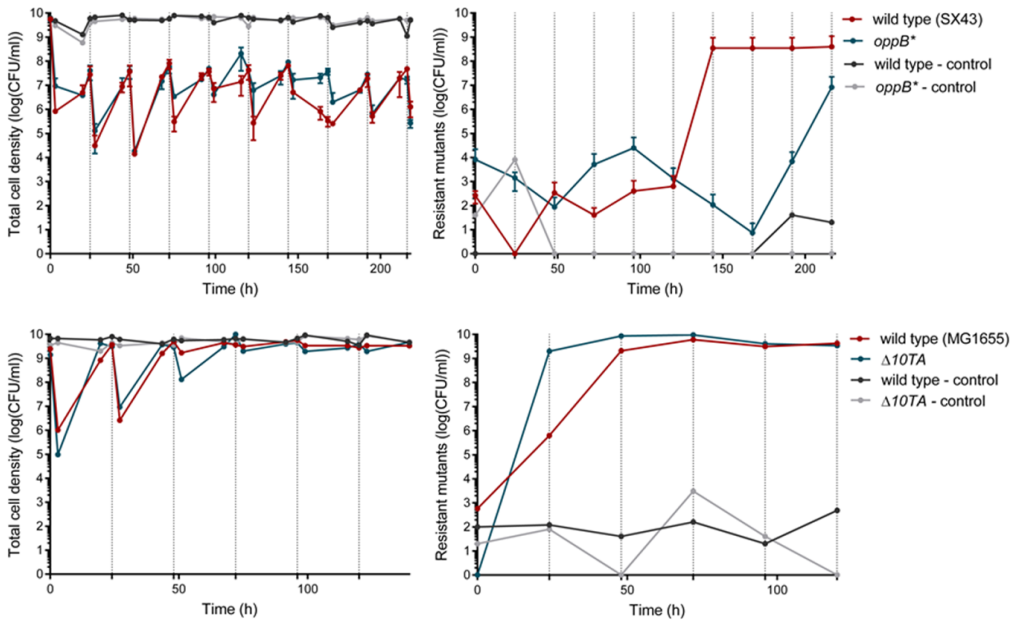

Figure 7.4: Total cell densities and densities of resistant mutants during experimental evolution in a chemostat. Populations were treated daily with ciprofloxacin (0.37 μg/ml). Total cell densities were determined three times a day by plating out samples on non-selective plates, whereas resistant mutants were quantified daily by plating out samples on ciprofloxacin-containing plates (4x MIC). For *oppB** and SX43, mean values of three biological replicates are plotted, with error bars representing the standard error of the mean.

7.2.6 Resistance mechanisms in evolved clones

After each evolution experiment, we investigated genetic regions prone to resistance mutations in the evolved clones, attempting to identify mechanisms causing antibiotic resistance. To confirm that satellite colonies on ampicillin plates indeed result from β-lactamase-producing resistant colonies, the promoter region of the *ampC* gene was sequenced in three central colonies of Δ*10TA*, BW25113, Δ*lon*, MG21, and *hipA7* (Table 7.1). The *ampC* promoter sequence of the original strains was determined as a control. *ampC* encodes a β-lactamase, but its native expression is too weak to render *E. coli* ampicillin resistant. However, mutations in a set of sequence elements, especially the -35 and -10 boxes, have been reported to affect promoter strength. The result is an increased expression of *ampC* and consequently, β-lactam resistance [89]. Indeed, a T $\rightarrow$ A transversion at position -32 was observed for a central colony of BW25113. This mutation restores the -35 box consensus sequence, TTGACA, and has been observed before in resistant clinical isolates [31, 89, 201, 216]. Additionally, a C $\rightarrow$ T transition at position -11 was observed for two central colonies of *hipA7*. This mutation reestablishes the -10 box consensus sequence, TATAAT, and was also observed by Jaurin *et al.* [89] and Corvec *et al.* [40]. While the optimal interbox distance is 17 bp, it is only 16 bp in the wild type *E. coli ampC* promoter, also contributing to the weak promoter strength. Not surprisingly, we observed a T insertion between position -15 and -14 in a central colony of Δ*lon* and Δ*10TA*, and a G insertion between position -17 and -16 in BW25113 and Δ*10TA*. Both insertions restore the optimal interbox distance. The *ampC* promoter region was also sequenced in clones evolved in serial transfer experiments (Table 7.1). A C $\rightarrow$ A transversion was detected at position +31 in the *ampC* attenuator of *hipA7*.

Similarly, we aimed to identify and compare mutations rendering ciprofloxacin resistance to clones evolved on plate, in serial transfer experiments, and in the chemostat. In Gram-negative bacteria, the DNA gyrase subunit GyrA constitutes the main target of quinolones, which explains why resistance mutations occur first in *gyrA*. Resistance-conferring mutations are constrained to a particular N-terminal region called the quinolone resistance-determining region (QRDR) and including amino acids between positions 51 and 106 [62]. Antibiotic susceptibility can be further reduced by additional step-wise mutations in *gyrB* (encoding the second subunit of DNA gyrase) and *parC* or *parE* (encoding two subunits of DNA topoisomerase IV) [86]. We sequenced the QRDR of *gyrA* and found mutations located on amino acid positions 82, 83, and 87 (Table 7.1). In most cases, a negatively charged aspartate (D) is replaced by a neutral amino acid (either tyrosine (Y) or glycine (G)).

In general, no notable differences in resistance mechanisms were observed between wild type and mutant strains evolved under the same experimental conditions.

Table 7.1: Mutations in clones evolved under ciprofloxacin or ampicillin stress in different experimental setups. Three clones were sequenced for each strain. Clones evolved in serial transfer experiments were taken from independent populations, while clones from chemostat experiments result from one population

Strain	Evolution experiment	Sequenced region	Nucleotide mutation	Amino acid substitution	Number of observations
BW25113	plate assay	*ampC* promoter	-32 T>A	-	1
hipA7	plate assay	*ampC* promoter	-11 C>T	-	1
Δ*lon*	plate assay	*ampC* promoter	-15_-14insT	-	1
Δ*10TA*	plate assay	*ampC* promoter	-15_-14insT	-	1
BW25113	plate assay	*ampC* promoter	-17_-16insG	-	1
Δ*10TA*	plate assay	*ampC* promoter	-17_-16insG	-	1
hipA7	serial transfer	*ampC* promoter	+31 C>A	-	3
*oppB**	chemostat	*gyrA* QRDR	259 G>T	D87Y	3
SX43	chemostat	*gyrA* QRDR	259 G>T	D87Y	2
MG1655	chemostat	*gyrA* QRDR	248 G>A	S83N	3
Δ*10TA*	chemostat	*gyrA* QRDR	248 G>A	S83N	3
*oppB**	plate assay	*gyrA* QRDR	260 A>G	D87G	1
SX43	plate assay	*gyrA* QRDR	260 A>G	D87G	1
SX43	plate assay	*gyrA* QRDR	245 A>G	D82G	1
MG1655	plate assay	*gyrA* QRDR	259 G>T	D87Y	1
Δ*10TA*	plate assay	*gyrA* QRDR	245 A>G	D82G	1
MG1655	serial transfer	*gyrA* QRDR	259 G>T	D87Y	2

7.3 Persistence versus resistance in environmental *E. coli* isolates

Significant variation in persister fractions of environmental *E. coli* isolates has already been reported [82, 207]. Based on these observations, the question raised as to whether this natural variation in persistence could be linked to the potential to develop resistance. To test this idea, we randomly selected 20 natural *E. coli* isolates from the ECOR collection, a panel of strains representing the genetic diversity in the species [170]. We quantified persister levels of all strains following ampicillin or ciprofloxacin treatment. Next, we tested their ability to develop resistance towards both antibiotics on solid medium, and investigated the correlation with persister fractions.

7.3.1 MIC values of ECOR isolates

MIC values of all ECOR isolates are summarized in Table C.1 (Appendix C). All strains are highly susceptible for ciprofloxacin and ampicillin, which enables a reliable comparison of persister levels. As an exception, ECOR 59 is resistant to an ampicillin concentration of at least 32 μg/ml.

7.3.2 Persister fractions of ECOR isolates

Killing curves were determined for all strains and persister fractions were extracted as described in paragraph 7.2.3. Exponential phase cultures were used for ampicillin treatment while ciprofloxacin treatment was performed in stationary phase (Figure 7.5). In contrast to the conventional setup,

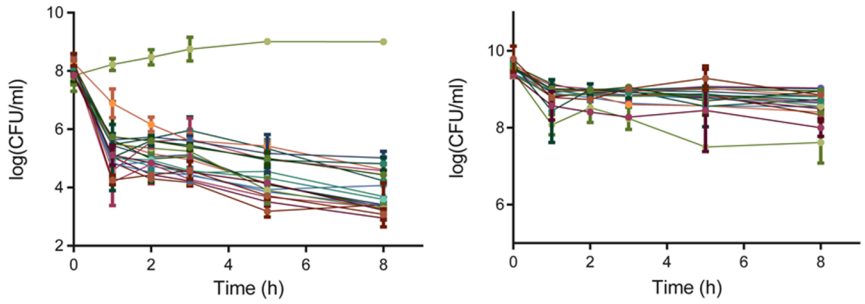

Figure 7.5: Time-kill curves of 20 ECOR strains, treated with ampicillin in exponential phase (left) and ciprofloxacin in stationary phase (right). Mean numbers of surviving cells from are plotted, with error bars indicating the standard error of the mean (n=3).

cultures were grown in 24-well plates instead of test tubes and cell densities were determined by spot plating. For ampicillin-treated cultures, a biphasic killing pattern was observed for all but one strain (ECOR 59) that was resistant to ampicillin. Ciprofloxacin treatment also resulted in biphasic killing curves, although the extent of killing was less pronounced than expected. Highly significant differences in persister fractions were observed among the 20 isolates following both ampicillin (0.000001-0.001; one-way analysis of variance (ANOVA) $F_{20} = 42.12$; $P < 0.0001$) and ciprofloxacin (0.02-0.34; one-way ANOVA $F_{20} = 9.584$; $P < 0.0001$) treatments. There was no statistically significant linear correlation between the MIC and persister fraction for ampicillin ($r = -0.098$; $P = 0.69$) or ciprofloxacin ($r = 0.31$; $P = 0.18$).

7.3.3 Resistance development of ECOR isolates on solid growth medium

All cultures were plated out on MHB agar plates containing either ampicillin (4x MIC) or ciprofloxacin (4x MIC). The emergence of resistant mutants was tracked over time as described in paragraph 7.2.2 (Figure 7.6).

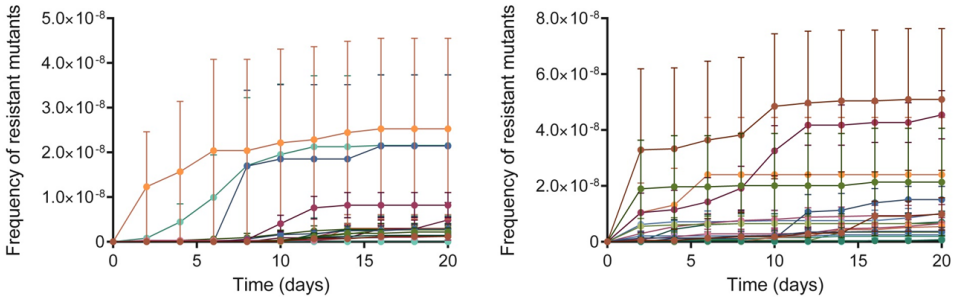

Figure 7.6: Resistance development of 20 ECOR strains plated out on solid growth medium supplemented with ampicillin (left) or ciprofloxacin (right) at a concentration of 4x MIC. The number of resistant colonies appearing over time is represented as the mean proportion of the total population density, which was measured at the start of the experiment. Error bars indicate the standard error of the mean (n=5).

A correlation analysis was performed on the logarithm of the persister level and the mutation rate. The latter was defined as the number of ciprofloxacin- or ampicillin-resistant mutants that emerged per cell as a function of time. According to the approach of Cirz *et al.* [35], a distinction was made between pre-existing and *de novo* mutants. Pre-existing mutants were defined as the mutants that had arisen in the overnight culture and were counted as the colonies appearing until 2 days of incubation on plate. Based on these numbers, a pre-exposure mutation rate was calculated. Colonies that appeared after day 2 were defined as *de novo* mutants and were used to calculate a post-exposure mutation rate. The total mutation rate was calculated with the total number of resistant mutants that appeared over time.

Correlation coefficients for persister levels, pre-exposure, post-exposure, and total mutation rates were analyzed for each antibiotic and between different antibiotics (Figure 7.7). In general, positive correlation coefficients were observed for parameters for the same antibiotic, whereas parameters for different antibiotics were not or slightly negatively correlated. Persister levels and mutation rates for the same antibiotic show a positive, but statistically insignificant correlation. As correlation coefficients range from 0.2 to 0.37, we can conclude that only part of the variance in resistance development is explained by the persister level.

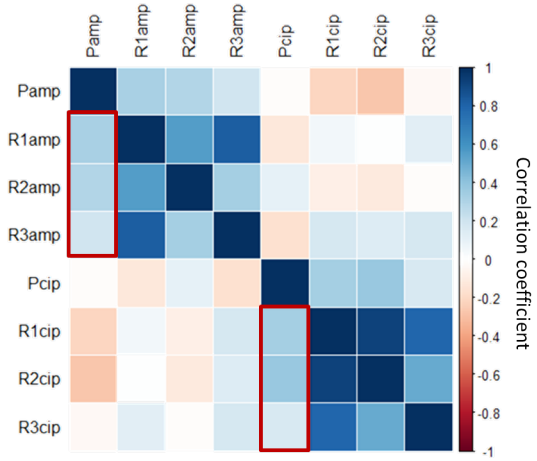

Figure 7.7: Correlation matrix of persister levels and mutation rates of 20 ECOR strains for ampicillin (amp) and ciprofloxacin (cip). Persister levels (Pamp and Pcip), total mutation rates (R1amp and R1cip), pre-exposure mutation rates (R2amp and R2cip), and post-exposure mutation rates (R3amp and R3cip) are shown for both antibiotics. Correlations between persister levels and mutation rates for the same antibiotic are indicated with a red frame.

7.4 Stress responses: catalysts of adaptive mutation?

As persisters constitute a protected compartment in a bacterial population, they remain viable when treated with antibiotics and can accumulate mutations. Although the presence of a refractory subpopulation could be sufficient to promote the emergence of resistance, stress responses may strongly accelerate this process [39]. Inspired by this hypothesis, we investigated the contribution of stress-induced mutagenesis to resistance evolution in high and low persistence mutants. First, we compared basal and stress-induced mutation rates among these strains. Next, we measured stress response activation and explored correlations with persister levels.

7.4.1 Mutation rates of high and low persistence mutants

Luria-Delbrück fluctuation assays were performed to determine mutation rates of Δ*10TA*, Δ*lon*, *oppB**, *hipA7*, and their respective wild types. Basal mutation rates were measured after 24 hours of unstressed growth, while stress-induced mutation rates were measured after a 24-hours exposure to sublethal antibiotic stress. The final population density strongly influences the number of mutations arising in a population. For this reason, sublethal stress was imposed by the highest antibiotic concentration that did not alter the final population density. To define this concentration, the OD_{595} of MG1655 populations was measured after 24 hours of growth in a range of antibiotic concentrations. We decided to conduct further experiments with a ciprofloxacin concentration of 1/8x MIC, while 1/4x MIC was still amenable for ampicillin. Corresponding to other experiments, ciprofloxacin stress was imposed on Δ*10TA*, Δ*lon*, and *oppB**, and ampicillin was used for *hipA7*.

Basal and stress-induced mutation rates (Figure 7.8) result from 20 parallel populations used to determine the number of mutational events (m) and 8 parallel populations used to calculate total cell densities. In order to compare mutation rates statistically, two-sided Student's t-tests were executed on m. This test is only valid when total cell densities can be assumed equal [192].

For the low persistence mutant Δ*10TA*, both mutation rates are significantly lower than those of the wild type strain. Δ*lon* shows a higher basal mutation rate than its wild type. The *hip* mutant *oppB** shows no significantly different basal mutation rate, but a considerably increased stress-induced mutation rate as compared to its wild type. Mutation rates of *hipA7* and its wild type could not be compared statistically, as the assumption of equal population densities was not valid.

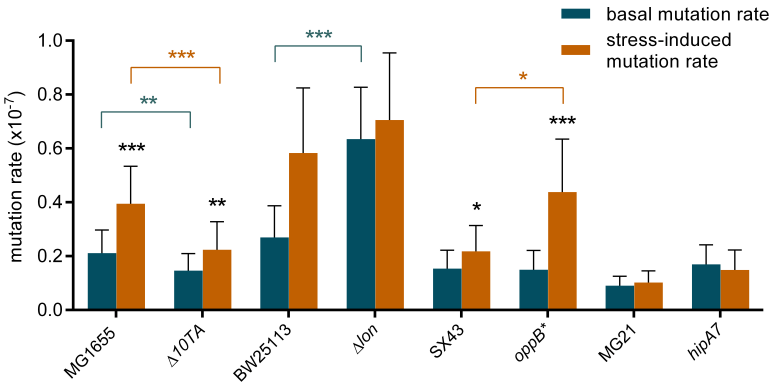

Figure 7.8: Basal and stress-induced mutation rates measured in a Luria-Delbrück fluctuation assay. The mutation rate is defined as the probability of mutation per cell per generation. Stress-induced mutation rates are measured by imposing ciprofloxacin stress (1/8x MIC) on Δ*10TA*, Δ*lon*, *oppB**, and their respective wild types MG1655, BW25113, and SX43, whereas ampicillin stress (1/4x MIC) was imposed on *hipA7* and its wild type MG21. Error bars represent upper limits of confidence intervals. Mutation rates were compared statistically using a two-sided Student's *t*-test on the absolute number of mutations ($* : P \leq 0.05; ** : P \leq 0.01; *** : P \leq 0.001$), assuming equal cell densities [192]. This assumption was not valid for *hipA7* and MG21.

7.4.2 Stress response promoter activity in high and low persistence mutants

Population-level measurements

As stress responses are believed to contribute to the generation and maintenance of persisters, their activity was compared in high and low persistence mutants. Reporter plasmids encoding fusions of *gfpmut2* to varying stress response promoters (Table 7.2) were used to measure transcriptional activity. As a proof of concept, exponential phase cultures of the reporter strains were subjected to 2 hour treatments known to activate the appropriate stress responses (Table 7.2). Stationary phase conditions were used as a positive control for the general stress response. Normalized fluorescence (fluorescence/OD_{595}) of the treated cultures was calculated as a measure for the average single-cell fluorescence, and compared to control measurements. Apparently, all promoter fusions (except *wrbA*) are appropriate reporters for the corresponding stress response (Figure 7.9).

Table 7.2: Overview of selected stress response genes for promoter activity measurements. Treatments known to activate the corresponding stress responses were used as a positive control

Stress response	Genes	Positive control
SOS response	*recA*, *polB*, *dinB*, *umuCD*	Mitomycin C (0.25 μg/ml)
Stringent response	*relA*, *wrbA*	Serine hydroxamate (1 mg/ml)
Extracytoplasmic stress response	*rpoE*	42 °C
General stress response	*rpoS*	Stationary phase
Oxidative stress response	*soxS*, *dps*	Paraquat (10 μM), H_2O_2 (5 mM)

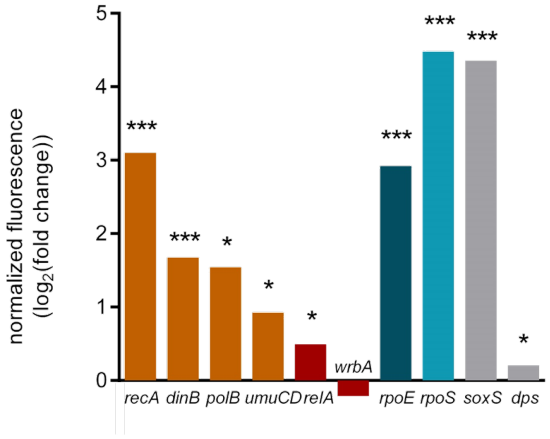

Figure 7.9: Positive control measurements of stress response promoter activity using transcriptional promoter-*gfpmut2* fusions. Treatments used to activate the stress responses are listed in Table 7.2. Results are represented as $\log_2$(fold change) of the normalized fluorescence (fluorescence/OD_{595}) compared to non-treated cultures (n=3) and tested for statistical significance with a two-sided Student's *t*-test ($* : P \leq 0.05; ** : P \leq 0.01; *** : P \leq 0.001$). As measurements from treated and non-treated cultures are not paired, error bars are not shown.

Subsequently, normalized fluorescence was measured for Δ*10TA*, Δ*lon*, *oppB**, *hipA7*, and their wild types transformed with all reporter plasmids. Measurements were taken either after 24 hours of growth under optimal conditions or sublethal antibiotic stress, or after 19 hours of growth followed by 5 hours of lethal antibiotic stress. Ciprofloxacin stress was imposed on Δ*10TA*, *oppB**, and their wild types, at sublethal (1/8x MIC) or lethal (625x MIC) concentrations. Ampicillin, carbenicillin, and ceftazidime stress was imposed on *hipA7* and its wild type at sublethal (1/4x MIC) or lethal (25x MIC) concentrations. Correction for background fluorescence was performed by subtraction of the normalized fluorescence of each strain transformed with an empty pUA66 vector. All data are summarized in Figure D.1 (Appendix D) and Figure 7.10.

In general, sublethal antibiotic stress caused a decreased promoter activity of the SOS response genes (*recA*, *dinB*, *polB*, and *umuCD*) in the low persistence mutant Δ*10TA* and an increased promoter activity in the *hip* mutants *oppB** and *hipA7* as compared to their wild types. Except for *polB*, the same trend was observed under optimal growth conditions, although the results are less conclusive. An inverse correlation was observed for Δ*10TA* under lethal antibiotic stress. For *hipA7*, data are represented for sublethal ampicillin treatment, as carbenicillin and ceftazidime treatment led to less consistent results (Figure D.1). Together, these data suggest a positive correlation between persister levels and average SOS response activities under sublethal antibiotic stress.

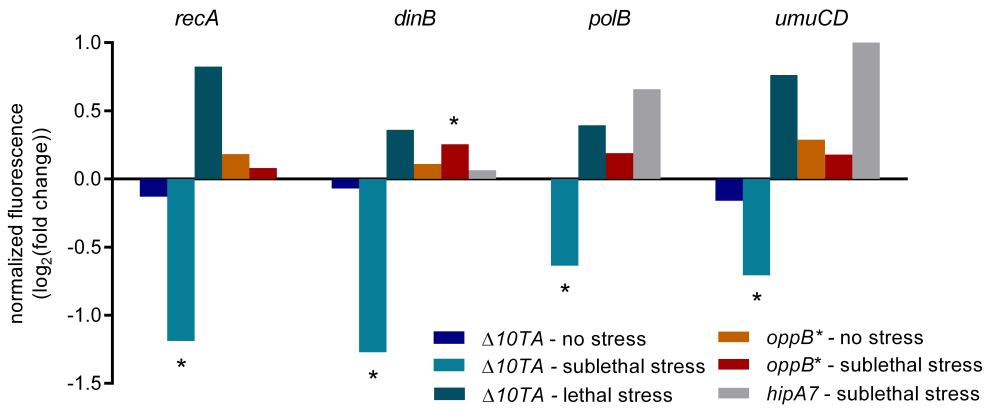

Figure 7.10: Promoter activity of SOS response genes (*recA*, *dinB*, *polB*, and *umuCD*) in Δ*10TA*, *oppB**, and *hipA7* under optimal growth conditions ('no stress'), sublethal, or lethal antibiotic stress. Fluorescence results from GFP expression from transcriptional promoter-*gfpmut2* fusions. Results are represented as $\log_2$(fold change) of the mean normalized fluorescence (fluorescence/OD_{595}) of the mutant and wild type strain, after subtraction of background fluorescence from an empty pUA66 vector. Statistical significance was tested with a two-sided Student's *t*-test ($* : P \leq 0.05$). As measurements from wild type and mutant strains are not paired, error bars are not shown.

Single-cell measurements using flow cytometry

In the experiments described above, stress response promoter activity was measured at the population level. Although these measurements are informative for average promoter activities, they do not capture underlying population distributions of fluorescence levels. Therefore, fluorescence of the reporter strains was measured at the single-cell level using flow cytometry. As the results of the population-level measurements were most promising for the SOS response genes, only these reporter strains were tested. Again, strains were either grown for 24 hours under optimal conditions or sublethal antibiotic stress, or grown for 19 hours followed by 5 hours of lethal antibiotic stress. The same antibiotic doses were used as for the population measurements. All data are summarized in Appendix D (Figure D.2). The population average shifts in the mutant strains largely correspond to those observed in the population measurements. In Figure 7.11, results are depicted for Δ*10TA*, *oppB**, and their wild types under sublethal or lethal ciprofloxacin stress. According to the population-level measurements, the average fluorescence of Δ*10TA* under sublethal stress is shifted to lower values as compared to its wild type (except for *recA*), while *oppB** shows higher average fluorescence levels than its wild type for all SOS response promoters. The population-level increase observed for Δ*10TA* under lethal stress was also confirmed at the single-cell level (except for *recA*).

In addition to fluorescence distributions, the potential correlation between SOS response activation and persister levels was investigated. 100,000 cells from the 5 % most strongly and 5 % most weakly fluorescent subpopulation were sorted and persister levels were quantified in the sorted fractions.

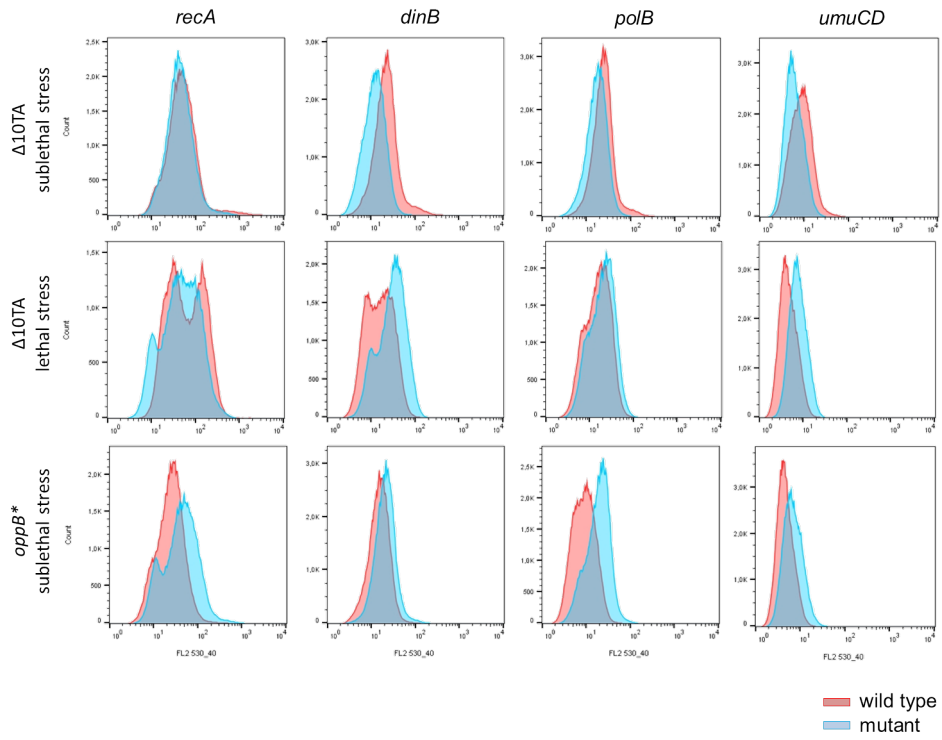

Figure 7.11: Single-cell promoter activity of SOS response genes (*recA*, *dinB*, *polB*, and *umuCD*). Fluorescence results from GFP expression from transcriptional promoter-*gfpmut2* fusions. Ciprofloxacin stress was imposed at sublethal (1/8x MIC) or lethal (625x MIC) concentrations.

For the non-stressed and sublethally stressed populations, sorting was followed by 5 hours of lethal antibiotic treatment and survival was tracked by plating (Figure 7.12). For the lethally stressed populations, sorted fractions were plated out directly. Lethal treatment after sorting in fresh MHB medium resulted in very limited survival, possibly due to persister resuscitation induced by optimal nutrient availability (data not shown). Therefore, subpopulations of *dinB*, *polB*, and *umuCD* reporter strains were sorted in spent MHB medium, preventing persisters from switching to the normal, growing state (Figure 7.12).

Figure 7.12 does not suggest any correlation between promoter activities (fluorescence levels) and persister fractions. Differences in survival between strains correspond to their persister fractions determined earlier (paragraph 7.2.3). As cells killed by ciprofloxacin do not lyse, dead cells were also sorted after lethal treatment, based on the remaining cellular GFP concentrations. In contrast, ampicillin causes lysis of dividing cells, indicating that only intact cells were sorted. Note that cultures were treated in stationary phase, leading to high overall survival in the case of ampicillin treatment.

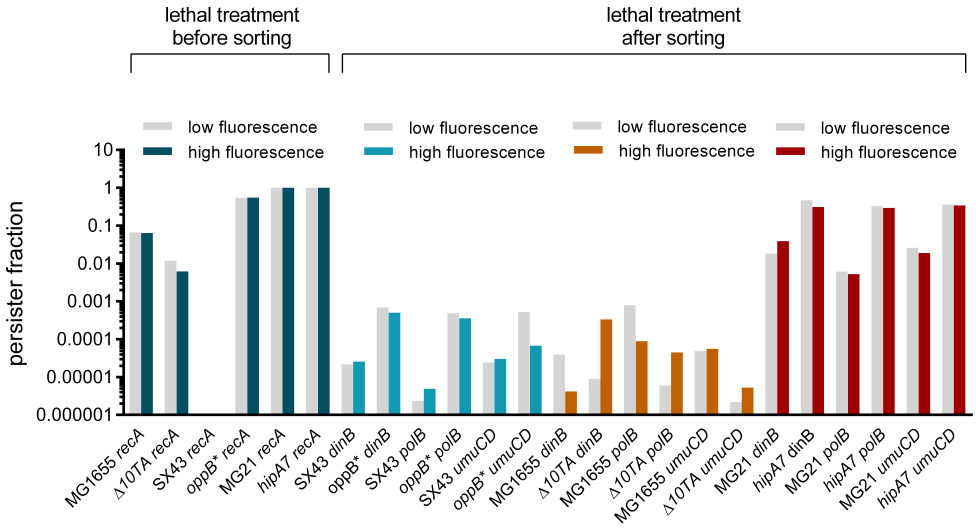

Figure 7.12: Persister fractions measured by lethal treatment of the 5 % most strongly and 5 % most weakly fluorescent subpopulations, either before or after sorting. For populations treated before sorting, persister fractions were calculated by comparing cell densities with a non-treated, but sorted population. For subpopulations treated after sorting in spent medium, persisters fractions were calculated as the ratio of cell densities after and before treatment.

7.5 Modelling

7.5.1 Estimation of model parameters

Population dynamics in a continuous culture were simulated with a theoretical model. In order to make realistic predictions on resistance development, some model parameters had to be estimated from experimental data. By measuring the growth rate during a one hour treatment as a function of the antibiotic concentration and fitting a pharmacodynamic function (see also paragraph 2.2.3), parameters such as the maximal and minimal growth rate, Hill coefficient, and MIC could be extracted. The growth rates in this equation are only representative for normal cells, as persisters are not killed during the one hour treatment. The pharmacodynamic function was determined for the strain SX43 with amikacin, assuming that the estimated parameters would be representative for other strains and antibiotics. Both exponential and stationary phase cultures were examined (Figure 7.13, Table 7.3).

Table 7.3: Fitted antibiotic susceptibility parameters of SX43 with amikacin (ψ_{max} = maximal growth rate, ψ_{min} = minimal growth rate, MIC = minimum inhibitory concentration, κ = Hill coefficient)

Parameter	Stationary phase	Exponential phase
ψ_{max}	0.136 ± 0.0645 (h^{-1})	0.870 ± 0.126 (h^{-1})
ψ_{min}	-2.19 ± 0.113 (h^{-1})	-6.68 ± 0.126 (h^{-1})
MIC	13.4 ± 1.66 (μg/ml)	0.449 ± 0.0483 (μg/ml)
κ	6.12 ± 1.86	1.78 ± 0.175

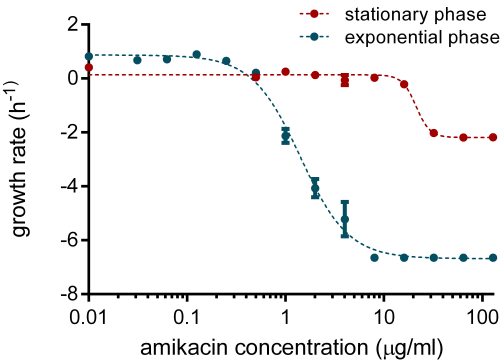

Figure 7.13: Pharmacodynamic function of SX43 with amikacin. Dashed lines visualize the Hill function [188] fitted on experimentally measured values, which are represented by dots. Error bars indicate the standard error of the mean (n=2).

7.5.2 Mathematical model of resistance evolution in a continuous culture

Complementing the experimental data, population models were built to examine the contribution of persistence to the evolution of resistance. We set up a system of differential equations and used it to verify whether higher persister levels enhance the emergence of *de novo* resistance mutations in a chemostat culture. The model was further extended with the incorporation of stress-induced mutagenesis, to investigate its contribution to the persistence-resistance link.

We established a model of persistence based on the first-order, linear differential equations proposed by Balaban *et al.* [17] (see also paragraph 4.2.2; Eq. 4.2). The evolution of resistance was considered by incorporating a third subpopulation of resistant mutants, which are generated out of the normal and persister subpopulations by mutation. As evolution towards high-level resistance is known to occur gradually over time, the resistant population was divided in subpopulations, characterized by gradually increasing MIC values. We assumed that mutations occur unidirectionally, with one mutation resulting in a fourfold increment of the MIC. The mutation rate was assumed equal for every transition.

The presence of antibiotics strongly influences the growth rate of normal cells. According to the model of Regoes *et al.* [188], pharmacodynamic parameters were incorporated as a Hill function (see also paragraph 2.2.3; Eq. 2.1). *In vivo* as well as in an *in vitro* continuous culture, the daily administration of a bolus of the drug preceeds an approximately exponential decay (Figure 7.14). In the theoretical model, continuous growth conditions translate into an extra term describing a decline of each subpopulation dependent on the dilution rate w. The resulting model is formulated mathematically in Eq. 7.2.

The model described in Eq. 7.2 includes subpopulations of normal cells (nW), persisters (pW),

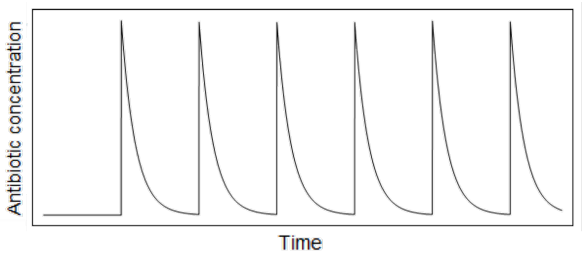

Figure 7.14: Graphical representation of the antibiotic concentration profile observed *in vivo* and simulated *in vitro* in a continuous culture. A daily bolus of the drug is followed by an exponential decay.

$$
\begin{cases}
n'_W(t) = \mu_{nW}(A) \times (1 - \frac{N_{tot}}{K}) \times n_W(t) - a_W \times \frac{N_{tot}}{K} \times n_W(t) \\
\qquad + b_W \times p_W(t) - w \times n_W(t) - m \times \mu_{nW} \times n_W(t) \\
p'_W(t) = \mu_{pW}(A) \times (1 - \frac{N_{tot}}{K}) \times p_W(t) - b_W \times p_W(t) \\
\qquad + a_W \times \frac{N_{tot}}{K} \times n_W(t) - w \times p_W(t) - m \times \mu_{pW} \times p_W(t) \\
n'_{R1}(t) = \mu_{nR1}(A) \times (1 - \frac{N_{tot}}{K}) \times n_{R1}(t) - w \times n_{R1}(t) \\
\qquad + m \times \mu_{nW} \times n_W(t) + m \times \mu_{pW} \times p_W(t) - m \times \mu_{nR1} \times n_{R1}(t) \\
n'_{R2}(t) = \mu_{nR2}(A) \times (1 - \frac{N_{tot}}{K}) \times n_{R2}(t) - w \times n_{R2}(t) \\
\qquad + m \times \mu_{nR1} \times n_{R1}(t) - m \times \mu_{nR2} \times n_{R2}(t) \\
n'_{R3}(t) = \mu_{nR3}(A) \times (1 - \frac{N_{tot}}{K}) \times n_{R3}(t) - w \times n_{R3}(t) + m \times \mu_{nR2} \times n_{R2}(t)
\end{cases}
\tag{7.2}
$$

and resistant mutants (n_{R1}, n_{R2}, and n_{R3}). To account for the effect of the total population size on the number of mutations, nW, pW, n_{R1}, n_{R2}, and n_{R3} are declared as total cell numbers instead of population densities. In contrast to the approach of Levin and Rozen [126], the growth rates μ_{nW}, μ_{nR1}, μ_{nR2}, and μ_{nR3} are dependent on the antibiotic concentration A according to Eq. 2.1, with parameters listed in Table 7.4. A gradually increasing fitness cost of resistance is taken into account, which is reflected in the parameter values of the maximal growth rate of resistant mutants (0.9 h^{-1}, 0.8 h^{-1}, and 0.7 h^{-1} respectively). We further assumed that the growth rate of persisters μ_{pW} is very small (0.00001 h^{-1}) and invariant in the face of changing antibiotic concentrations. A logistic factor $(1 - \frac{N_{tot}}{K})$ is added to the growth rates to guarantee that the populations cannot grow infinitely but eventually reach the carrying capacity K. Additionally, we

considered the fact that persister formation is often enhanced when a culture reaches stationary phase. According to Johnson and Levin [91], the switching rate a from normal to persister cells is proportional to $(\frac{N_{tot}}{K})$ to incorporate this effect.

Since we were specifically interested in the emergence of resistance by *de novo* mutations, we assumed that there are no resistant mutants present at $t = 0$ ($prop_R = 0$). However, this does not always correspond to our own experimental observations (Figure 7.4) and could lead to a discrepancy between our model and experimental data. In this first model, mutation resulting in a fourfold increase of the MIC is represented by a basal mutation rate m, which has the same value for normal cells and persisters. As m denotes a site-specific mutation rate per replication, it is multiplied by the growth rate to obtain the overall mutation rate. However, in addition to this growth-dependent mutation, slowly or non-growing bacterial cultures have also been shown to yield a large number of mutations [138]. Therefore, mutagenesis of persister cells can be highly underestimated in this model.

The differential equation system in Eq. 7.2 was solved numerically in *Wolfram Mathematica* v10, using parameter values listed in Table 7.4. These parameters are largely based on the experimental parameters used in the lab and the parameter estimations resulting from the pharmacodynamic function. The resulting population dynamics for a wild type strain are represented in Figure 7.15. For these particular parameters, the simulation predicts a relatively rapid increase of the proportion of resistant mutants, completely taking over the population after about 200 hours. Next, we considered the same situation in a strain with higher persister levels, assuming that the high persistence phenotype is lost by resistance mutations (Figure 7.15). Resistant mutants emerge considerably faster in this population, reaching the maximum cell density after 80 hours.

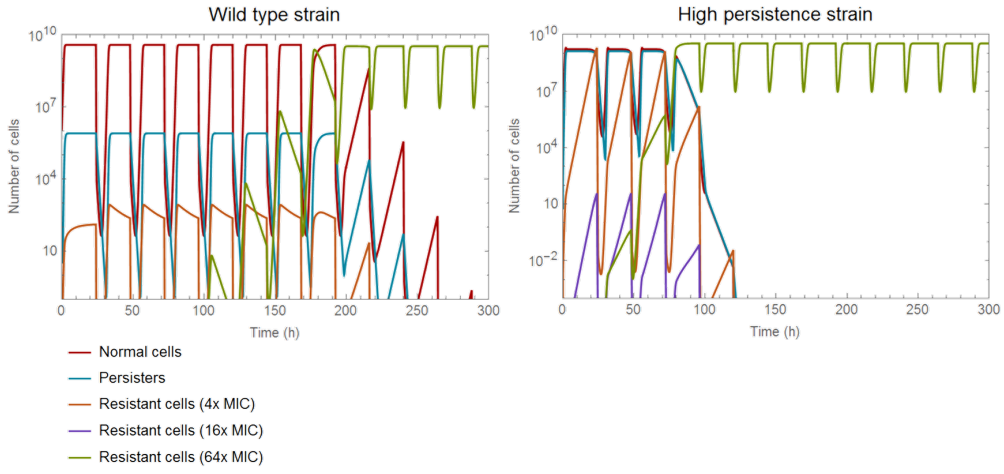

Figure 7.15: Population dynamics of normal cells, persisters and resistant mutants with gradually increasing resistance levels in a model of a continuous culture, starting from a wild type strain (left) or a high persistence strain (right) with parameters listed in Table 7.4.

Levin and Rozen [126] extended their model with the incorporation of resistant persisters, supporting the hypothesis that persisters provide a reservoir for resistant mutants. Although the presence of this subpopulation might seem counterintuitive, resistant persisters can serve as an intermediate state of persisters that have accumulated resistance mutations. We investigated how the presence of resistant persisters affects the final outcome of our simulations. As this extra subpopulation appeared to have a negligible effect on the dynamics of the other subpopulations (not shown), we did not further pursue this extra complexity.

Table 7.4: Overview of the model parameters and their numerical values (*hip* strain = high persistence strain)

Parameter	Description	Value
μ_{nWmax}	maximal growth rate of wild type strain	1 h^{-1}
μ_{nWmin}	minimal growth rate of wild type strain	-6 h^{-1}
μ_{pWmax}	maximal growth rate of wild type persisters	0.00001 h^{-1}
μ_{nR1max}	maximal growth rate of resistant strain 1	0.9 h^{-1}
μ_{nR2max}	maximal growth rate of resistant strain 2	0.8 h^{-1}
μ_{nR3max}	maximal growth rate of resistant strain 3	0.7 h^{-1}
μ_{nRmin}	minimal growth rate of resistant strains	-6 h^{-1}
MIC_W	minimum inhibitory concentration for wild type strain	0.008 μg/ml
MIC_{R1}	minimum inhibitory concentration for resistant strain 1	0.032 μg/ml
MIC_{R2}	minimum inhibitory concentration for resistant strain 2	0.128 μg/ml
MIC_{R3}	minimum inhibitory concentration for resistant strain 3	0.512 μg/ml
κ_W	Hill coefficient of wild type strain	1
κ_R	Hill coefficient of resistant strains	1
K	carrying capacity	5×10^9
a	switching rate normal cells $\rightarrow$ persisters	wild type strain: 0.00001 h^{-1} *hip* strain: 0.5 h^{-1}
b	switching rate persisters $\rightarrow$ normal cells	0.14 h^{-1}
m	basal site-specific mutation rate per replication	8 $\times 10^{-10}$
A_{max}	antibiotic peak concentration	0.37 μg/ml
w	dilution rate	0.231 h^{-1}
p_{init}	initial number of persisters	1
t_{init}	total initial cell density	2×10^5
$prop_R$	initial proportion of resistant cells	0
τ	max. fold increase in mutation rate	wild type: 4 *hip* strain: 100
s_n	steepness of curve	wild type 4 *hip* strain: 4

Incorporation of stress-induced mutagenesis

Until now, we considered mutation towards resistance by taking into account a basal site-specific mutation rate per replication, m. However, as this mutation rate is growth-based, it strongly underestimates mutation occurring in the slowly growing persister subpopulation. Furthermore, bacterial responses to different types of stress have been shown to increase mutation rates, thereby serving as a potential accelerator of adaptive evolution in unfavorable environments [14]. As proposed by Ram and Hadany [184], we modeled this stress-induced mutagenesis by making the

mutation rate U_n inversely proportional to the fitness of a cell according to Eq. 7.3. The growth rate μ_n was used as a fitness measure (Figure 7.16). Additionally, we assume no mutation in case of a negative growth rate, which implies the presence of lethal stress.

$$U_n(\mu_n) = \begin{cases} m + (\tau - 1) \times m \times e^{-s \times \mu_n} & \mu_n \geq 0 \\ 0 & \mu_n < 0 \end{cases} \tag{7.3}$$

In Eq. 7.3, τ represents the fold increase in mutation rate under conditions of maximal stress ($\mu_n = 0$). m is the basal mutation rate, which is the same as in Eq. 7.2 and refers to the mutation rate under conditions of minimal stress ($\mu_n = \mu_{nmax}$). s is a measure for the steepness of the curve.

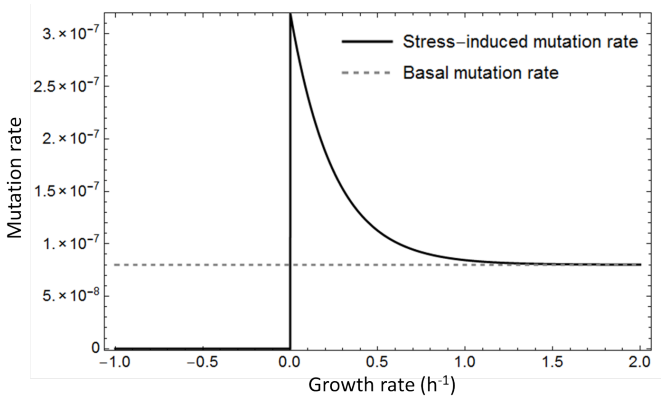

Figure 7.16: Graphical representation of a model of stress-induced mutagenesis, with the mutation rate being inversely proportional to the growth rate for positive growth rates and zero for negative growth rates ($\tau_n = 4$, $s_n = 4$, $m = 8 \times 10^{-10}$).

This stress-induced mutation rate was incorporated into our model by replacing m in Eq. 7.2 by U_n given by Eq. 7.3. For persisters, mutation was considered independent of the growth rate. Using additional parameter values (τ and s_n) listed in Table 7.4, a graphical representation of the population dynamics resulting from this model is provided in Figure 7.17. Generally, the incorporation of stress-induced mutagenesis generates surprisingly small differences with the basic model (Figure 7.15). Varying the parameter values of τ and s only slightly affects the outcome (not shown). We can conclude that our model does not support stress-induced mutagenesis as a major contributor to the correlation between persistence and resistance.

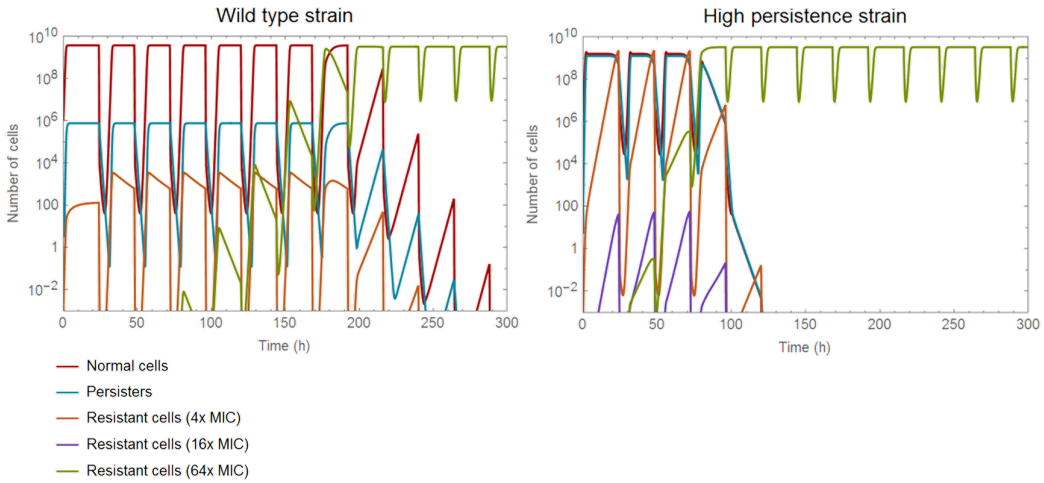

Figure 7.17: Population dynamics of normal cells, persisters and resistant mutants in a model incorporating stress-induced mutagenesis, starting from a wild type strain (left) or a high persistence strain (right). Simulations were performed with parameters listed in Table 7.4.

Chapter 8

Discussion

8.1 Experimental evolution of antibiotic resistance in high and low persistence mutants

8.1.1 Persistence catalyzes resistance evolution on solid growth medium

Apart from some theoretical hypotheses [39, 126, 169], the contribution of persistence to resistance evolution so far remained unexplored experimentally. By recording the emergence of resistant colonies on solid medium, we demonstrated that resistance evolution is catalyzed by the presence of persisters. In particular, strains characterized by high persister levels (*oppB** and *hipA7*) not only showed a faster emergence, but also a higher frequency of resistant mutants, while the opposite was observed in a strain with low persister levels (Δ*10TA*) (Figure 7.1). Killing curves reveal that between-strain differences in persister levels are maximal in stationary phase, at the moment of plating. After one day of antibiotic exposure on solid medium, susceptible cells are killed [35] whereas persisters are able to survive much longer. Although rates of cell division are negligible, these viable cells remain prone to DNA damage [234]. The time of survival on plate determines the extent of DNA damage, and therefore the number of mutations that accumulate.

Despite the clear results for *oppB**, Δ*10TA*, and *hipA7*, the same correlation was not detected in all tested strain-antibiotic combinations. More resistant colonies were encountered for Δ*10TA* than for its wild type on plates with ampicillin, and the emergence of resistance was less prominent in *hipA7* than its wild type on plates with ciprofloxacin (Figure B.2). As we did not determine persister levels with these antibiotics, these results are difficult to interpret in terms of the persistence-resistance correlation. Furthermore, Δ*lon* exhibited slower resistance development than its wild type whereas persister levels did not differ significantly (Figure 7.2). Despite a similar experimental set-up, the observed persister levels of Δ*lon* do not confirm the results of Maisonneuve *et al.* [147]. One explanation could be the different genetic background, as strain-specific effects of persistence genes have been observed earlier [104, 198]. However, in other studies, Δ*lon* mutants also not always displayed decreased persistence [199, 239]. Lon protease plays a role in the regulation of multiple physiological processes and central stress responses [222], which could explain the observed differences.

On plates supplemented with ampicillin, *hipA7* not only showed more resistant colonies than its wild type, but also a remarkably increased emergence of satellite colonies after 5-8 days. Medaney *et al.* [153] argued that this phenomenon can be attributed to the presence of persisters, which are able to survive a period of antibiotic exposure before detoxification by β-lactamase-producing resistant colonies takes place. For putative satellite colonies emerging on wild type plates, their non-resistant nature was confirmed by the absence of growth when restreaked on fresh, antibiotic-containing agar. Remarkably, suspected satellite colonies of the *hipA7* mutant were still able to grow on these plates, suggesting that they might not represent true satellite colonies.

As we wondered whether persistence also accelerates the emergence of resistance in other settings, we built a theoretical model to simulate resistance evolution in a continuous culture. Even when stress-induced mutagenesis is not considered, the model predicts an accelerated emergence and spread of resistant mutants due to higher persister levels (Figure 7.15). The considerably increased viability of persisters in the presence of lethal antibiotic doses is key to this phenomenon.

8.1.2 The contribution of persistence to resistance depends on the treatment conditions

Inspired by our theoretical model predictions and observations on the emergence of resistance on solid media, we verified whether similar evolutionary dynamics were encountered in other experimental setups. Unexpectedly, we could not support our hypothesis with evolution experiments involving either serial transfer or continuous growth. To understand the discrepancy between the results of these experiments and the plate assay, experimental parameters and growth characteristics should be considered thoroughly.

Plate assays versus serial transfer experiments

In the serial transfer experiments, strains were evolved under a constant, sublethal antibiotic selection pressure that was adjusted to the changing MIC. Except for the slower resistance development in Δ*10TA*, the MIC of high and low persistence strains followed similar trajectories (Figure 7.3). The bottleneck imposed during serial transfer determines the extent of genetic drift and therefore the chance that a beneficial mutation reaches fixation. Although the bottleneck in our experiments ($1:10,000$) was stronger than normally advocated [228], we obtained resistance levels that are comparable to those reported in literature [172]. In contrast to the plate assays, in which single mutations are probably sufficient to overcome the constant antibiotic doses, the high resistance levels obtained in serial transfer experiments probably require an accumulation of multiple mutations.

In addition to the population bottleneck, the timing of antibiotic treatment strongly influences

population dynamics. In the plate assay, stationary phase cultures containing relatively high numbers of persisters were exposed to supra-MIC antibiotic doses. In contrast, small fractions of populations evolved in serial transfer experiments were inoculated daily in fresh, antibiotic-containing medium. Importantly, fresh medium triggers persister resuscitation [100], potentially diminishing the effect of persistence at the moment of antibiotic exposure.

An agar plate supplemented with antibiotics represents a strongly simplified environment in which a cell's growth capacity is determined by the presence of resistance mutations, without being influenced by its fitness relative to other genotypes. In other words, competition does not play a role and the time at which a resistant mutant emerges is only of minor importance. Conversely, strains evolved in serial transfer experiments experience a much larger influence of competition. The first beneficial mutation that provides a sufficiently high resistance level can take over the population and define the direction of future fitness trajectories. Because of random chance associated with this process, the direction of further genotypic changes may be constrained. Furthermore, the fitness cost of resistance under sub-MIC conditions can explain why several resistant mutants, although emerging rapidly in high persistence mutants, are outcompeted in a batch culture while they would survive on plate.

Continuous culture: theoretical predictions versus experimental observations

To investigate the contribution of persistence to resistance evolution in clinically relevant settings, we simulated an *in vivo* pharmacokinetic profile in a chemostat. The exponentially decaying antibiotic concentration, combined with the applied peak concentration and half-life of the antibiotic, indeed mimicked the conditions of an infection environment. While alternating periods of lethal antibiotic treatment and antibiotic-free growth do not select for resistance [221], we expected that the gradual decrease of the antibiotic concentration to sub-MIC levels would favor resistant mutants in the chemostat [9].

Compared to the other evolution experiments, population dynamics in a chemostat culture are more complex and difficult to predict due to the constantly changing antibiotic concentration. In this light, our mathematical model is crucial to provide insight into the behavior of a population in a continuous culture. The model predicts a similar correlation between persistence and resistance evolution as observed on plate. Surprisingly, our experimental data do not support these predictions, as resistance development was slightly delayed in a *hip* mutant ($oppB^*$), and slightly accelerated in a low persistence mutant ($\Delta 10TA$). Yet, it is important to note that we detected resistance development in only one culture per strain, questioning the statistical relevance of these observations.

Pharmacodynamical parameters (Hill coefficient, minimal and maximal growth rate) can constitute a first point of difference between the theoretical predictions and experimental observations. The cellular physiology of bacteria in a continuously growing population neither corresponds to exponential phase, nor to stationary phase physiology [59]. Parameter values used in the model were measured in exponential phase, possibly resulting in deviations from the actual values.

Before each new drug bolus was added, the cultures were found to be at steady state, with a population density equal to the carrying capacity. These conditions are characterized by nutrient limitation, resulting in a growth rate that is identical to the low dilution rate. At the same time, bacteria encounter low levels of antibiotic stress, as the initial bolus has been diluted to sub-MIC values. Given that both nutrient stress [64] and antibiotic stress [46, 91, 116] can trigger persister formation, the question arises as to when persister levels reach their maximum during a treatment cycle. In the model, we assumed that persister formation increases with the population density, reaching a maximum before the addition of a new bolus. Hence, between-strain variation in persister levels in the model are maximal at the start of antibiotic treatment. As we did not incorporate the effect of antibiotics on persister formation, persister level differences, and therefore the actual effects of persistence, might be overestimated at this point.

The growth deficit of persister cells is considered their most obvious fitness cost. This effect is incorporated in the model by assuming a slow growth rate. However, additional costs have been identified. Van den Bergh *et al.* [221] observed drastically reduced fitness in antibiotic-free conditions, which could not be explained by a diminished growth rate. Indeed, it has been suggested that persistence has hidden costs such as stationary phase mortality and a lengthened lag phase [206], which are not addressed in the model. As a consequence of these non-incorporated costs, the fitness of *hip* mutants, and thus their contribution to the generation of resistant mutants, is likely overestimated in the model.

Competition between persistence and resistance, two alternative antibiotic survival strategies, could slow down resistance evolution in *hip* mutants. Possibly, the spread of resistance is limited by the small selective advantage of a resistant mutant versus a *hip* mutant under our treatment conditions, rather than by the supply rate of resistance mutations that might still be higher in the *hip* mutant. This is also supported by the observation that some chemostat cultures did not develop resistance. Simulating competition between a wild type, high persistence, and resistant strain with a model of a continuous culture illustrates how the treatment conditions are decisive for the evolutionary outcome (not shown). A high treatment frequency combined with a high or intermediate peak dose results in an antibiotic concentration that is almost permanently above the MIC, thereby selecting for resistance. When very high peak doses are encountered at a low frequency, persistence comes out as the most favorable strategy and is thus able to slow down

selection for resistance.

On the other hand, Vogwill *et al.* [226] proposed that certain environments can simultaneously select for persistence and resistance, indicating that both strategies can be considered as complementary. If true, selection for high persister levels in low persistence strains could complicate our conclusions on the persistence-resistance correlation. Unfortunately, the increased survival provided by resistance mechanisms interfere with an accurate measurement of persister levels, preventing us from tracking persister levels during chemostat evolution. Hence, we cannot completely rule out selection for high persistence in strains with initially low persister levels.

Despite valuable insights provided by our population model, some imperfections of this theoretical approach should be noted. First of all, mutagenesis was considered as a deterministic process occurring with a fixed probability, while a model involving stochastic mutation (e.g. by simulating a Monte Carlo process) would provide more realistic predictions. Secondly, persisters in the model were assumed to be dormant, according to the currently established paradigm. However, recent studies challenge this view [171, 229] and motivate another theoretical implementation of persistence. The mutation rate of persisters, which is now growth-based, would increase in this case, strengthening the role of persisters as an evolutionary reservoir of resistant mutants. Finally, the availability of more experimental data would allow us to fit models onto the data and extract parameters that cannot be measured directly, thereby enabling an even more mutual interaction between theoretical models and experimental observations.

8.2 Persistence versus resistance in environmental *E. coli* isolates

Using mutants with drastically increased or reduced persister levels, a correlation was found between persistence and resistance development on solid growth medium. To investigate whether these findings were confirmed in genetically diverse natural isolates, we randomly selected 20 strains from the ECOR collection and determined their MIC values, persister levels, and resistance evolution in the presence of ciprofloxacin and ampicillin.

A correlation analysis suggests that persister levels are partially predictive for the rate of resistance mutations emerging on plate (Figure 7.7). This positive correlation was however not statistically significant. The high degree of survival detected in stationary phase cultures treated with ciprofloxacin resulted in a smaller range of persister levels than initially anticipated. Conducting future experiments in exponential phase is likely to extend this range and provide more statistical power to find correlations. When treating exponential phase cultures of ECOR strains with norfloxacin, another fluoroquinolone, Stewart and Rozen [207] indeed observed that persister levels varied over

four orders of magnitude. In addition, increasing the number of resistant colonies by reducing the antibiotic concentration in the agar plates could maximize the reliability of these data. Satellite colonies on ampicillin plates could be circumvented by investigating other β-lactams such as carbenicillin or ceftazidime.

8.3 The SOS response accelerates adaptive mutagenesis in high persistence mutants

After having established a link between persistence and resistance development, we set out to investigate the underlying mechanisms. An enhanced survival capacity may be not the only feature of persistence that promotes resistance development. Several stress responses trigger and enable the active maintenance of the persister state (see also paragraph 1.3.4). The same stress responses have been shown to catalyze adaptive evolution, and can therefore provide a link between persistence and resistance [39].

8.3.1 Sublethal ciprofloxacin concentrations promote mutagenesis

Sublethal doses of bactericidal antibiotics can effectively induce mutagenesis [76, 109, 163]. Supporting this statement, sublethal ciprofloxacin doses were found to increase mutation rates in MG1655, Δ*10TA*, SX43, and *oppB** (Figure 7.8). Using a similar approach, Kohanski *et al.* [109] and Nair *et al.* [163] noted a comparable effect of norfloxacin, also a quinolone, on *E. coli* and *P. aeruginosa* mutation rates respectively. Conversely, ampicillin treatment of *hipA7* and MG21 did not significantly affect mutation rates. An unequal impact of ciprofloxacin and ampicillin on mutation rates can be attributed to their mode of action. By corrupting the function of DNA gyrase, fluoroquinolones are well-known DNA-damaging agents and strong inducers of the SOS response [128, 166, 179]. As the target of ampicillin is not directly involved in mutagenesis, the modest impact on the mutation rate was not unexpected. However, mutagenic effects of sublethal β-lactam levels have already been reported, resulting in similar stress-induced mutation rates as with fluoroquinolones [76, 109, 163]. According to Gutierrez *et al.* [76], this β-lactam-induced mutagenesis is executed by the error-prone polymerase PolIV and regulated by the sigma factor RpoS. Distinct experimental conditions, such as the antibiotic concentration and culture volume, can explain why we did not observe this effect.

Both untreated and ciprofloxacin-treated cultures of Δ*lon* exhibited remarkably high mutation rates (Figure 7.8). These findings can be attributed to increased cellular concentrations of UmuD, a subunit of the SOS-induced error-prone polymerase PolV, in the absence of Lon. In particular, Lon is held responsible for proteolysis of UmuD, thereby tuning cellular UmuD concentrations to the need for error-prone DNA repair [60, 73].

8.3.2 Persister levels correlate with stress-induced mutation rates and SOS response activation under sublethal antibiotic stress

Remarkably, the induction of mutagenesis by sublethal ciprofloxacin doses was found to be enhanced in the *hip* mutant *oppB** and diminished in the low persistence mutant Δ*10TA* (Figure 7.8). Assuming that persisters are slowly dividing cells, the impact on the mutation rate per genome replication is likely even higher than measured. Survival of normal cells is generally not affected by sub-MIC antibiotic concentrations. Hence, these results strongly suggest that the ability of persisters to survive lethal drug exposure is not the only feature catalyzing resistance.

The observed correlation between stress-induced mutation rates and persister levels suggests a stronger induction of stress responses in *hip* mutants when facing antibiotic stress. By measuring fluorescence of strains encoding promoter-*gfpmut2* fusions, we investigated the transcription level of genes involved in the stringent response, SOS response, general stress response, oxidative stress response, and extracytoplasmic stress response (Figures 7.10, 7.11, D.1, and D.2). As the data for the SOS response revealed a remarkable and consistent trend, we focus the discussion on these findings. Under sublethal ciprofloxacin stress, a higher transcriptional activity of the SOS response genes *recA*, *dinB*, *polB*, and *umuCD* was found in *hip* mutants, while a lower activity was detected in low persistence strains. These differences were observed at the population level as well as at the single-cell level. Although the population-average fluorescence shift is usually small, it was encountered consistently in all replicate samples. The fluorescence distributions do not reveal multimodality (Figure 7.11), indicating that the shifted average fluorescence level results from a population-wide change rather than from a small fraction of cells deviating from the bulk of the population. It is important to note that expression was only measured at the level of transcription, ignoring any posttranscriptional and posttranslational regulation mechanisms.

Of all stress responses, the SOS response has the strongest mutagenic effect. Importantly, Cirz *et al.* [35] provided evidence for the central role of the SOS response in the evolution of quinolone resistance, emphasizing the impact of our results. Concisely, the bacterial response to ciprofloxacin involves DNA damage, followed by induction of the SOS response and error-prone DNA repair which causes adaptive mutations [202] (Figure 3.2). According to our results, high persistence mutations enhance this process at the level of SOS induction.

To investigate if persisters experience similar levels of DNA damage and SOS induction upon lethal antibiotic treatment, we sorted populations after lethal ciprofloxacin treatment and determined the number of surviving persisters in subpopulations with high and low levels of SOS induction (Figure 7.12). No correlation was found between persister fractions and fluorescence levels, indicating that persisters not necessarily undergo lower levels of DNA damage and SOS induction upon

lethal ciprofloxacin stress. These findings support conclusions drawn by Völzing and Brynildsen [227], stating that persisters towards ofloxacin experience the same level of DNA damage and SOS induction as susceptible cells, but the persistence phenotype does rely on DNA repair when the antibiotic stress is relieved. The central role of the SOS response in persistence towards ciprofloxacin was already suggested by Dörr *et al.* [46]. Yet, according to their findings, persisters experience lower levels of DNA damage and SOS induction than the bulk of the population, as too extensive damage compromises the survival potential. Völzing and Brynildsen [227] ascribe this discrepancy to the fact that their measurements were performed in stationary phase, whereas Dörr *et al.* [46] investigated exponential phase cultures.

To investigate if persisters correspond to cells with a high SOS induction in unstressed or sublethally stressed populations, subpopulations with high and low SOS promoter activity were sorted and the persister level of the subpopulations was determined. Single-cell expression levels of the SOS-dependent error-prone polymerases did not correlate with persistence, indicating that high persistence mutations cause a population-wide increase in SOS response, yet the increased persister level does not seem to be a direct consequence.

Together, the fluctuation assays, stress response measurements, and flow cytometry experiments suggest that sublethal ciprofloxacin levels promote both mutagenesis and the population-wide SOS response activity in *hip* mutants, but an increased activity in the persister fraction does not seem to be responsible for this phenomenon. However, as this generally increased SOS response activity also affects the surviving persister fraction, it can be sufficient to accelerate resistance evolution. Higher numbers of persisters in these strains even amplify this effect. Stated otherwise, antibiotic tolerance of persisters combined with an active or even elevated SOS response in these cells is sufficient to constitute an important evolutionary reservoir of resistant mutants.

On the other hand, an elevated population-wide SOS response activity could increase the number of resistance-conferring mutations in all cells. Therefore, we are not sure whether persisters indeed constitute the major pool of resistant mutants. In future experiments, it would be interesting to monitor resistance development of a culture consisting solely of persisters. An overnight culture could be treated with lethal antibiotic doses in order to kill all non-persisters. The resulting persister fraction could be plated out on antibiotic-containing agar plates and the emergence of resistant colonies could be surveyed as was done in the plate assays. However, the preceding antibiotic treatment that is required to isolate persisters can influence adaptive evolution and complicate comparisons with non-treated cultures.

Population dynamics predicted by our theoretical model are only slightly influenced when stress-induced mutagenesis is incorporated. This can be attributed to a lack of known underlying mechanisms that can be translated properly into mathematical equations. We now used a model

proposed by Ram and Hadany [184], in which the mutation rate is inversely proportional to the fitness of the cells. However, as mutation rates are still expressed as the number of mutations per cell division, the negligible growth rate of persisters in the model results in an underestimation of mutations occurring in this subpopulation. We can conclude that the current model of stress-induced mutagenesis is largely based on theoretical assumptions and definitely needs to be supported and fine-tuned by experimental data.

8.4 Conclusion and future perspectives

This work highlights the contribution of persistence to the emergence of resistance. The presence of persisters catalyzes the development of resistance in lab strains grown on solid medium. In natural *E. coli* isolates, persistence is likely to play the same role although statistical evidence is currently lacking. Yet, the contribution of persistence strongly depends on the growth conditions. Evolution of resistance in serial transfer experiments is only slightly affected by altered persister levels, probably due to the timing of antibiotic treatment and the effect of competition. Although theoretical models suggest that persisters accelerate resistance development under *in vivo*-like conditions, evolution experiments in a chemostat do not support these predictions.

The SOS response is a potential mechanism that links persistence and resistance towards ciprofloxacin. Strains with higher persister levels show a stronger population-wide expression of SOS-dependent error-prone polymerases, which is also reflected in their increased stress-induced mutation rate. The SOS induction in persisters is similar to the bulk of the population. Still, high persistence strains can show a higher adaptive potential through the increased number of surviving persisters combined with an elevated SOS response activity in the face of antibiotic treatment.

Our findings establish several directions for future research. To provide evidence for the causal role of SOS polymerases in the increased mutation rates and resistance evolution, mutant strains could be generated that exhibit high persister levels but the lack genes encoding for error-prone polymerases (*dinB*, *polB*, and *umuCD*). If evolution experiments and fluctuation assays with these strains reveal a central role for these polymerases in resistance evolution, the SOS response can be proposed as a target to counteract rapid resistance development towards quinolones.

Persistence contributes to resistance development on plate, but its impact in clinical settings remains unclear. The chemostat constitutes a convenient tool to investigate which treatment conditions (e.g. antibiotic peak dose, treatment frequency, etc.) cause the largest effect of altered persister levels on resistance development. The clinical relevance of these findings could then be explored in important pathogens and clinical isolates of chronic infections, which have been selected *in vivo* for higher persister levels.

Although we considered the spread of resistance mutations as a consequence of vertical transmission, horizontal gene transfer can also play a dominant role in this process. Importantly, it has been shown that the induction of the SOS response by fluoroquinolones promotes transfer of mobile genetic elements [220]. Combined with our results, this can imply an even stronger effect on the spread of resistance in high persistence mutants. Hence, a study on the contribution of horizontal gene transfer using naturally competent strains could help unraveling the mechanisms underlying the persistence-resistance correlation. Eventually, novel insights could underscore the importance of anti-persister therapies, and provide new targets to prevent the emergence and spread of resistant pathogens.

Bibliography

[1] Acosta, M. B., Ferreira, R. C., Padilla, G., Ferreira, L. C. and Costa, S. O. (2000). Altered expression of oligopeptide-binding protein (OppA) and aminoglycoside resistance in laboratory and clinical *Escherichia coli* strains. *Journal of Medical Microbiology*, 49(5):409–413.

[2] Adams, K. N., Takaki, K., Connolly, L. E., Wiedenhoft, H., Winglee, K., Humbert, O., Edelstein, P. H., Cosma, C. L. and Ramakrishnan, L. (2011). Drug tolerance in replicating mycobacteria mediated by a macrophage-induced efflux mechanism. *Cell*, 145(1):39–53.

[3] Ades, S. E. (2008). Regulation by destruction: design of the σ^E envelope stress response. *Current Opinion in Microbiology*, 11(6):535–540.

[4] Akiyama, Y., Kanehara, K. and Ito, K. (2004). RseP (YaeL), an *Escherichia coli* RIP protease, cleaves transmembrane sequences. *The EMBO Journal*, 23(22):4434–4442.

[5] Alekshun, M. N. and Levy, S. B. (2007). Molecular mechanisms of antibacterial multidrug resistance. *Cell*, 128(6):1037–1050.

[6] Altuvia, S., Weinstein-Fischer, D., Zhang, A., Postow, L. and Storz, G. (1997). A small, stable RNA induced by oxidative stress: Role as a pleiotropic regulator and antimutator. *Cell*, 90(1):43–53.

[7] Amato, S. M., Orman, M. A. and Brynildsen, M. P. (2013). Metabolic control of persister formation in *Escherichia coli*. *Molecular Cell*, 50(4):475–487.

[8] Andersson, D. I. and Hughes, D. (2010). Antibiotic resistance and its cost: is it possible to reverse resistance? *Nature Reviews Microbiology*, 8(4):260–271.

[9] Andersson, D. I. and Hughes, D. (2014). Microbiological effects of sublethal levels of antibiotics. *Nature Reviews Microbiology*, 12(7):465–478.

[10] Andrews, J. M. (2001). Determination of minimum inhibitory concentrations. *Journal of Antimicrobial Chemotherapy*, 48:5–16.

[11] Ankomah, P. and Levin, B. R. (2014). Exploring the collaboration between antibiotics and the immune response in the treatment of acute, self-limiting infections. *Proceedings of the National Academy of Sciences of the United States of America*, 111(23):8331–8338.

[12] Baba, T., Ara, T., Hasegawa, M., Takai, Y., Okumura, Y., Baba, M., Datsenko, K. A., Tomita, M., Wanner, B. L. and Mori, H. (2006). Construction of *Escherichia coli* K-12 in-frame, single-gene knockout mutants: the Keio collection. *Molecular Systems Biology*, 2:2006.0008.

[13] Baek, S., Li, A. H. and Sassetti, C. M. (2011). Metabolic regulation of mycobacterial growth and antibiotic sensitivity. *PLoS Biology*, 9(5):e1001065.

[14] Baharoglu, Z. and Mazel, D. (2014). SOS, the formidable strategy of bacteria against aggressions. *FEMS Microbiology Reviews*, 38(6):1126–1145.

[15] Balaban, N. Q. (2011). Persistence: mechanisms for triggering and enhancing phenotypic variability. *Current Opinion in Genetics and Development*, 21(6):768–775.

[16] Balaban, N. Q., Gerdes, K., Lewis, K. and McKinney, J. D. (2013). A problem of persistence: still more questions than answers? *Nature Reviews Microbiology*, 11(8):587–91.

[17] Balaban, N. Q., Merrin, J., Chait, R., Kowalik, L. and Leibler, S. (2004). Bacterial persistence as a phenotypic switch. *Science*, 305:1622–1625.

[18] Barrick, J. E. and Lenski, R. E. (2013). Genome dynamics during experimental evolution. *Nature Reviews Genetics*, 14(12):827–839.

[19] Battesti, A., Majdalani, N. and Gottesman, S. (2011). The RpoS-mediated general stress response in *Escherichia coli*. *Annual Review of Microbiology*, 65:189–213.

[20] Baysarowich, J., Koteva, K., Hughes, D. W., Ejim, L., Griffiths, E., Zhang, K., Junop, M. and Wright, G. D. (2008). Rifamycin antibiotic resistance by ADP-ribosylation: Structure and diversity of Arr. *Proceedings of the National Academy of Sciences of the United States of America*, 105(12):4886–4891.

[21] Beaber, J. W., Hochhut, B. and Waldor, M. K. (2004). SOS response promotes horizontal dissemination of antibiotic resistance genes. *Nature*, 427:72–74.

[22] Becker, G., Klauck, E. and Hengge-Aronis, R. (1999). Regulation of RpoS proteolysis in *Escherichia coli*: the response regulator RssB is a recognition factor that interacts with the turnover element in RpoS. *Proceedings of the National Academy of Sciences of the United States of America*, 96(11):6439–6444.

[23] Bhargava, N., Sharma, P. and Capalash, N. (2014). Pyocyanin stimulates quorum sensing-mediated tolerance to oxidative stress and increases persister cell populations in *Acinetobacter baumannii*. *Infection and Immunity*, 82(8):3417–3425.

[24] Bigger, J. W. (1944). Treatment of staphylococcal infections with penicillin by intermittent sterilisation. *The Lancet*, ii(8):497–500.

[25] Blango, M. G. and Mulvey, M. A. (2010). Persistence of uropathogenic *Escherichia coli* in the face of multiple antibiotics. *Antimicrobial Agents and Chemotherapy*, 54(5):1855–1863.

[26] Blattner, F., Plunkett G, I., Bloch, C., Perna, N., Burland, V., Riley, M., Collado-Vides, J., Glasner, J., Rode, C., Mayhew, G., Gregor, J., Davis, N., Kirkpatrick, H., Goeden, M., Rose, D., Mau, B. and Shao, Y. (1997). The complete genome sequence of *Escherichia coli* K-12. *Science*, 277:1453–1462.

[27] Breidenstein, E. B. M., de la Fuente-Núñez, C. and Hancock, R. E. W. (2011). *Pseudomonas aeruginosa*: All roads lead to resistance. *Trends in Microbiology*, 19(8):419–426.

[28] Brennan, R. G. and Link, T. M. (2007). Hfq structure, function and ligand binding. *Current Opinion in Microbiology*, 10(2):125–133.

[29] Butala, M., Žgur-Bertok, D. and Busby, S. J. W. (2009). The bacterial LexA transcriptional repressor. *Cellular and Molecular Life Sciences*, 66(1):82–93.

[30] Campbell, E. A., Korzheva, N., Mustaev, A., Murakami, K., Nair, S., Goldfarb, A. and Darst, S. A. (2001). Structural mechanism for rifampicin inhibition of bacterial RNA polymerase. *Cell*, 104(6):901–912.

[31] Caroff, N., Espaze, E., Gautreau, D., Richet, H. and Reynaud, A. (2000). Analysis of the effects of -42 and -32 *ampC* promoter mutations in clinical isolates of *Escherichia coli* hyperproducing AmpC. *Journal of Antimicrobial Chemotherapy*, 45(6):783–788.

[32] Cataudella, I., Sneppen, K., Gerdes, K. and Mitarai, N. (2013). Conditional cooperativity of toxin - antitoxin regulation can mediate bistability between growth and dormancy. *PLoS Computational Biology*, 9(8):e1003174.

[33] Chiang, S. M. and Schellhorn, H. E. (2012). Regulators of oxidative stress response genes in *Escherichia coli* and their functional conservation in bacteria. *Archives of Biochemistry and Biophysics*, 525(2):161–169.

[34] Chou, H., Chiu, H., Delaney, N. F., Segrè, D. and Marx, C. J. (2011). Diminishing returns epistasis among beneficial mutations decelerates adaptation. *Science*, 332(6034):1190–1192.

[35] Cirz, R. T., Chin, J. K., Andes, D. R., de Crécy-Lagard, V., Craig, W. A. and Romesberg, F. E. (2005). Inhibition of mutation and combating the evolution of antibiotic resistance. *PLoS Biology*, 3(6):1024–1033.

[36] Cisneros-Farrar, F. and Parsons, L. C. (2007). Antimicrobials: Classifications and uses in critical care. *Critical Care Nursing Clinics of North America*, 19(1):43–51.

[37] Claudi, B., Spröte, P., Chirkova, A., Personnic, N., Zankl, J. and Schürmann, N. (2014). Phenotypic variation of *Salmonella* in host tissues delays eradication by antimicrobial chemotherapy. *Cell*, 158:722–733.

[38] Cochran, J. W. and Byrne, R. W. (1974). Isolation and properties of a ribosome-bound factor required for ppGpp and pppGpp synthesis in *Escherichia coli* isolation and properties of a ribosome-bound required for ppGpp and pppGpp synthesis in *Escherichia coli*. *The Journal of Biological Chemistry*, 249(2):353–360.

[39] Cohen, N. R., Lobritz, M. A. and Collins, J. J. (2013). Microbial persistence and the road to drug resistance. *Cell Host and Microbe*, 13(6):632–642.

[40] Corvec, S., Caroff, N., Espaze, E., Marraillac, J. and Reynaud, A. (2002). -11 Mutation in the *ampC* promoter increasing resistance to β-Lactams in a clinical *Escherichia coli* strain. *Antimicrobial Agents and Chemotherapy*, 46(10):3265–3267.

[41] Dalton, T., Cegielski, P., Akksilp, S., Asencios, L., Caoili, J. C., Cho, S. N., Erokhin, V. V., Ershova, J., Gler, M. T., Kazennyy, B. Y., Kim, H. J., Kliiman, K., Kurbatova, E., Kvasnovsky, C., Leimane, V., Van Der Walt, M., Via, L. E., Volchenkov, G. V., Yagui, M. A. and Kang, H. (2012). Prevalence of and risk factors for resistance to second-line drugs in people with multidrug-resistant tuberculosis in eight countries: A prospective cohort study. *The Lancet*, 380(12):1406–1417.

[42] Datsenko, K. A. and Wanner, B. L. (2000). One-step inactivation of chromosomal genes in *Escherichia coli* K-12 using PCR products. *Proceedings of the National Academy of Sciences of the United States of America*, 97(12):6640–6645.

[43] Davies, J. and Davies, D. (2010). Origins and evolution of antibiotic resistance. *Microbiology and Molecular Biology Reviews*, 74(3):417–433.

[44] De Groote, V. N., Fauvart, M., Kint, C. I., Verstraeten, N., Jans, A., Cornelis, P. and Michiels, J. (2011). *Pseudomonas aeruginosa* fosfomycin resistance mechanisms affect non-inherited fluoroquinolone tolerance. *Journal of Medical Microbiology*, 60:329–336.

[45] Ding, X., Baca-DeLancey, R. R. and Rather, P. N. (2001). Role of SspA in the density-dependent expression of the transcriptional activator AarP in Providencia stuartii. *FEMS Microbiology Letters*, 196:25–29.

[46] Dörr, T., Lewis, K. and Vulić, M. (2009). SOS response induces persistence to fluoroquinolones in *Escherichia coli*. *PLoS Genetics*, 5(12):1–9.

[47] Dörr, T., Vulić, M. and Lewis, K. (2010). Ciprofloxacin causes persister formation by inducing the TisB toxin in *Escherichia coli*. *PLoS Biology*, 8(2):1–8.

[48] Doughtery, T. J. and Pucci, M. J. (2012). *Antibiotic discovery and development*. Springer.

[49] Drlica, K. (2003). The mutant selection window and antimicrobial resistance. *Journal of Antimicrobial Chemotherapy*, 52(1):11–17.

[50] Drlica, K., Malik, M., Kerns, R. J. and Zhao, X. (2008). Quinolone-mediated bacterial death. *Antimicrobial Agents and Chemotherapy*, 52(2):385–392.

[51] Durfee, T., Hansen, A., Zhi, H., Blattner, F. R. and Jin, D. J. (2008). Transcription profiling of the stringent response in *Escherichia coli*. *Journal of Bacteriology*, 190(3):1084–1096.

[52] Dykhuizen, D. E. and Hartl, D. L. (1983). Selection in chemostats. *Microbiology Reviews*, 47(2):150–168.

[53] Elowitz, M. B., Siggia, E. D., Levine, A. J. and Swain, P. S. (2002). Stochastic gene expression in a single cell. *Science*, 297:1183–1187.

[54] Eng, R. H. K., Padberg, F. T., Smith, S. M., Tan, E. N. and Cherubin, C. E. (1991). Bactericidal effects of antibiotics on slowly growing and nongrowing bacteria. *Antimicrobial Agents Chemotherapy*, 35(9):1824–1828.

[55] Fang, F. C. (2013). Antibiotic and ROS linkage questioned. *Nature Biotechnology*, 31(5):415–416.

[56] Fasani, R. A. and Savageau, M. A. (2013). Molecular mechanisms of multiple toxin-antitoxin systems are coordinated to govern the persister phenotype. *Proceedings of the National Academy of Sciences of the United States of America*, 110(27):E2528–E2537.

[57] Fauvart, M., De Groote, V. N. and Michiels, J. (2011). Role of persister cells in chronic infections: clinical relevance and perspectives on anti-persister therapies. *Journal of Medical Microbiology*, 60:699–709.

[58] Feng, J., Kessler, D. A., Ben-jacob, E. and Levine, H. (2013). Growth feedback as a basis for persister bistability. *Proceedings of the National Academy of Sciences*, 111(1):544–549.

[59] Ferenci, T. (2008). Bacterial physiology, regulation and mutational adaptation in a chemostat environment. *Advances in Microbial Physiology*, 53:169–230.

[60] Frank, E. G., Ennis, D. G., Gonzalez, M., Levine, A. S. and Woodgate, R. (1996). Regulation of SOS mutagenesis by proteolysis. *Proceedings of the National Academy of Sciences of the United States of America*, 93(19):10291–10296.

[61] Fridman, O., Goldberg, A., Ronin, I., Shoresh, N. and Balaban, N. Q. (2014). Optimization of lag time underlies antibiotic tolerance in evolved bacterial populations. *Nature*, 513:418–421.

[62] Friedman, S., Lu, T. and Drlica, K. (2001). Mutation in the DNA gyrase A gene of *Escherichia coli* that expands the quinolone resistance-determining region. *Antimicrobial Agents and Chemotherapy*, 45(8):2378–2380.

[63] Fu, H., Yuan, J. and Gao, H. (2015). Microbial oxidative stress response: Novel insights from environmental facultative anaerobic bacteria. *Archives of Biochemistry and Biophysics*, 584:28–35.

[64] Fung, D. K. C., Chan, E. W. C., Chin, M. L. and Chan, R. C. Y. (2010). Delineation of a bacterial starvation stress response network which can mediate antibiotic tolerance development. *Antimicrobial Agents and Chemotherapy*, 54(3):1082–1093.

[65] Gardete, S. and Tomasz, A. (2014). Mechanisms of vancomycin resistance in *Staphylococcus aureus*. *The Journal of Clinical Investigation*, 124(7):2836–2840.

[66] Gardner, A., West, S. A. and Griffin, A. S. (2007). Is bacterial persistence a social trait? *PLoS ONE*, 2(8):e752.

[67] Gefen, O. and Balaban, N. Q. (2009). The importance of being persistent: heterogeneity of bacterial populations under antibiotic stress. *FEMS Microbiology Reviews*, 33:704–717.

[68] Geli, P., Laxminarayan, R., Dunne, M. and Smith, D. L. (2012). "One-Size-Fits-All"? Optimizing treatment duration for bacterial infections. *PLoS ONE*, 7(1):e29838.

[69] Gerdes, K. and Maisonneuve, E. (2012). Bacterial persistence and toxin-antitoxin loci. *Annual Review of Microbiology*, 66(1):103–123.

[70] Germain, E., Castro-Roa, D., Zenkin, N. and Gerdes, K. (2013). Molecular mechanism of bacterial persistence by HipA. *Molecular Cell*, 52(2):248–254.

[71] Gerrish, P. J. and Lenski, R. E. (1998). The fate of competing beneficial mutations in an asexual population. *Genetica*, 102/103:127–144.

[72] Gibson, J. L., Lombardo, M. J., Thornton, P. C., Hu, K. H., Galhardo, R. S., Beadle, B., Habib, A., Magner, D. B., Frost, L. S., Herman, C., Hastings, P. J. and Rosenberg, S. M. (2010). The σ^E stress response is required for stress-induced mutation and amplification in *Escherichia coli*. *Molecular Microbiology*, 77(2):415–430.

[73] Gonzalez, M., Frank, E. G., Levine, a. S. and Woodgate, R. (1998). Lon-mediated proteolysis of the *Escherichia coli* UmuD mutagenesis protein: *in vitro* degradation and identification of residues required for proteolysis. *Genes & Development*, 12(24):3889–3899.

[74] Grant, S. S. and Hung, D. T. (2013). Persistent bacterial infections, antibiotic tolerance, and the oxidative stress response. *Virulence*, 4(4):273–283.

[75] Gullberg, E., Cao, S., Berg, O. G., Ilbäck, C., Sandegren, L., Hughes, D. and Andersson, D. I. (2011). Selection of resistant bacteria at very low antibiotic concentrations. *PLoS Pathogens*, 7(7):e1002158.

[76] Gutierrez, A., Laureti, L., Crussard, S., Abida, H., Rodríguez-Rojas, A., Blázquez, J., Baharoglu, Z., Mazel, D., Darfeuille, F., Vogel, J. and Matic, I. (2013). β-lactam antibiotics promote bacterial mutagenesis via an RpoS-mediated reduction in replication fidelity. *Nature Communications*, 4:1–9.

[77] Hall, B. M., Ma, C.-X., Liang, P. and Singh, K. K. (2009). Fluctuation AnaLysis CalculatOR: a web tool for the determination of mutation rate using Luria-Delbruck fluctuation analysis. *Bioinformatics*, 25(12):1564–1565.

[78] Hansen, S., Lewis, K. and Vulić, M. (2008). Role of global regulators and nucleotide metabolism in antibiotic tolerance in *Escherichia coli*. *Antimicrobial Agents and Chemotherapy*, 52(8):2718–2726.

[79] Helaine, S., Cheverton, A. M., Watson, K. G., Faure, L. M., Matthews, S. A. and Holden, D. W. (2014). Internalization of *Salmonella* by macrophages induces formation of nonreplicating persisters. *Science*, 343:204–208.

[80] Henderson-Begg, S. K., Livermode, D. and Hall, L. (2006). Effect of subinhibitory concentrations of antibiotics on mutation frequency in *Streptococcus pneumoniae*. *Journal of Antimicrobial Chemotherapy*, 57(5):849–854.

[81] Hirsch, M. and Elliott, T. (2002). Role of ppGpp in rpoS stationary-phase regulation in *Escherichia coli*. *Journal of Bacteriology*, 184(18):5077–5087.

[82] Hofsteenge, N., van Nimwegen, E. and Silander, O. K. (2013). Quantitative analysis of persister fractions suggests different mechanisms of formation among environmental isolates of *E. coli*. *BMC microbiology*, 13(1):25.

[83] Holden, B. D. W. (2015). Persisters unmasked. *Science*, 347:30–32.

[84] Hong, S. H., Wang, X., O'Connor, H. F., Benedik, M. J. and Wood, T. K. (2012). Bacterial persistence increases as environmental fitness decreases. *Microbial Biotechnology*, 5(4):509–522.

[85] Hu, Y. and Coates, A. R. M. (2005). Transposon mutagenesis identifies genes which control antimicrobial drug tolerance in stationary-phase *Escherichia coli*. *FEMS Microbiology Letters*, 243(1):117–124.

[86] Jacoby, G. (2005). Mechanisms of resistance to quinolones. *Clinical Infectious Diseases*, 41:S120–126.

[87] James, T. W. (1961). Continuous culture of microorganisms. *Annual Review of Microbiology*, 15:27–46.

[88] Jansen, G., Barbosa, C. and Schulenburg, H. (2013). Experimental evolution as an efficient tool to dissect adaptive paths to antibiotic resistance. *Drug Resistance Updates*, 16(6):96–107.

[89] Jaurin, B., Grundström, T. and Normark, S. (1982). Sequence elements determining *ampC* promoter strength in *E. coli*. *The EMBO Journal*, 1(7):875–881.

[90] Jayaraman, R. (2008). Bacterial persistence: some new insights into an old phenomenon. *Journal of Biosciences*, 33:795–805.

[91] Johnson, P. J. T. and Levin, B. R. (2013). Pharmacodynamics, population dynamics, and the evolution of persistence in *Staphylococcus aureus*. *PLoS Genetics*, 9(1):e1003123.

[92] Jørgensen, K. M., Wassermann, T., Jensen, P. Ø., Hengzuang, W., Molin, S., Høiby, N. and Ciofu, O. (2013). Sublethal ciprofloxacin treatment leads to rapid development of high-level ciprofloxacin resistance during long-term experimental evolution of *Pseudomonas aeruginosa*. *Antimicrobial Agents and Chemotherapy*, 57(9):4215–4121.

[93] Kaiser, P., Regoes, R. R., Dolowschiak, T., Wotzka, S. Y., Lengefeld, J., Slack, E., Grant, A. J., Ackermann, M. and Hardt, W. (2014). Cecum lymph node dendritic cells harbor slow-growing bacteria phenotypically tolerant to antibiotic treatment. *PLoS Biology*, 12(2):e1001793.

[94] Kaspy, I., Rotem, E., Weiss, N., Ronin, I., Balaban, N. Q. and Glaser, G. (2013). HipA-mediated antibiotic persistence via phosphorylation of the glutamyl-tRNA-synthetase. *Nature Communications*, 4:3001.

[95] Kawecki, T. J., Lenski, R. E., Ebert, D., Hollis, B., Olivieri, I. and Whitlock, M. C. (2012). Experimental evolution. *Trends in Ecology and Evolution*, 27(10):547–560.

[96] Kayama, S., Murakami, K., Ono, T., Ushimaru, M., Yamamoto, A., Hirota, K. and Miyake, Y. (2009). The role of *rpoS* gene and quorum-sensing system in ofloxacin tolerance in *Pseudomonas aeruginosa*. *FEMS Microbiology Letters*, 298(2):184–192.

[97] Kearse, M., Moir, R., Wilson, A., Stones-Havas, S., Cheung, M., Sturrock, S., Buxton, S., Cooper, A., Markowitz, S., Duran, C., Thierer, T., Ashton, B., Meintjes, P. and Drummond, A. (2012). Geneious Basic: An integrated and extendable desktop software platform for the organization and analysis of sequence data. *Bioinformatics*, 28(12):1647–1649.

[98] Keren, I., Minami, S., Rubin, E. and Lewis, K. C. (2011). Characterization and transcriptome analysis of *Mycobacterium tuberculosis* persisters. *mBio*, 2(3):e00100–11.

[99] Keren, I., Kaldalu, N., Spoering, A., Wang, Y. and Lewis, K. (2004). Persister cells and tolerance to antimicrobials. *FEMS Microbiology Letters*, 230(1):13–18.

[100] Keren, I., Shah, D., Spoering, A., Kaldalu, N. and Lewis, K. (2004). Specialized persister cells and the mechanism of multidrug tolerance in *Escherichia coli*. *Journal of Bacteriology*, 186(24):8172–8180.

[101] Keren, I., Wu, Y., Inocencio, J., Mulcahy, L. R. and Lewis, K. (2013). Killing by bactericidal antibiotics does not depend on reactive oxygen species. *Science*, 339:1213–1216.

[102] Kim, D. Y. (2015). Two stress sensor proteins for the expression of σ^E regulon: DegS and RseB. *Journal of Microbiology*, 53(5):306–310.

[103] Kim, J.-S., Heo, P., Yang, T.-J., Lee, K.-S., Jin, Y.-S., Kim, S.-K., Shin, D. and Kweon, D.-H. (2011). Bacterial persisters tolerate antibiotics by not producing hydroxyl radicals. *Biochemical and Biophysical Research Communications*, 413(1):105–110.

[104] Kim, Y. and Wood, T. K. (2010). Toxins Hha and CspD and small RNA regulator Hfq are involved in persister cell formation through MqsR in *Escherichia coli*. *Biochemical and Biophysical Research Communications*, 391(1):209–213.

[105] Kint, C. I., Verstraeten, N., Fauvart, M. and Michiels, J. (2012). New-found fundamentals of bacterial persistence. *Trends in Microbiology*, 20(12):577–585.

[106] Kivisaar, M. (2003). Stationary phase mutagenesis: Mechanisms that accelerate adaptation of microbial populations under environmental stress. *Environmental Microbiology*, 5(10):814–827.

[107] Klemm, E. J., Gkrania-Klotsas, E., Hadfield, J., Forbester, J. L., Harris, S. R., Hale, C., Heath, J. N., Wileman, T., Clare, S., Kane, L., Goulding, D., Otto, T. D., Kay, S., Doffinger, R., Cooke, F. J., Carmichael, A., Lever, A. M. L., Parkhill, J., MacLennan, C. A., Kumararatne, D., Dougan, G. and Kingsley, R. A. (2016). Emergence of host-adapted *Salmonella* Enteritidis through rapid evolution in an immunocompromised host. *Nature Microbiology*, 1:15023.

[108] Koh, R. S. and Dunlop, M. J. (2012). Modeling suggests that gene circuit architecture controls phenotypic variability in a bacterial persistence network. *BMC Systems Biology*, 6(1):47.

[109] Kohanski, M. A., DePristo, M. A. and Collins, J. J. (2010). Sublethal antibiotic treatment leads to multidrug resistance via radical-induced mutagenesis. *Molecular Cell*, 37(3):311–320.

[110] Kohanski, M. A., Dwyer, D. J. and Collins, J. J. (2010). How antibiotics kill bacteria: from targets to networks. *Nature Reviews Microbiology*, 8(6):423–435.

[111] Kohanski, M. A., Dwyer, D. J., Hayete, B., Lawrence, C. A. and Collins, J. J. (2007). A common mechanism of cellular death induced by bactericidal antibiotics. *Cell*, 130(5):797–810.

[112] Korch, S. B., Henderson, T. A. and Hill, T. M. (2003). Characterization of the *hipA7* allele of *Escherichia coli* and evidence that high persistence is governed by (p)ppGpp synthesis. *Molecular Microbiology*, 50(4):1199–1213.

[113] Korch, S. B. and Hill, T. M. (2006). Ectopic overexpression of wild-type and mutant *hipA* genes in *Escherichia coli*: Effects on macromolecular synthesis and persister formation. *Journal of Bacteriology*, 188(11):3826–3836.

[114] Kussell, E., Kishony, R., Balaban, N. Q. and Leibler, S. (2005). Bacterial persistence: A model of survival in changing environments. *Genetics*, 169:1807–1814.

[115] Kussell, E. and Leibler, S. (2005). Phenotypic diversity, population growth, and information in fluctuating environments. *Science*, 309:2075–2078.

[116] Kwan, B. W., Valenta, J. A., Benedik, M. J. and Wood, T. K. (2013). Arrested protein synthesis increases persister-like cell formation. *Antimicrobial Agents and Chemotherapy*, 57(3):1468–1473.

[117] Lachmann, M. and Jablonka, E. (1996). The inheritance of phenotypes: an adaptation to fluctuating environments. *Journal of Theoretical Biology*, 181(1):1–9.

[118] LaFleur, M. D., Qi, Q. and Lewis, K. (2010). Patients with long-term oral carriage harbor high-persister mutants of *Candida albicans*. *Antimicrobial Agents and Chemotherapy*, 54(1):39–44.

[119] Lange, R. and Hengge-Aronis, R. (1994). The cellular concentration of the σ^S subunit of RNA polymerase in *Escherichia coli* is controlled at the levels of transcription, translation, and protein stability. *Genes & Development*, 8(13):1600–1612.

[120] Lázár, V., Pal Singh, G., Spohn, R., Nagy, I., Horváth, B., Hrtyan, M., Busa-Fekete, R., Bogos, B., Méhi, O., Csörgő, B., Pósfai, G., Fekete, G., Szappanos, B., Kégl, B., Papp, B. and Pál, C. (2013). Bacterial evolution of antibiotic hypersensitivity. *Molecular Systems Biology*, 9:700.

[121] Lee, H. H., Molla, M. N., Cantor, C. R. and Collins, J. J. (2010). Bacterial charity work leads to population-wide resistance. *Nature*, 467(7311):82–85.

[122] Lenski, R. E., Rose, M. R., Simpson, S. C. and Tadler, S. C. (1991). Long-term experimental evolution in *Escherichia coli*. I. Adaptation and divergence during 2,000 generations. *The American Naturalist*, 138(6):1315–1341.

[123] Lenski, R. E. (2011). Evolution in action: a 50,000-generation salute to Charles Darwin. *Microbe*, 6(1):30–33.

[124] Leung, V. and Lévesque, C. M. (2012). A stress-inducible quorum-sensing peptide mediates the formation of persister cells with noninherited multidrug tolerance. *Journal of Bacteriology*, 194(9):2265–2274.

[125] Levin, B. R., Concepción-Acevedo, J. and Udekwu, K. I. (2014). Persistence: A copacetic and parsimonious hypothesis for the existence of non-inherited resistance to antibiotics. *Current Opinion in Microbiology*, 21:18–21.

[126] Levin, B. R. and Rozen, D. E. (2006). Non-inherited antibiotic resistance. *Nature Reviews Microbiology*, 4:556–562.

[127] Levy, S. B. and Marshall, B. (2004). Antibacterial resistance worldwide: causes, challenges and responses. *Nature Medicine Supplement*, 10(12):S122–S129.

[128] Lewin, C. S., Howard, B. M. A., Ratcliffe, N. T. and Smith, J. T. (1989). 4-Quinolones and the SOS response. *Journal of Medical Microbiology*, 29(2):139–144.

[129] Lewis, K. (2007). Persister cells, dormancy and infectious disease. *Nature Reviews Microbiology*, 5:48–56.

[130] Lewis, K. (2010). Persister cells. *Annual Review of Microbiology*, 64:357–372.

[131] Li, X.-Z. and Nikaido, H. (2009). Efflux-mediated drug resistance in bacteria: an update. *Drugs*, 69(12):1555–1623.

[132] Li, Y. and Zhang, Y. (2007). PhoU is a persistence switch involved in persister formation and tolerance to multiple antibiotics and stresses in *Escherichia coli*. *Antimicrobial Agents and Chemotherapy*, 51(6):2092–2099.

[133] Lieberman, T. D., Michel, J.-B., Aingaran, M., Potter-Bynoe, G., Roux, D., Davis, M. R., Skurnik, D., Leiby, N., LiPuma, J. J., Goldberg, J. B., McAdam, A. J., Priebe, G. P. and Kishony, R. (2011). Parallel bacterial evolution within multiple patients identifies candidate pathogenicity genes. *Nature Genetics*, 43(12):1275–1280.

[134] Lin, D., Gibson, I. B., Moore, J. M., Thornton, P. C., Leal, S. M. and Hastings, P. J. (2011). Global chromosomal structural instability in a subpopulation of starving *Escherichia coli* cells. *PLoS Genetics*, 7(8):e1002223.

[135] Liu, A., Fong, A., Becket, E., Yuan, J., Tamae, C., Medrano, L., Maiz, M., Wahba, C., Lee, C., Lee, K., Tran, K. P., Yang, H., Hoffman, R. M., Salih, A. and Miller, J. H. (2011). Selective advantage of resistant strains at trace levels of antibiotics: a simple and ultrasensitive color test for detection of antibiotics and genotoxic agents. *Antimicrobial Agents and Chemotherapy*, 55(3):1204–1210.

[136] Liu, H. and Tomasz, A. (1985). Penicillin tolerance in multiply drug-resistant neutral isolates of *Streptococcus pneumoniae*. *Journal of Infectious Diseases*, 152(2):365–372.

[137] Liu, Y. and Imlay, J. A. (2013). Cell death from antibiotics without the involvement of reactive oxygen species. *Science*, 339:1210–1213.

[138] Loewe, L., Textor, V. and Scherer, S. (2003). High deleterious genomic mutation rate in stationary phase of *Escherichia coli*. *Science*, 302:1558–1560.

[139] López, E., Elez, M., Matic, I. and Blázquez, J. (2007). Antibiotic-mediated recombination: ciprofloxacin stimulates SOS-independent recombination of divergent sequences in *Escherichia coli*. *Molecular Microbiology*, 64(1):83–93.

[140] Lou, C., Li, Z. and Ouyang, Q. (2008). A molecular model for persister in *E. coli*. *Journal of Theoretical Biology*, 255:205–209.

[141] Louie, A., Brown, D. L., Liu, W., Kulawy, R. W., Deziel, M. R. and Drusano, G. L. (2007). *In vitro* infection model characterizing the effect of efflux pump inhibition on prevention of resistance to levofloxacin and ciprofloxacin in *Streptococcus pneumoniae*. *Antimicrobial Agents and Chemotherapy*, 51(11):3988–4000.

[142] Luria, S. and Delbrück, M. (1943). Mutations of bacteria from virus sensitivity to virus resistance. *Genetics*, 28(6):491–511.

[143] Maddamsetti, R., Lenski, R. E. and Barrick, J. E. (2015). Adaptation, clonal interference, and frequency-dependent interactions in a long-term evolution experiment with *Escherichia coli*. *Genetics*, 200(2):619–631.

[144] Magnusson, L. U., Farewell, A. and Nyström, T. (2005). ppGpp: a global regulator in *Escherichia coli*. *Trends in Microbiology*, 13(5):236–242.

[145] Maisonneuve, E., Castro-Camargo, M. and Gerdes, K. (2013). (p)ppGpp controls bacterial persistence by stochastic induction of toxin-antitoxin activity. *Cell*, 154(5):1140–1150.

[146] Maisonneuve, E. and Gerdes, K. (2014). Molecular mechanisms underlying bacterial persisters. *Cell*, 157(3):539–548.

[147] Maisonneuve, E., Shakespeare, L. J., Jørgensen, M. G. and Gerdes, K. (2011). Bacterial persistence by RNA endonucleases. *Proceedings of the National Academy of Sciences of the United States of America*, 108(32):13206–13211.

[148] Mayers, D. L. (2009). *Antimicrobial Drug Resistance*, volume 1. Humana Press.

[149] McClure, W. R. and Cech, C. L. (1978). On the mechanism of rifampicin inhibition of RNA synthesis. *Journal of Biological Chemistry*, 253(24):8949–8956.

[150] McDermott, W. (1958). Microbial Persistence. *The Yale Journal of Biology and Medicine*, 30:257–291.

[151] McKenzie, G. J., Harris, R. S., Lee, P. L. and Rosenberg, S. M. (2000). The SOS response regulates adaptive mutation. *Proceedings of the National Academy of Sciences of the United States of America*, 97(12):6646–6651.

[152] Mechler, L., Herbig, A., Paprotka, K., Fraunholz, M., Nieselt, K. and Bertram, R. (2015). A novel point mutation promotes growth phase-dependent daptomycin tolerance in *Staphylococcus aureus*. *Antimicrobial Agents and Chemotherapy*, 59:5366–5376.

[153] Medaney, F., Dimitriu, T., Ellis, R. J. and Raymond, B. (2015). Live to cheat another day: bacterial dormancy facilitates the social exploitation of β-lactamases. *The ISME Journal*, 10(3):778–787.

[154] Meredith, H. R., Srimani, J. K., Lee, A. J., Lopatkin, A. J. and You, L. (2015). Collective antibiotic tolerance: mechanisms, dynamics and intervention. *Nature Chemical Biology*, 11(3):182–188.

[155] Michel, B. (2005). After 30 years of study, the bacterial SOS response still surprises us. *PLoS Biology*, 3(7):1174–1176.

[156] Michiels, J. and Fauvart, M. (2016). *Bacterial persistence - Methods and protocols*. Springer Science+Business Media, New York.

[157] Mika, F. and Hengge, R. (2005). A two-component phosphotransfer network involving ArcB, ArcA, and RssB coordinates synthesis and proteolysis of σ^S (RpoS) in *E. coli*. *Genes & Development*, 19(22):2770–2781.

[158] Möker, N., Dean, C. R. and Tao, J. (2010). *Pseudomonas aeruginosa* increases formation of multidrug-tolerant persister cells in response to quorum-sensing signaling molecules. *Journal of Bacteriology*, 192(7):1946–1955.

[159] Montero, M., Rahimpour, M., Viale, A. M., Almagro, G., Eydallin, G., Sevilla, Á., Cánovas, M., Bernal, C., Lozano, A. B., Muñoz, F. J., Baroja-Fernández, E., Bahaji, A., Mori, H., Codoñer, F. M. and Pozueta-Romero, J. (2014). Systematic production of inactivating and non-inactivating suppressor mutations at the *relA* locus that compensate the detrimental effects of complete *spoT* loss and affect glycogen content in *Escherichia coli*. *PLoS ONE*, 9(9):e106938.

[160] Moyed, H. S. and Bertrand, K. P. (1983). *hipA*, a newly recognized gene of *Escherichia coli* K-12 that affects frequency of persistence after inhibition of murein synthesis. *Microbiology*, 155(2):768–775.

[161] Mulcahy, L. R., Burns, J. L., Lory, S. and Lewis, K. (2010). Emergence of *Pseudomonas aeruginosa* strains producing high levels of persister cells in patients with cystic fibrosis. *Journal of Bacteriology*, 192(23):6191–6199.

[162] Murakami, K., Ono, T., Viducic, D., Kayama, S., Mori, M., Hirota, K., Nemoto, K. and Miyake, Y. (2005). Role for *rpoS* gene of *Pseudomonas aeruginosa* in antibiotic tolerance. *FEMS Microbiology Letters*, 242(1):161–167.

[163] Nair, C. G., Chao, C., Ryall, B. and Williams, H. D. (2013). Sub-lethal concentrations of antibiotics increase mutation frequency in the cystic fibrosis pathogen *Pseudomonas aeruginosa*. *Letters in Applied Microbiology*, 56(2):149–154.

[164] Navarro Llorens, J. M., Tormo, A. and Martínez-García, E. (2010). Stationary phase in gram-negative bacteria. *FEMS Microbiology Reviews*, 34(4):476–495.

[165] Neu, H. and Reeves, D. (1986). *Ciprofloxacin*, volume 1. Springer.

[166] Newmark, K. G., O'Reilly, E. K., Pohlhaus, J. R. and Kreuzer, K. N. (2005). Genetic analysis of the requirements for SOS induction by nalidixic acid in *Escherichia coli*. *Gene*, 356:69–76.

[167] Nguyen, D., Joshi-Datar, A., Lepine, F., Bauerle, E., Olakanmi, O., Beer, K., McKay, G., Siehnel, R., Schafhauser, J., Wang, Y., Britigan, B. E. and Singh, P. K. (2011). Active starvation responses mediate antibiotic tolerance in biofilms and nutrient-limited bacteria. *Science*, 334(6058):982–6.

[168] Nilsson, O. (2012). Vancomycin resistant enterococci in farm animals – occurrence and importance. *Infection Ecology & Epidemiology*, 2:16959.

[169] Novak, R., Henriques, B., Charpentier, E., Normark, S. and Tuomanen, E. (1999). Emergence of vancomycin tolerance in *Streptococcus pneumoniae*. *Nature*, 399:590–593.

[170] Ochman, H. and Selander, R. (1984). Standard reference strains of *Escherichia coli* from natural populations. *Journal of Bacteriology*, 157(2):690–693.

[171] Orman, M. A. and Brynildsen, M. P. (2013). Dormancy is not necessary or sufficient for bacterial persistence. *Antimicrobial Agents and Chemotherapy*, 57(7):3230–3239.

[172] Oz, T., Guvenek, A., Yildiz, S., Karaboga, E., Tamer, Y. T., Mumcuyan, N., Ozan, V. B., Senturk, G. H., Cokol, M., Yeh, P. and Toprak, E. (2014). Strength of selection pressure is an important parameter contributing to the complexity of antibiotic resistance evolution. *Molecular Biology and Evolution*, 31(9):2387–2401.

[173] Pál, C., Papp, B. and Lázár, V. (2015). Collateral sensitivity of antibiotic-resistant microbes. *Trends in Microbiology*, 23(7):401–407.

[174] Palmer, K. L., Kos, V. N. and Gilmore, M. S. (2010). Horizontal gene transfer and the genomics of enterococcal antibiotic resistance. *Current Opinion in Microbiology*, 13(5):632–639.

[175] Patra, P. and Klumpp, S. (2013). Population dynamics of bacterial persistence. *PLoS ONE*, 8(5):e62814.

[176] Pearl, S., Gabay, C., Kishony, R., Oppenheim, A. and Balaban, N. Q. (2008). Nongenetic individuality in the host-phage interaction. *PLoS Biology*, 6(5):0957–0964.

[177] Pedersen, K., Christensen, S. K. and Gerdes, K. (2002). Rapid induction and reversal of a bacteriostatic condition by controlled expression of toxins and antitoxins. *Molecular Microbiology*, 45(2):501–510.

[178] Pennington, J. M. and Rosenberg, S. M. (2007). Spontaneous DNA breakage in single living *Escherichia coli* cells. *Nature Genetics*, 39(6):797–802.

[179] Piddock, L. J. and Walters, R. N. (1992). Bactericidal activities of five quinolones for *Escherichia coli* strains with mutations in genes encoding the SOS response or cell division. *Antimicrobial Agents and Chemotherapy*, 36(4):819–825.

[180] Pomposiello, P. J. and Demple, B. (2001). Redox-operated genetic switches: The SoxR and OxyR transcription factors. *Trends in Biotechnology*, 19(3):109–114.

[181] Ponder, R. G., Fonville, N. C. and Rosenberg, S. M. (2005). A switch from high-fidelity to error-prone DNA double-strand break repair underlies stress-induced mutation. *Molecular Cell*, 19(6):791–804.

[182] Poole, K. (2012). Stress responses as determinants of antimicrobial resistance in Gram-negative bacteria. *Trends in Microbiology*, 20(5):227–234.

[183] Raghavan, A. and Chatterji, D. (1998). Guanosine tetraphosphate-induced dissociation of open complexes at the *Escherichia coli* ribosomal protein promoters rplJ and rpsA P1: nanosecond depolarization spectroscopic studies. *Biophysical Chemistry*, 75(1):21–32.

[184] Ram, Y. and Hadany, L. (2014). Stress-induced mutagenesis and complex adaptation. *Proceedings of the Royal Society B: Biological Sciences*, 281(1792):45.

[185] Ramirez, M., Rajaram, S., Steininger, R. J., Osipchuk, D., Roth, M. A., Morinishi, L. S., Evans, L., Ji, W., Hsu, C.-H., Thurley, K., Wei, S., Zhou, A., Koduru, P. R., Posner, B. A., Wu, L. F. and Altschuler, S. J. (2016). Diverse drug-resistance mechanisms can emerge from drug-tolerant cancer persister cells. *Nature Communications*, 7:1–8.

[186] Rao, S. P. S., Alonso, S., Rand, L., Dick, T. and Pethe, K. (2008). The protonmotive force is required for maintaining ATP homeostasis and viability of hypoxic, nonreplicating *Mycobacterium tuberculosis*. *Proceedings of the National Academy of Sciences of the United States of America*, 105(33):11945–11950.

[187] Ratcliff, W. C. and Travisano, M. (2014). Experimental evolution of multicellular complexity in *Saccharomyces cerevisiae*. *BioScience*, 64(5):383–393.

[188] Regoes, R. R., Wiuff, C., Zappala, R. M., Garner, K. N., Baquero, F. and Levin, B. R. (2004). Pharmacodynamic functions: A multiparameter approach to the design of antibiotic treatment regimens. *Antimicrobial Agents and Chemotherapy*, 48(10):3670–3676.

[189] Renggli, S., Keck, W., Jenal, U. and Ritz, D. (2013). Role of autofluorescence in flow cytometric analysis of *Escherichia coli* treated with bactericidal antibiotics. *Journal of Bacteriology*, 195(18):4067–4073.

[190] Rhodius, V. A., Suh, W. C., Nonaka, G., West, J. and Gross, C. A. (2006). Conserved and variable functions of the σ^E stress response in related genomes. *PLoS Biology*, 4(1):0043–0059.

[191] Rodriguez, M. and Costa, S. (1999). Spontaneous kanamycin-resistant *Escherichia coli* mutant with altered periplasmic oligopeptide permease protein (OppA) and impermeability to aminoglycosides. *Revista de Microbiologia*, 30:153–156.

[192] Rosche, W. A. and Foster, P. L. (2000). Determining mutation rates in bacterial populations. *Methods*, 20:4–17.

[193] Rosenberg, S. M., Shee, C., Frisch, R. L. and Hastings, P. J. (2012). Stress-induced mutation via DNA breaks in *Escherichia coli*: A molecular mechanism with implications for evolution and medicine. *Bioessays*, 34:885–892.

[194] Rotem, E., Loinger, A., Ronin, I., Levin-Reisman, I., Gabay, C., Shoresh, N., Biham, O. and Balaban, N. Q. (2010). Regulation of phenotypic variability by a threshold-based mechanism underlies bacterial persistence. *Proceedings of the National Academy of Sciences*, 107(28):12541–12546.

[195] Rowley, G., Spector, M., Kormanec, J. and Roberts, M. (2006). Pushing the envelope: extracytoplasmic stress responses in bacterial pathogens. *Nature Reviews Microbiology*, 4(5):383–394.

[196] Schumacher, M. A., Piro, K. M., Xu, W., Hansen, S., Lewis, K. and Brennan, R. G. (2009). Molecular mechanisms of HipA-mediated multidrug tolerance and its neutralization by HipB. *Science*, 323:396–401.

[197] Schweder, T., Lee, K. H., Lomovskaya, O. and Matin, A. (1996). Regulation of *Escherichia coli* starvation sigma factor (σS) by ClpXP protease. *Journal of Bacteriology*, 178(2):470–476.

[198] Shah, D., Zhang, Z., Khodursky, A. B., Kaldalu, N., Kurg, K. and Lewis, K. (2006). Persisters: a distinct physiological state of *E. coli*. *BMC Microbiology*, 6:53.

[199] Shan, Y., Lazinski, D., Rowe, S., Camilli, A. and Lewis, K. (2015). Genetic basis of persister tolerance to aminoglycosides in *Escherichia coli*. *mBio*, 6(2):e00078–15.

[200] Sharma, S. V., Lee, D. Y., Li, B., Quinlan, M. P., Takahashi, F., Maheswaran, S., McDermott, U., Azizian, N., Zou, L., Fischbach, M. A., Wong, K. K., Brandstetter, K., Wittner, B., Ramaswamy, S., Classon, M. and Settleman, J. (2010). A chromatin-mediated reversible drug-tolerant state in cancer cell subpopulations. *Cell*, 141(1):69–80.

[201] Simner, P. J., Zhanel, G. G., Pitout, J., Tailor, F., McCracken, M., Mulvey, M. R., Lagacé-Wiens, P. R., Adam, H. J. and Hoban, D. J. (2011). Prevalence and characterization of extended-spectrum β-lactamase– and AmpC β-lactamase–producing *Escherichia coli*: results of the CANWARD 2007–2009 study. *Diagnostic Microbiology and Infectious Disease*, 69(3):326–334.

[202] Smith, P. A. and Romesberg, F. E. (2007). Combating bacteria and drug resistance by inhibiting mechanisms of persistence and adaptation. *Nature Chemical Biology*, 3(9):549–556.

[203] Speer, B. S., Shoemaker, N. B. and Salyers, A. A. (1992). Bacterial resistance to tetracycline: Mechanisms, transfer, and clinical significance. *Clinical Microbiology Reviews*, 5(4):387–399.

[204] Spellberg, B. and Doi, Y. (2015). The rise of fluoroquinolone-resistant *Escherichia coli* in the community: Scarier than we thought. *Journal of Infectious Diseases*, 212:1853–1855.

[205] Spoering, A. L. and Lewis, K. (2001). Biofilms and planktonic cells of *Pseudomonas aeruginosa* have similar resistance to killing by antimicrobials. *Journal of Bacteriology*, 183(23):6746–6751.

[206] Stepanyan, K., Wenseleers, T., Duéñez-Guzmán, E. A., Muratori, F., Van den Bergh, B., Verstraeten, N., De Meester, L., Verstrepen, K. J., Fauvart, M. and Michiels, J. (2015). Fitness trade-offs explain low levels of persister cells in the opportunistic pathogen *Pseudomonas aeruginosa*. *Molecular Ecology*, 24:1572–1583.

[207] Stewart, B. and Rozen, D. E. (2012). Genetic variation for antibiotic persistence in *Escherichia coli*. *Evolution*, 66(3):933–939.

[208] Strateva, T. and Yordanov, D. (2009). *Pseudomonas aeruginosa* - A phenomenon of bacterial resistance. *Journal of Medical Microbiology*, 58(9):1133–1148.

[209] Tam, V. H., Louie, A., Deziel, M. R., Liu, W. and Drusano, G. L. (2007). The relationship between quinolone exposures and resistance amplification is characterized by an inverted U: a new paradigm for optimizing pharmacodynamics to counterselect resistance. *Antimicrobial Agents Chemotherapy*, 51(2):744–777.

[210] Tan, C., Smith, R. P., Srimani, J. K., Riccione, K. A., Prasada, S., Kuehn, M. and You, L. (2012). The inoculum effect and band-pass bacterial response to periodic antibiotic treatment. *Molecular Systems Biology*, 8:617.

[211] Taylor, M. J., Tanna, S. and Sahota, T. (2010). Pharmacokinetics in drug discovery. *Journal of Pharmaceutical Sciences*, 99(10):4215–4227.

[212] Temkin, E., Adler, A., Lerner, A. and Carmeli, Y. (2014). Carbapenem-resistant Enterobacteriaceae: Biology, epidemiology, and management. *Annals of the New York Academy of Sciences*, 1323:22–42.

[213] Thattai, M. and Van Oudenaarden, A. (2004). Stochastic gene expression in fluctuating environments. *Genetics*, 167:523–530.

[214] Toprak, E., Veres, A., Michel, J.-B., Chait, R., Hartl, D. L. and Kishony, R. (2011). Evolutionary paths to antibiotic resistance under dynamically sustained drug selection. *Nature Genetics*, 44(1):101–105.

[215] Toprak, E., Veres, A., Yildiz, S., Pedraza, J. M., Chait, R., Paulsson, J. and Kishony, R. (2013). Building a morbidostat: an automated continuous-culture device for studying bacterial drug resistance under dynamically sustained drug inhibition. *Nature Protocols*, 8(3):555–567.

[216] Tracz, D. M., Boyd, D. A., Bryden, L., Hizon, R., Giercke, S., Caeseele, P. V. and Mulvey, M. R. (2005). Increase in *ampC* promoter strength due to mutations and deletion of the attenuator in a clinical isolate of cefoxitin-resistant *Escherichia coli* as determined by RT-PCR. *Journal of Antimicrobial Chemotherapy*, 55:768–772.

[217] Tsutsui, A., Suzuki, S., Yamane, K., Matsui, M., Konda, T., Marui, E., Takahashi, K. and Arakawa, Y. (2011). Genotypes and infection sites in an outbreak of multidrug-resistant *Pseudomonas aeruginosa*. *Journal of Hospital Infection*, 78(4):317–322.

[218] Tuomanen, E., Cozens, R., Tosch, W., Zak, O. and Tomasz, A. (1986). The rate of killing of *Escherichia coli* by β-lactam antibiotics is strictly proportional to the rate of bacterial growth. *Journal of General Microbiology*, 132(5):1297–1304.

[219] Tupin, A., Gualtieri, M., Roquet-Banères, F., Morichaud, Z., Brodolin, K. and Leonetti, J. P. (2010). Resistance to rifampicin: At the crossroads between ecological, genomic and medical concerns. *International Journal of Antimicrobial Agents*, 35(6):519–523.

[220] Úbeda, C., Maiques, E., Knecht, E., Lasa, Í., Novick, R. P. and Penadés, J. R. (2005). Antibiotic-induced SOS response promotes horizontal dissemination of pathogenicity island-encoded virulence factors in staphylococci. *Molecular Microbiology*, 56(3):836–844.

[221] Van den Bergh, B., Michiels, J. E., Wenseleers, T., Windels, E. M., Vanden Boer, P., Kestemont, D., De Meester, L., Verstrepen, K. J., Verstraeten, N., Fauvart, M. and Michiels, J. (2016). Frequency of antibiotic application drives rapid evolutionary adaptation of *Escherichia coli* persistence. *Nature Microbiology*, 1(3):16020.

[222] Van Melderen, L. and Aertsen, A. (2009). Regulation and quality control by Lon-dependent proteolysis. *Research in Microbiology*, 160(9):645–651.

[223] Vàzquez-Laslop, N., Lee, H. and Neyfakh, A. A. (2006). Increased persistence in *Escherichia coli* caused by controlled expression of toxins or other unrelated proteins. *Journal of Bacteriology*, 188(10):3494–3497.

[224] Verstraeten, N., Knapen, W. J., Kint, C. I., Liebens, V., Van den Bergh, B., Dewachter, L., Michiels, J. E., Fu, Q., David, C. C., Fierro, A. C., Marchal, K., Beirlant, J., Versées, W., Hofkens, J., Jansen, M., Fauvart, M. and Michiels, J. (2015). Obg and membrane depolarization are part of a microbial bet-hedging strategy that leads to antibiotic tolerance. *Molecular Cell*, 59:1–13.

[225] Viducic, D., Ono, T., Murakami, K., Susilowati, H., Kayama, S., Hirota, K. and Miyake, Y. (2006). Functional analysis of *spoT*, *relA* and *dksA* genes on quinolone tolerance in *Pseudomonas aeruginosa* under nongrowing condition.

[226] Vogwill, T., Comfort, A. C., Furió, V. and MaClean, R. C. (2016). Persistence and resistance as complementary bacterial adaptations to antibiotics. *Journal of Evolutionary Biology*, n/a–n/a.

[227] Völzing, K. G. and Brynildsen, M. P. (2015). Stationary-phase persisters to ofloxacin sustain DNA damage and require repair systems only during recovery. *mBio*, 6(5):e00731–15.

[228] Wahl, L. M., Gerrish, P. J. and Saika-Voivod, I. (2002). Evaluating the impact of population bottlenecks in experimental evolution. *Genetics*, 162(2):961–971.

[229] Wakamoto, Y., Dhar, N., Chait, R., Schneider, K., Signorino-Gelo, F., Leibler, S. and McKinney, J. (2013). Dynamic persistence of antibiotic-stressed *Mycobacteria*. *Science*, 339:91–95.

[230] Walsh, N. P., Alba, B. M., Bose, B., Gross, C. A. and Sauer, R. T. (2003). OMP peptide signals initiate the envelope-stress response by activating DegS protease via relief of inhibition mediated by its PDZ domain. *Cell*, 113(1):61–71.

[231] Wayne, L. G. and Sohaskey, C. D. (2001). Nonreplicating persistence of *Mycobacterium tuberculosis*. *Annual Review of Microbiology*, 55:139–163.

[232] Weber, H., Polen, T., Heuveling, J., Wendisch, V. F. and Hengge, R. (2005). Genome-wide analysis of the general stress response network in *Escherichia coli* : σ^S-dependent genes, promoters, and sigma factor selectivity. *Journal of Bacteriology*, 187(5):1591–1603.

[233] WHO (2014). Antimicrobial resistance: Global report on surveillance 2014. *World Health Organization*.

[234] Wimberly, H., Shee, C., Thornton, P. C., Sivaramakrishnan, P., Rosenberg, S. M. and Hastings, P. J. (2013). R-loops and nicks initiate DNA breakage and genome instability in non-growing *Escherichia coli*. *Nature Communications*, 4:2115.

[235] Wolf, L. N. and Barrick, J. E. (2012). Tracking winners and losers in *E. coli* evolution experiments. *Microbe*, 7(3):124–128.

[236] Wong, A., Rodrigue, N. and Kassen, R. (2012). Genomics of adaptation during experimental evolution of the opportunistic pathogen *Pseudomonas aeruginosa*. *PLoS Genetics*, 8(9):e1002928.

[237] Wood, T. K., Knabel, S. J. and Kwan, B. W. (2013). Bacterial persister cell formation and dormancy. *Applied and Environmental Microbiology*, 79(23):7116–7121.

[238] Wu, N., Chen, B., Tian, S. and Chu, Y. (2014). The inoculum effect of antibiotics against CTX-M-extended-spectrum β-lactamase-producing *Escherichia coli*. *Annals of Clinical Microbiology and Antimicrobials*, 13(1):45.

[239] Wu, N., He, L., Cui, P., Wang, W., Yuan, Y., Liu, S., Xu, T., Zhang, S., Wu, J., Zhang, W. and Zhang, Y. (2015). Ranking of persister genes in the same *Escherichia coli* genetic background demonstrates varying importance of individual persister genes in tolerance to different antibiotics. *Frontiers in Microbiology*, 6:1003.

[240] Wu, Y., Vulić, M., Keren, I. and Lewis, K. (2012). Role of oxidative stress in persister tolerance. *Antimicrobial Agents and Chemotherapy*, 56(9):4922–4926.

[241] Xiao, H., Kalman, M., Ikehara, K., Zemel, S., Glaser, G. and Cashel, M. (1991). Residual guanosine 3',5'-bispyrophosphate synthetic activity of *relA* null mutants can be eliminated by *spoT* null mutations. *Journal of Biological Chemistry*, 266(9):5980–5990.

[242] Xiaodong, C. (2007). Exact stochastic simulation of coupled chemical reactions with delays. *Journal of Chemical Physics*, 126(12):124108.

[243] Xie, X. S., Choi, P. J., Li, G.-W., Lee, N. K. and Lia, G. (2008). Single-molecule approach to molecular biology in living bacterial cells. *Annual Review of Biophysics*, 37:417–44.

[244] Yang, L., Jelsbak, L., Marvig, R. L., Damkiaer, S., Workman, C. T., Rau, M. H., Hansen, S. K., Folkesson, A., Johansen, H. K., Ciofu, O., Hoiby, N., Sommer, M. O. A. and Molin, S. (2011). Evolutionary dynamics of bacteria in a human host environment. *Proceedings of the National Academy of Sciences*, 108(18):7481–7486.

[245] Zaslaver, A., Bren, A., Ronen, M., Itzkovitz, S., Kikoin, I., Shavit, S., Liebermeister, W., Surette, M. G. and Alon, U. (2006). A comprehensive library of fluorescent transcriptional reporters for *Escherichia coli*. *Nature Methods*, 3(8):623–628.

[246] Zhang, Q., Lambert, G., Liao, D., Kim, H., Robin, K., Tung, C.-K., Pourmand, N. and Austin, R. H. (2011). Acceleration of emergence of bacterial antibiotic resistance in connected microenvironments. *Science*, 333:1764–1767.

[247] Ziv, N., Brandt, N. J. and Gresham, D. (2013). The use of chemostats in microbial systems biology. *Journal of Visualized Experiments*, 80:e50168.

Appendices

Appendix A

MIC values of high and low persistence mutants

Table A.1: MIC values of ciprofloxacin (CIP), ampicillin (AMP), amikacin (AMK), carbenicillin (CAR), and ceftazidime (CEF) for high and low persistence mutants and their wild types. When different MIC values were obtained for different replicates, the MIC is reported as a range

Strain	**CIP** (μ**g/ml**)	**AMP** (μ**g/ml**)	**AMK** (μ**g/ml**)	**CAR** (μ**g/ml**)	**CEF** (μ**g/ml**)
SX43	0.008	4	2		
nuoN*	0.008	4	2-4		
oppB*	0.008	4	1-4		
gadC*	0.008	4	2		
MG21	0.008	4	2-4	16	0.5
hipA7	0.016	4	2	16	0.5
MG1655	0.008	4	2		
Δ*10TA*	0.008	4	2-4		
BW25113	0.008	4	2-4		
Δ*rpoS*	0.008	4	2-4		
Δ*relAspoT*	0.008	4	2-4		
Δ*lon*	0.016	4	2-4		

Appendix B

Resistant mutant plate assay: supplemental data

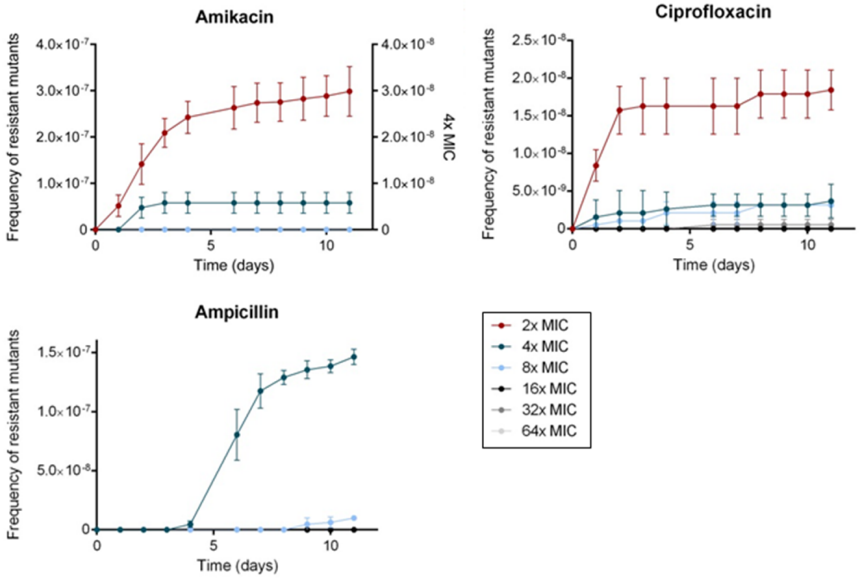

Figure B.1: Optimization of antibiotic concentration and treatment period of the resistant mutant plate assay with MG1655. The number of resistant colonies appearing over time is represented as the mean proportion of the total population density at the start of the experiment (n=2). Agar plates were supplemented with either amikacin, ciprofloxacin, or ampicillin at different concentrations. The selection pressure exerted by the antibiotic is expressed as a multiple of the MIC. Error bars represent the standard error of the mean. Note the different scale for amikacin (4x MIC), indicated on the right axis. For ampicillin (2x MIC), the colony density was too high to distinguish single colonies.

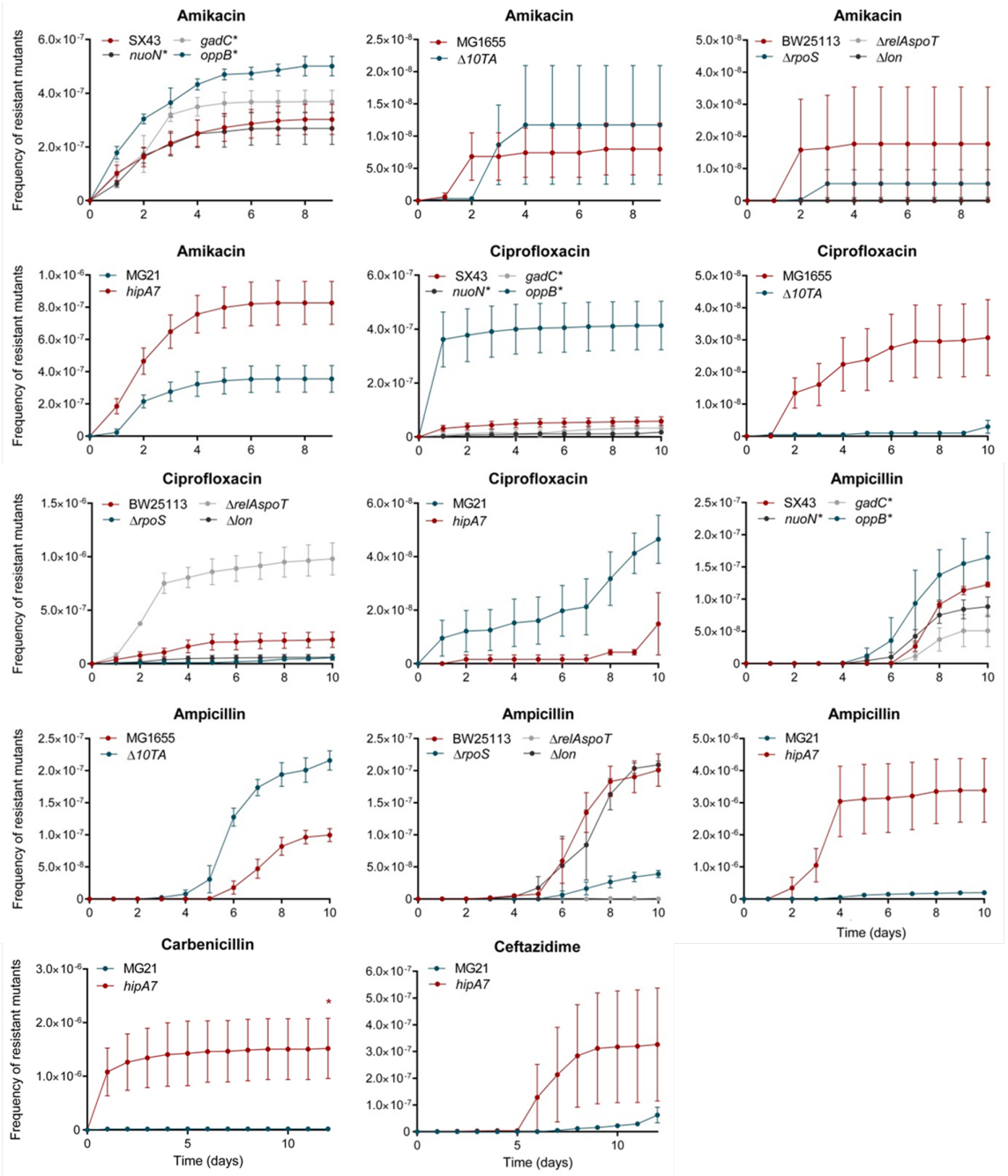

Figure B.2: Frequencies of resistant mutants emerging on solid growth medium supplemented with amikacin (4x MIC), ciprofloxacin (2x MIC), ampicillin (4x MIC), carbenicillin (4x MIC), or ceftazidime (4x MIC). The number of resistant colonies appearing over time is represented as the mean proportion of the total population density, which was measured at the start of the experiment. Error bars indicate the standard error of the mean of 3 biological replicates, except for the data shown in the main text (9 biological replicates). End points were compared statistically with a two-sided Student's t-test ($* : P \leq 0.05; ** : P \leq 0.01; *** : P \leq 0.001$).

Appendix C

MIC values of ECOR isolates

Table C.1: MIC values of ciprofloxacin and ampicillin for strains of the ECOR collection

Strain	**CIP** (μ**g/ml**)	**AMP** (μ**g/ml**)
ECOR 1	0.008	4
ECOR 8	0.001	2
ECOR 15	0.008	4
ECOR 16	0.008	4
ECOR 21	0.008	2
ECOR 26	0.016	8
ECOR 30	0.016	8
ECOR 36	0.008	8
ECOR 37	0.008	4
ECOR 41	0.008	4
ECOR 42	0.002	4
ECOR 43	0.004	4
ECOR 47	0.008	4
ECOR 49	0.004	8
ECOR 51	0.008	4
ECOR 57	0.008	8
ECOR 58	0.008	8
ECOR 59	0.016	>32
ECOR 65	0.016	4
ECOR 70	0.008	8

Appendix D

Stress response promoter activity: supplemental data

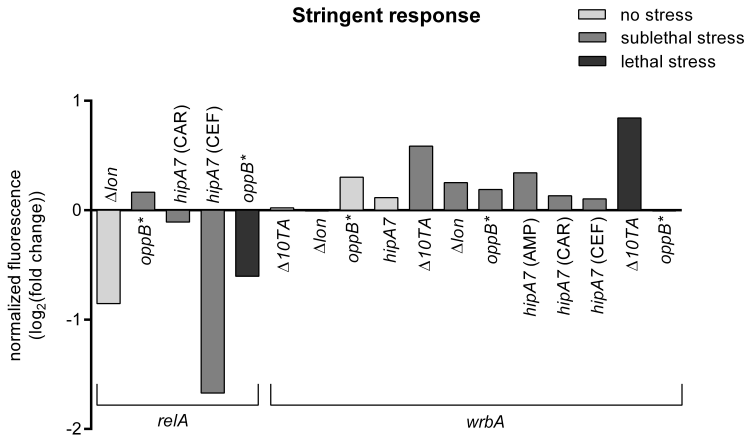

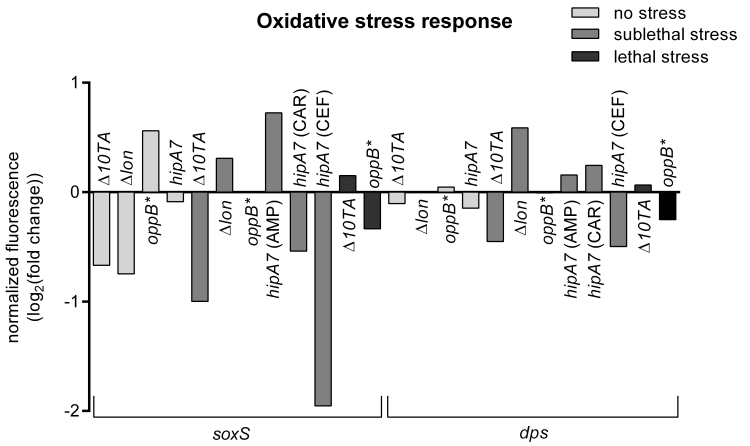

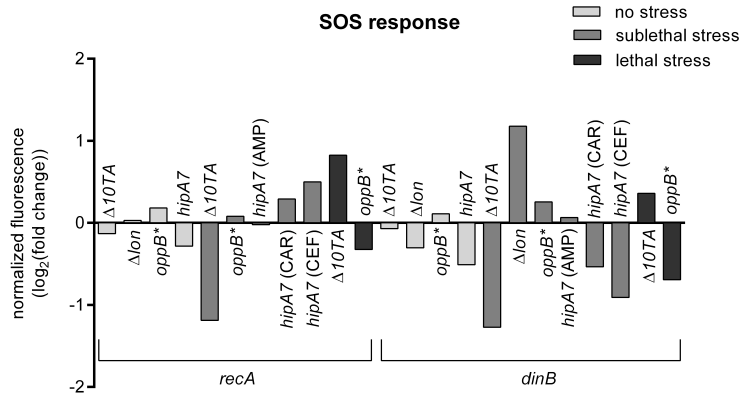

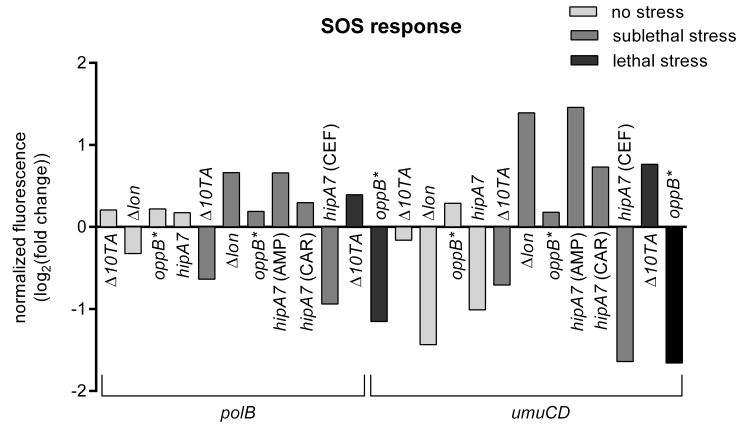

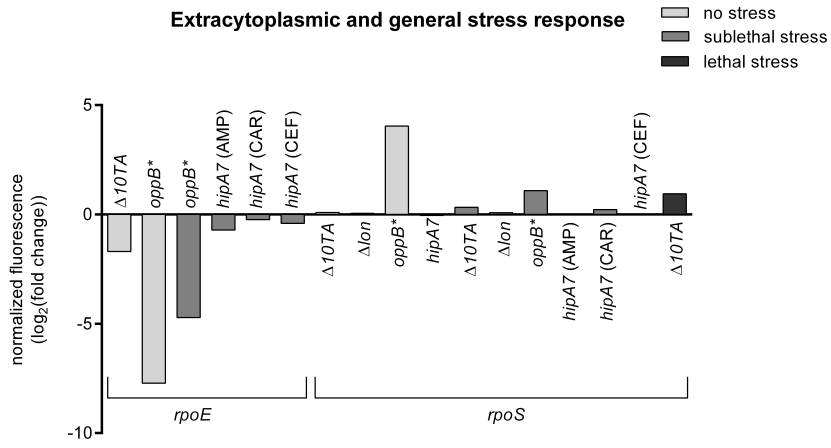

Figure D.1: Promoter activity of stress response genes in different strains under optimal growth conditions ('no stress'), sublethal, or lethal antibiotic stress. Normalized fluorescence (fluorescence/OD_{595}) results from GFP expression from transcriptional promoter-*gfpmut2* fusions. Results are represented as $\log_2$(fold change) of the normalized fluorescence of the mutant strain to the wild type strain, after subtraction of background fluorescence from an empty pUA66 vector.

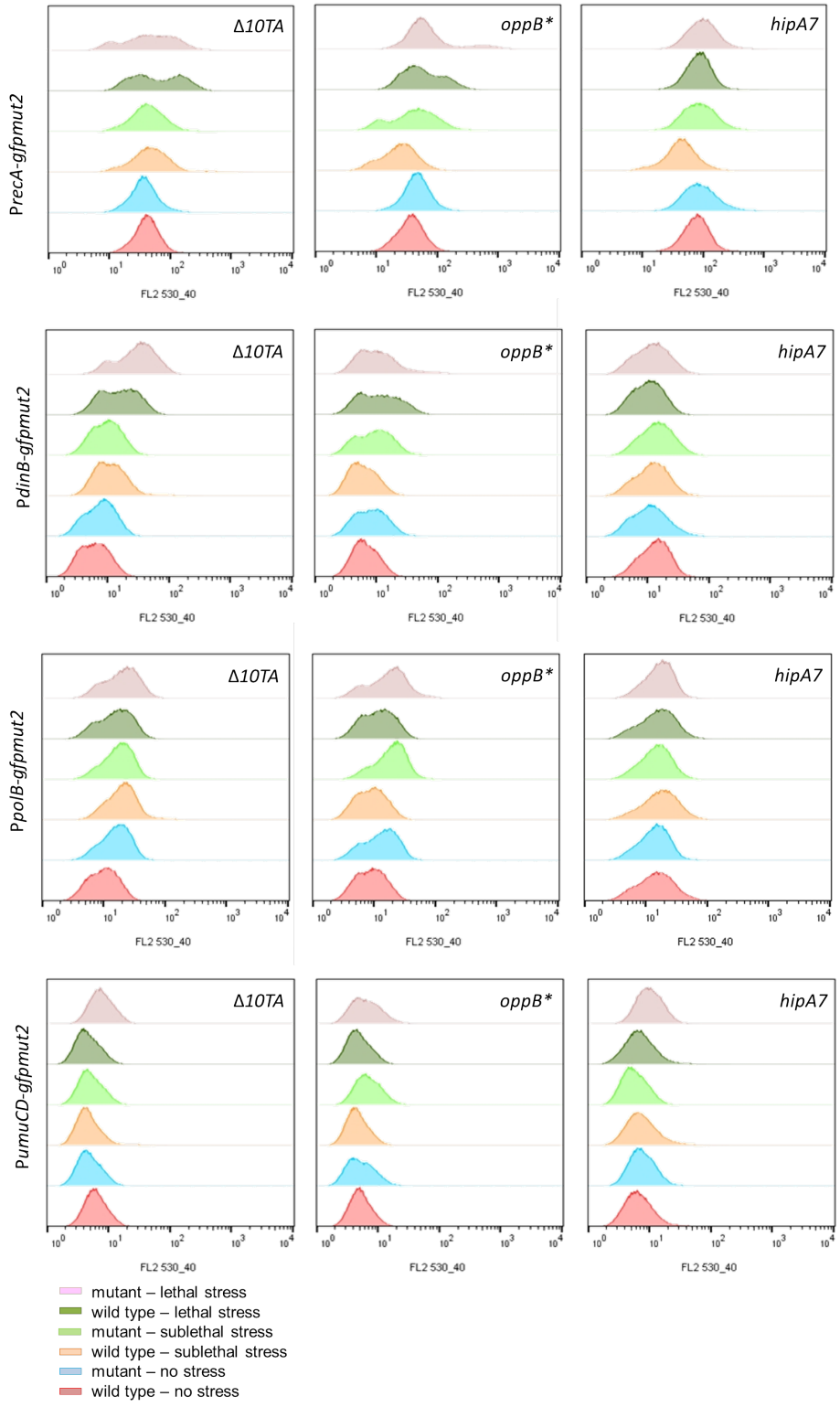

Figure D.2: Single-cell promoter activity of SOS response genes (*recA*, *dinB*, *polB*, and *umuCD*). Fluorescence results from GFP expression from transcriptional promoter-*gfpmut2* fusions. Ciprofloxacin stress was imposed on Δ*10TA*, *oppB**, and their wild types, at sublethal (1/8x MIC) or lethal (625x MIC) concentrations. Ampicillin stress was imposed on *hipA7* and its wild type, at sublethal (1/4x MIC) or lethal (25x MIC) concentrations.

Summary in layman's terms

The discovery of antibiotics was a milestone in medical history. Unfortunately, the introduction of any new antibiotic is accompanied with the emergence of bacteria that are resistant to the drug. When treated with antibiotics, resistant bacteria are not killed but keep on growing. Increasing numbers of infected patients cannot be treated properly because the disease-causing bacterium is resistant to all available antibiotics. On the other hand, several infections do not harbor resistant bacteria but are still difficult to treat. These chronic infections, of which tuberculosis is a prime example, are attributed to the presence of small numbers of persisters. Persisters are dormant bacteria that able to survive antibiotic treatment, even though they are genetically identical to the drug-susceptible cells. When the antibiotic is removed, persisters can re-initiate growth and cause a relapse of the disease.

In addition to the complication of antibiotic therapy, a recent hypothesis states that persisters can accelerate the emergence of resistance. We tested this hypothesis by simulating the evolution of resistance in the lab. When we evolved strains under simplified antibiotic treatment conditions, we indeed observed a faster emergence of resistance when more persisters were present. However, this trend was not observed under conditions that mimick daily treatment of an infected patient, indicating that the contribution of persistence to resistance largely depends on the treatment conditions.

Bacteria have various defense mechanisms to cope with environmental stress. Persister formation is supposed to rely on the same mechanisms. We found that these mechanisms are indeed more active in strains with high persister levels, but the activity in persisters did not seem to differ from the rest of the population. Remarkably, a higher activity of these defense mechanisms was associated with a higher rate of resistant cells emerging in the population. These results suggest that the mechanisms that are involved in persister formation can govern the acceleration of resistance development.

This work contributes to a better understanding of the role of persistence in the emergence and spread of resistant pathogens. The identification of mechanisms underlying this threatening phenomenon offers new targets and opportunities to combat infectious diseases.